ADVANCES IN ANATOMY, EMBRYOLOGY AND CELL BIOLOGY

Lorenzo Alibardi

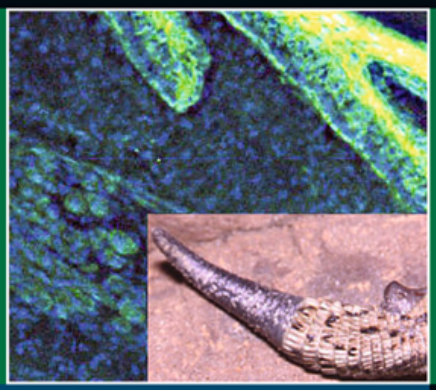

Morphological and Cellular Aspects of Tail and Limb Regeneration in Lizards

A Model System With Implications for Tissue Regeneration in Mammals

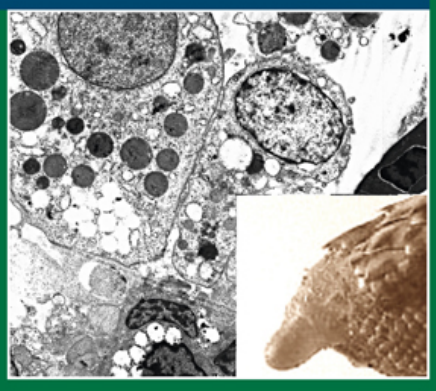

Springer

Reviews and critical articles covering the entire field of normal anatomy (cytology, histology, cyto- and histochemistry, electron microscopy, macroscopy, experimental morphology and embryology and comparative anatomy) are published in Advancesin Anatomy, Embryology and Cell Biology. Papers dealing with anthropology and clinical morphology that aim to encourage cooperation between anatomy andrelated disciplines will also be accepted. Papers are normally commissioned. Original papers and communications may be submitted and will be considered for publication provided they meet the requirements of a review article and thus fit into the scope of "Advances". English language is preferred.
It is a fundamental condition that submitted manuscripts have not been and will not simultaneously be submitted or published elsewhere. With the acceptance of a manuscript for publication, the publisher acquires full and exclusive copyright for all languages and countries.
Twenty-five copies of each paper are supplied free of charge.

Manuscripts should be addressed to

207
Advances in Anatomy, Embryology and Cell Biology

For further volumes:
http://www.Springer.com/series/102

Lorenzo Alibardi

Morphological and Cellular Aspects of Tail and Limb Regeneration in Lizards

A Model System With Implications for Tissue Regeneration in Mammals

With 28 figures

Springer

Dr. Lorenzo Alibardi
Università di Bologna
Dipto. Biologia Evoluzionistica
Sperimentale
via Selmi, 3
40126 Bologna
Italy
lorenzo.alibardi@unibo.it

ISSN 0301-5556
ISBN 978-3-642-03732-0 e-ISBN 978-3-642-03733-7
DOI 10.1007/978-3-642-03733-7
Springer Heidelberg Dordrecht London New York

Library of Congress Control Number: 2009938016

Cover design: WMXDesign GmbH, Heidelberg, Germany

Printed on acid-free paper

Springer is part of Springer Science+Business Media (www.springer.com)

Abstract

The present review deals with the analysis of the cytological processes occurring during tissue regeneration in the tail and limb of lizards. These reptiles are considered as a model to understand the process of tissue regeneration in all amniotes. The review begins with some evaluative considerations on the origin of tail regeneration in comparison with the failure of limb regeneration, a unique case among amniotes. The formation of the tail in the embryo and the possible accumulation of stem cells in autotomy planes of the tail are discussed. The histological and ultrastructural processes occurring during blastema formation and tail regeneration and during limb cicatrization are presented. The comparison stresses the scarce to absent inflammatory reaction present in the tail in contrast to the massive inflammatory response in the limb leading to scarring. In fact the experimental inducement of a strong inflammation in the tail also leads to scarring. The importance of the nervous system in stimulating tail regeneration in lizards is emphasized. The presence of growth factors and extracellular matrix proteins during wound healing of the tail and limb is introduced. The review concludes by stressing the importance of the lizard model of tissue regeneration for medical studies and applications.

Acknowledgements

The study of tissue regeneration in lizards has been the main theme of my research interests since I was a high school student and used to attend the biology laboratories at the Institute of Animal Biology of the University of Padua, Italy (often skipping some high school classes), back in 1974. After the completion of my high school curriculum, I enrolled at the University of Padua and could finally start active research on regeneration in reptiles and amphibians in 1977, entering the laboratory of experimental embryology of M. Sala. The initial morphological, histochemical, and experimental work was followed by biochemical analysis on the variation of different molecules in the regenerating tail and limb of lizards in the physiology and biochemistry laboratory of F. Ghiretti at the University of Padua. From 1980 to 1996 my main interests concentrated on the ultrastructural characterization of various tissues formed in the regenerating tail and limbs of lizards.

The relative isolation, lack of a laboratory in which to pursue this study in Italy, and uncertain academic fate drove me to move abroad. In 1987–1988 I worked in the Department of Biological Sciences, University of Waikato, New Zealand, on the ultrastructural analysis of the regenerating spinal cord in lizards and in the lizard-like reptile *Sphenodon punctatus*, in collaboration with V.B. Meyer-Rochow. In 1989–1990 the study was continued in the Department of Biology, University of Illinois at Chicago, USA, working with S.B. Simpson Jr., especially on the regenerating spinal cord of lizards using autoradiographic, ultrastructural, and tract-tracing neuroanatomical methods, and in vitro cell cultures. In 1991–1992 the ultrastructural, immunocytochemical, and autoradiographic study of the dynamics of tissue regeneration in lizards was continued in the cell biology laboratory of L. Moffat and J. McAvoy, in the Department of Histology and Embryology of the University of Sydney, Australia.

Owing largely to my research activity on other topics (skin of vertebrates and on mammalian auditory nuclei), the work on regenerating tissues was carried on with some discontinuity during the following years. From 1993 to part of 1994

I worked at the University of the West Indies in Kingston, Jamaica, and, from 1994 to most of 1995 the work was carried out at the University of Connecticut in Storrs, USA. From 1995, the research was slowly continued at the University of Bologna in Italy, mainly on the ultrastructural, immunocytochemical, and electrophoretic analysis of the variation of the type and number of blood cells and proteins during regeneration. The analysis mainly concentrated on the regenerating skin of the tail and limb using ultrastructural immunocytochemistry. The study of tissue and spinal cord regeneration in lizards is presently being continued using biochemical methods in conjunction with immunocytochemical analysis of growth factors and extracellular matrix proteins.

The research work was initially supported by the Italian Ministry of Public Education (MPI) while I was at the University of Padua (60% grants), the Ministry of Foreigner Affairs (ME, the scholarships for New Zealand and Australia), and the Italian National Center for Scientific Research (CNR, scholarship to the USA). Other support came from the University of Waikato (NZ Grant Committee), the University of Sydney (Australian DEET), and internal grants from the University of Illinois at Chicago, the University of the West Indies at Kingston, and the University of Connecticut at Storrs while I was working there. However, a large part of my past and present work derives from self-support in conjunction with some funding from the University of Bologna Grants (60%). L. Dipietrangelo (University of Bologna) has helped with reference listing and photography.

The present review is dedicated to S.B. Simpson Jr. (former Director of the Department of Biological Sciences, University of Illinois, Chicago) for his fundamental contribution to the topic, teaching, and friendship. Finally, I warmly thank R. Putz (University of Munich, Germany) for giving me the chance to summarize in the present review the efforts of many researchers as well as my own efforts.

Foreword

The present review covers a very neglected field in regeneration studies, namely, tissue and organ regeneration in reptiles, especially represented by the lizard model of regeneration. The term "regeneration" is intended here as "the ability of an adult organism to recover damaged or completely lost body parts or organs." The process of recovery is further termed "restitutive regeneration" when the lost part is reformed and capable of performing the complete or partial physiological activity performed by the original, lost body part. Lizards represent the only amniotes that at the same time show successful organ regeneration, in the tail, and organ failure, in the limb (Marcucci 1930a, b; Simpson 1961, 1970, 1983). This condition offers a unique opportunity to study at the same time mechanisms that in different regions of the same animal control the success or failure of regeneration. The lizard model is usually neglected in the literature despite the fact that the lizard is an amniote with a basic histological structure similar to that of mammals, and it is therefore a better model than the salamander (an anamniote) model to investigate regeneration issues.

The present review draws attention to the lizard model; the lizard represents the best nonmammalian amniote to analyze the molecular factors involved in the regeneration of various tissues in the tail (successful organ regeneration) compared with the limb (failure of organ regeneration). The present account is intended as an ultrastructural and cell biology continuation of the previous, mainly anatomical and histological summary of this process in lizards (Bellairs and Bryant 1985). Historical information on the studies that have been carried out on the regeneration of the tail and limbs in lizards is reported in several old articles (Fraisse 1885; Misuri 1910; Terni 1920; Woodland 1920). Among the information missing from the literature about reptilian regeneration is the comprehensive visual documentation of the process of tissue regeneration at the ultrastructural level, a very different situation from what is known in amphibians, fish, and mammals (Schmidt 1967; Carlson 2007). The review also provides summaries of published and unpublished images of the fine structure and cell biology of regenerating tissues in the tail and limb in lizards of different species,

studied by the author over many years. Mainly owing to time and space limitations, the present account reports some experimental data on tissue regeneration in lizards and few biochemical data on enzymes and on the general metabolism operating during tail regeneration. The scope of the review is to make a cytological summary of the topic, indicate the future trends of this neglected field of investigation, and draw the attention of the scientific community to the usefulness of adopting the reptilian model for studies on tissue regeneration in the era of molecular biology. This is particularly relevant after the publication by the Broad Institute of MIT, in Boston, of the genome of the American green anolid lizard *Anolis carolinensis* (UCSC genome browser at http://genome.ucsc.edu).

The first chapter of this review deals with the place that reptilian regeneration occupies among vertebrate regeneration, and emphasizes the importance of comparing different factors involved in regeneration in amniotes. This chapter is an attempt to explain why lizards are gifted with a large power of tissue regeneration in the tail but limited power of regeneration in other body regions. Why and how this process has evolved in lizards among the other amniotes is also analyzed. The main microscopic features of the process of regeneration in the tail and limbs are introduced. The last section considers some different local or systemic factors influencing lizard regeneration or failure, and concludes with an analysis of the possible influence of the immune system on the process.

The second and third chapters deal with the ultrastructural and cellular analysis of the process of regeneration of the tail compared with the process of cicatrization of the limb. The two chapters allow one to appreciate some of the differences in cell composition between the injured tail and limb, which will determine the successful regeneration in the tail in contrast to the failure of regeneration in the limb. In the latter, the cellular aspects of inflammation are stressed in comparison with mammalian inflammation, granulation tissue formation, and repair. The third chapter finishes by introducing some immunological analyses of growth factors, intercellular matrix proteins, and keratins expressed during tissue regeneration in the lizard.

The fourth and final chapter briefly stresses the utility of lizards as a model system for studies on tissue regeneration in amniotes and what lizard regeneration can teach us in terms of the consequences for medical treatments of human injuries, wound healing, and possible recovery.

Contents

1	**Regeneration in Reptiles and Its Position Among Vertebrates**	1
1.1	Regeneration in the First Amniotes, the Reptiles	2
1.2	Significance of Tail Regeneration in Lizards: Zoological Background	7
1.3	Regeneration in Lizards: Growth Rates	14
1.4	Embryos of Lizards Fail To Regenerate Limbs and Tail	15
1.5	Histological and Histochemical Aspects of Tail Regeneration	17
1.5.1	Wound Healing and Blastema Formation	19
1.5.2	The Blastema Grows into a Cone	21
1.5.3	Tail Growth and Tissue Differentiation	26
1.5.4	Tail Scalation and Maturation	29
1.6	Histological Aspects of Limb Regeneration and Cicatrization	30
1.7	Single Tissue Regeneration in the Lizard Tail	35
1.8	Failure of Tail Regeneration and Cicatrization	47
2	**Tail Regeneration: Ultrastructural and Cytological Aspects**	51
2.1	Wound Healing to Blastema Formation	51
2.2	Tissue Differentiation	58
2.2.1	Epidermis	58
2.2.2	Blood Vessels, Fat, and Meninges	59
2.2.3	Muscles	64
2.2.4	Cartilage	67
2.2.5	Spinal Cord and Central Nerves	70
2.2.6	Spinal Ganglia and Peripheral Nerves	76
2.3	Growth Factors, Extracellular Matrix Proteins, and Keratins	77
2.3.1	Growth Factors	77
2.3.2	Extracellular Matrix Proteins	82
2.3.3	Intermediate Filament Proteins	84
3	**Limb Regeneration: Ultrastructural and Cytological Aspects**	89
3.1	Wound Healing and Blastema Formation	89
3.2	Scar Formation in the Limb as Compared with the Inducement of Tail Scarring	91
4	**Conclusion and Perspectives: Implications for Human Regeneration**	95
References		99
Index		111

Chapter 1
Regeneration in Reptiles and Its Position Among Vertebrates

The analysis of the distribution of the regenerative power in Eumetazoa indicates that many phyla include species where regeneration is present, sometimes in species very similar to species that do not show any regenerative ability (Reichman 1984; Goss 1987; Alvarado 2000; Brookes et al. 2001). This observation suggests that when some conditions are present and receive a positive selective pressure, an organism, even a complex one, can regenerate lost parts.

In vertebrates an uneven distribution of the regenerative power of tissues and organs is present, but epimorphic regeneration (regeneration from localized body regions) is very limited, mainly to fins in some fish, to many organs in aquatic amphibians, and to the tail of lizards. Vertebrates possess a complex histological composition, and dedifferentiation of some tissues appears to be the prevalent mechanism capable of forming a regenerative blastema of mesenchymal cells in contact with a wound epithelium (Han et al. 2005). Dedifferentiation is not necessary or occurs only partially in tissues where stem cells are present and contribute to the formation of the regenerative blastema (VanBekkum 2004). The formation of a minimal mass of mesenchymal cells capable of proliferation and successive differentiation into specialized and functional tissues is critical for organ regeneration.

The process of regeneration is probably monitored by a number of regulatory checkpoints that control dangerous and uncontrolled proliferation (Alvarado 2000). Whereas successful regeneration implies that all the regulative steps are passed positively, failure of regeneration can derive from not fulfilling one or a few of the requirements of these checkpoints. In particular, in amniotes there are multiple regeneration barriers that prevent limb regeneration. These barriers are represented by biological processes related to a variable inflammatory response (Ferguson and O'Kane 2004), the neurotrophic influence (Singer 1978), and the lack of an apical cap epidermis for sustaining organ growth (Han et al. 2005).

In general, in vertebrates the power of restitutive regeneration decreases from urodele amphibians to larval anuran amphibians and fish, then to some adult anuran amphibians and reptiles (lizards), and finally birds and mammals. Restitutive regeneration is almost absent in birds and mammals (Schmidt 1967; Goss 1969, 1987; Bryant 1970; Reichman 1984; Tsonis 2002; Galis et al. 2003; Han et al. 2005;

Maginnis 2006; Carlson 2007). Also in the modern literature on regeneration studies, the capability of tissue or organ regeneration in reptiles, even the noteworthy regeneration of the tail in lizards, is named in few cases. The process of reptilian tissue regeneration, for unclear reasons, has been almost completely underestimated and neglected in the last 30 years.

1.1 Regeneration in the First Amniotes, the Reptiles

Reptiles are amniotes, and from reptilian ancestors both sauropsids (extant reptiles, including birds) and mammals originated over time (Colbert et al. 2001). Anatomically and physiologically, extant reptiles differ in many aspects from mammals but their histological features are quite similar, definitely more than between mammals and amphibians, making them an attractive model to study tissue and organ regeneration, in particular considering the outstanding regeneration capability of lizards.

For unclear reasons, the study of lizard regeneration, and of reptiles in general, has always been very limited in comparison with research performed on the other vertebrates, and the ability of reptilian tissues to regenerate in particular has been greatly neglected. Aside from the relative difficulty (perhaps unpleasantness) of working with reptiles, another reason may be related to the idea that the lizard model has been (erroneously) considered too distant from the human situation (see the discussion in Simpson 1970, 1983; Simpson and Duffy 1994). Most information about reptilian tissue regeneration derives from the study of the regenerating tail of lizards, an organ that measures a few centimeters in length in most of the species studied. A few other examples of organ regeneration among reptiles include regeneration of the tail and jaws of crocodilians and the shell of turtles (Bellairs and Bryant 1985; Carlson 2007).

Reptiles can be regarded as vertebrates with intermediate regenerative ability, lower than that of cyclostomes, fish, and amphibians (anamniotes) but higher than that of homeothermic amniotes (birds and mammals). In particular, lizards can regenerate many tissues, including nerve cells, part of the lower mandibular arch, and parts of the limb, and have a noteworthy ability to regenerate the tail (Simpson 1961; Bryant 1970; Bellairs and Bryant 1985; Figs. 1.1, 1.2). Caudal regeneration, however, varies in different species of lizards, from the restitution of most of the original tail length to the production of short knobs (Fig. 1.1a–j). The caudal spinal cord, but in general not more rostral parts of the cord (lumbar or thoracic), can regenerate, producing a simple spinal cord (Simpson 1968, 1983; Egar et al. 1970; Alibardi 1990–1991). The regeneration of the spinal cord in the lumbar and thoracic regions, however, deserves more study in relation to still-unexplained reports (see later).

Lizards can repair large amputations of the maxilla and mandibular arch with the initial production of a cartilaginous tissue that can later calcify. The lens of the

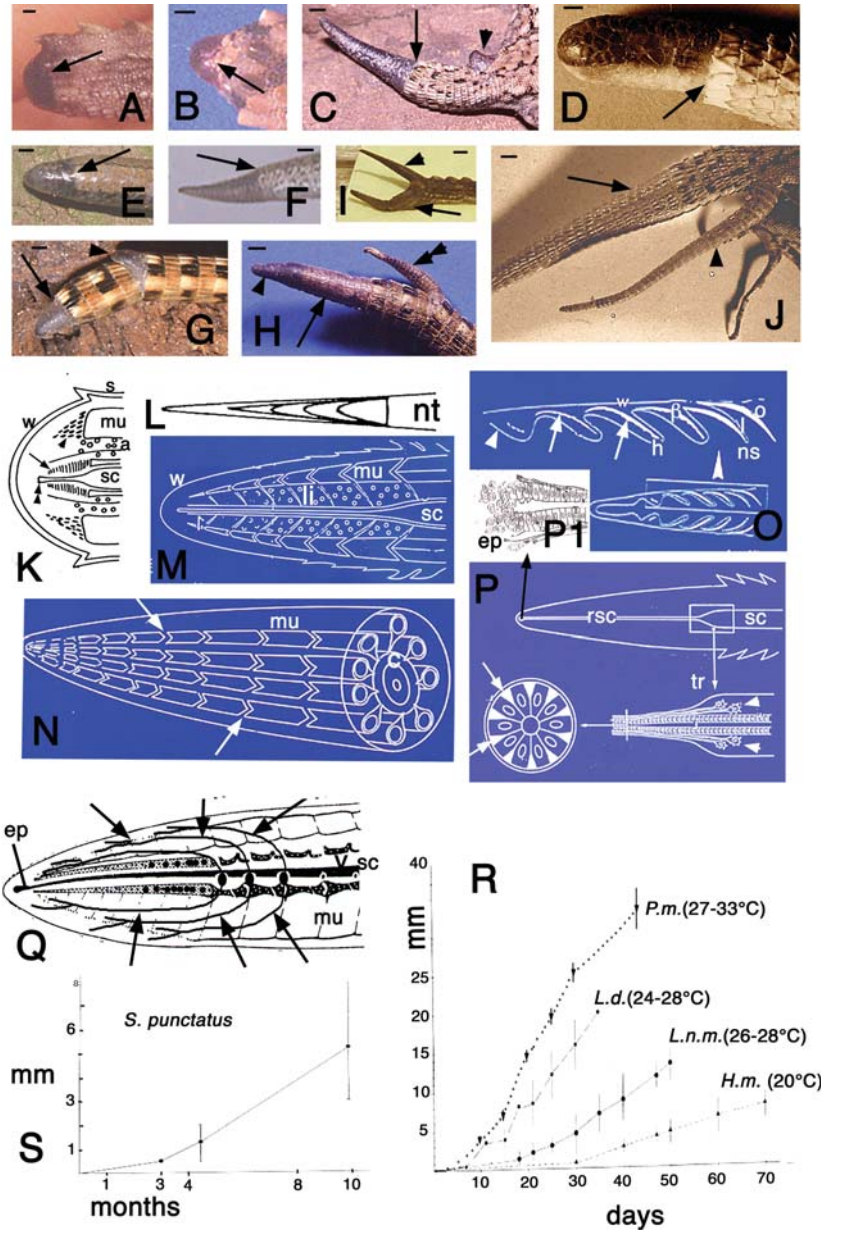

Fig. 1.1 Gross aspects of regenerating tails in different species (**a–j**), regenerating tails (**k–q**), and growth curves for tail regeneration in different species (**r–s**). **a** A blastema of about 45 days in a juvenile of the tuatara *Sphenodon punctatus* (the *arrowhead* indicates the amputation point). *Bar* 1 mm. **b** Blastema of 15 days in the gecko *Tarentola mauritanica* (the *arrow* indicates the fracture point). *Bar* 1 mm. **c** Elongating tail (the *arrow* indicates the

eye can partially regenerate, and a good regeneration is present in the optic nerve, capable of remaking anatomical (but not functional) connections with specific regions of the optic tectum (Beazley et al. 1997; Dunlop et al. 2004). Also part of the cerebral cortex and of the optic tectum of the mesencephalon can regenerate (Minelli et al. 1978, 1980; Del Grande et al. 1981; Lopez-Garcia et al. 1992).

Bone fractures are efficiently repaired, more rapidly at higher temperatures (32–37°C), and two different mechanisms are involved in the healing process. In long bones, such as the femur and the humerus, the fracture results in the formation of cartilage (secondary cartilage) from the periosteum (Pritchard and

Fig. 1.1 (continued) amputation level) and an induced regenerative cone (*arrowhead*) after spinal cord implantation in the lacertid *Podarcis muralis*. *Bar* 2 mm. **d** Club-like regenerated tail of about 2.5 months in the agamid lizard *Agama agama* (the *arrow* indicates the fracture point). *Bar* 1 mm. **e** Short regenerating cone of the limbless anguid lizard *Chalcided chalcides* (the *arrow* indicates the breaking point). *Bar* 1 mm. **f** Elongating cone of the scincid lizard *Leiolopisma nigriplantare maccanni* (the *arrow* points to the breaking point). *Bar* 2 mm. **g** Broken tail of *P. muralis* showing that a second regenerative blastema (*arrowhead*) is forming near the proximal broken tail in addition to the normal regenerating cone (*arrow*). *Bar* 1 mm. **h** Supernumerary tail (*double arrowhead*) of about 4 weeks in *P. muralis* derived from an autotransplant of a small piece of cartilaginous tube containing ependyma. An elongating cone (*arrowhead*) is regenerating on a previously regenerated tail (*arrow*). *Bar* 2 mm. **i** Double tail (the *arrow* indicates the normal regenerated tail, the *arrowhead* points to the supernumerary tail) in *S. puctatus*. *Bar* 1 mm. **j** Long supernumerary tail (*arrowhead*) of about 5 weeks in *Podarcis sicula* derived from an autotransplant of the spinal cord. The *arrow* indicates the normal regenerated tail. *Bar* 2 mm. **k** Tail blastema with ependymal ampulla (*double arrowhead*), procartilaginous aggregates (*arrow*), and promuscles (*arrowhead*). **l** Progressive stages of tail regeneration. **m** The regenerating tail and the localization of the new adipomeres (fat bodies) and muscles. **n** Organization of the regenerated, segmented muscles (*arrows* on the intermuscular planes). **o** Regenerating scales (*bottom image*). The detail (indicated by the *white arrowhead*) shows the entire sequence of scale regeneration, from the initial epidermal peg by the tip of the tail (*arrowhead*) to the deep peg with formation of the shedding line (*arrows*). Beneath the shedding line a new β-layer is formed and neogenic scales are formed with an outer and an inner surface underneath the shedding epidermis (*dashes on the right*). **p** *Top*: the passage region (*square*) from normal and regenerating spinal cord. The regenerating spinal cord (*bottom image*) is made of ependymal cells with a few neurons (*arrowheads*). The cross section of the ependymal tube and the axonal channels (*arrows*) is shown at the *bottom left*. **q** Regenerated nerves into the new tail (*arrows*) that are connected to the last three hypertrophic spinal ganglia (compare their size with the size of the two more proximal ganglia on the *right*). The apical part of the regenerating ependymal tube is enlarged into the ependymal ampulla. **r** Variation in growth curves of regenerating tails in lizards under different temperatures (*P.m.*, *P. sicula*; *L.d.*, *Lampropholis delicata*; *L.n.m.*, *L. nigriplantare maccanni*; *H.m.*, *Hoplodactylus maculatum*). **s** Growth curves of the regenerating tail of *S. punctatus* at 22–24°C. *β* β-keratin layer, *c* cartilage/cartilaginous tube, *ep* ependymal ampulla, *h* hinge region among scales, *i* inner scale surface, *li* lipid-containing (fat) tissues, *mu* muscles, *nt* normal tail (stump), *o* outer scale surface, *rsc* regenerating spinal cord, *s* scales, *sc* spinal cord, *st* stump of the normal tail, *tr* transition zone between normal and regenerating spinal cord, *v* vertebrae, *w* wound epidermis

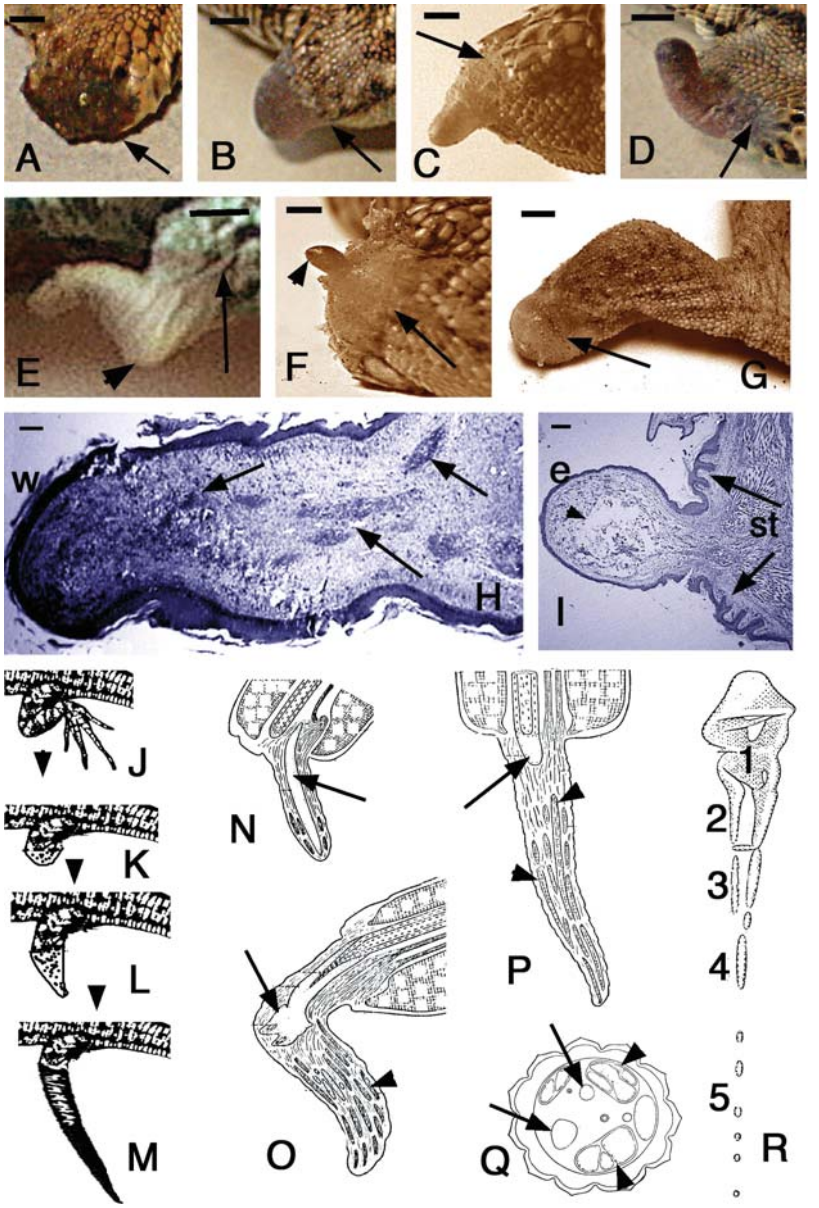

Fig. 1.2 Gross view of hindlimb amputation in *P. muralis* (**a–f**) and *S. punctatus* (**g**), histological aspects of regenerating limbs in *P. muralis* (**h, i**), and hindlimb regeneration in *P. muralis* (**j–r**). **a** Stump covered by a scab (*arrow*) after 4–5 days from the amputation. *Bar* 1 mm. **b** Twenty days after amputation a regenerative cone is formed (the *arrow* indicates the amputation level). *Bar* 2 mm. **c** Twenty-five days after amputation an elongating cone is present (the *arrow* indicates the level of amputation). *Bar* 2 mm.

Ruzicka 1950). Also, vertebrae can reform hemal and neural arches through the formation of cartilaginous bridges (Alibardi, personal observations; see the later description). However, in dermal bones of the skull no secondary cartilage is produced, and only osteoblasts repair the broken bone with new bone (Irwin and Ferguson 1986).

Amphisbaenids (fossorial lizard-like reptiles) do not possess autotomy planes (preformed breaking points) in the tail and do not regenerate a new tail (Bellairs and Bryant 1985). Not much is known about regeneration power in snakes, which do not seem to be able even to regenerate the tip of their tails (Alibardi, personal observations), contrary to previous, occasional assertions (Fraisse 1885). Skin recovery has been reported (Maderson 1971; Maderson et al. 1978; Smith and Barker 1988) but no data on the regeneration of inner organs in snakes are available in the main literature. Also the fracture of dermal bones of the skull is rapidly repaired without production of secondary cartilage (as instead occurs in mammals and birds) but through a direct reossification (Irwin and Ferguson 1986).

Also, the living fossil *Sphenodon punctatus* (sphenodontids, lepidosaurians), a lizard-like reptile with a complete diapsid skull presently living on few offshore islands of New Zealand, has regenerative power similar to that of agamid lizards (Fig. 1.1a, d, i). The process of tail regeneration is very slow (compare Fig. 1.1s with Fig. 1.1r), and needs over 1 year to reform a stiff and often blunt squamous tail (Woodland 1920; Byerly 1925; Alibardi, personal observations). Inside the regenerated tail, large masses of muscle myomeres, a cartilaginous tube longer

Fig. 1.2 (continued) **d** Twenty-five days after amputation in a case with a bending outgrowth (the *arrow* indicates the level of amputation). *Bar* 2 mm. **e** A 40-day regenerated limb with a bent outgrowth forming and angle (*arrowhead*). The *arrow* indicates the level of amputation. *Bar* 2 mm. **f** Thin and short outgrowth (*arrowhead*) over the stump at about 30 days after amputation (the *arrow* indicates the level of amputation). *Bar* 1 mm. **g** Scar over the limb stump of a juvenile tuatara at 3 months after amputation (the *arrow* indicates the amputation level). The limb was lost following accidental injury. *Bar* 2 mm. **h** Longitudinal section of a regenerating limb of about 25 days showing muscle bundles (*arrows*) among dense connective tissue. *Bar* 40 μm. **i** Short outgrowth of about 1 month (like in **f**) showing connective tissue and large blood vessels (*arrow*), whereas most muscles remain in the stump. The *arrows* indicate epidermal pegs of neogenic scales of the limb scar. *Bar* 40 μm. **j**–**m** The sequence of limb regeneration leading to scarring (**j**, **k**), short outgrowths (**l**), or tail-like appendages in rare cases (**m**). **n**–**p** Regenerated limbs of different extension and anatomical complexity produced after amputation. The cartilaginous, partly calcified rod can occupy most of the outgrowth (*arrow* in **n**) or only the proximal part (*arrows* in **o**, **p**), whereas the remaining organ consists of dense connective tissue and muscle bundles (*arrowheads* in **o**–**q**). **q** The anatomical structure in cross section (*arrows* indicate bones, *arrows* indicate muscles) and **r** the skeleton of a tail-like appendage found in nature. In **r**, *1* represents the distal extremity of the femur, *2* corresponds to the fibula and tibia, *3* to the tarsal and metatarsal region, and *4* to the phalanx, possibly corresponding to the second toe. *b* original bone (femur), *bv* blood vessels, *e* epidermis, *rc* regenerated cartilaginous rod, *rm* regenerated muscle bundles, *s* scales, *st* stump. (**n**–**p** Modified from Marcucci 1930a; **q**, **r** modified from Marcucci 1925)

than 10 cm in larger individuals together a variety of tissues and a rudimentary spinal cord are regenerated (Fig. 1.1k–q). The skin regenerates smaller scales with a different morphological pattern of distribution with respect to those of the original tail. However, the structure of the epidermis is similar to that of previous scales (Alibardi 1999; Alibardi and Maderson 2003). Like in lizards, also the limb in this species cannot regenerate (Alibardi, personal observations; Fig. 1.2g).

In chelonians (turtles and tortoises) part of the damaged shell can be repaired and new osteoderms (dermal bones) are formed beneath the horny scutes, but the new scales appear with irregular morphology in comparison with the original scutes (Bellairs and Bryant 1985). The healing process takes over 1 year, depending on the extent of injury, and the recovered area of the shell is covered with atypical scales. Tail regeneration generally does not occur in *Pseudemis nelsonii* and *Chrysemis picta* (Alibardi, personal observations), but a possible regeneration of the tail has been reported in the turtle *Emydura* sp., although no histological details are available (Kuchling 2005).

Finally, occasional cases of tail regeneration have been observed in crocodilians (crocodiles, alligator, caiman; Bellairs and Bryant 1985; Webb and Manolis 1989; Carlson 2007). The new tail can measure over 40 cm in length and the segmented vertebrae of the amputated tail are replaced with a calcified rod of cartilage. The histological aspects of this process are not known but it probably occurs like the process that takes place in the lizard tail, but over a much longer period. The frequency of this phenomenon in crocodilians is not precisely known, but it seems to be very low. Also, in some cases of extensive but not lethal injury to the maxilla, a large portion of the skeletal tissue is regenerated as cartilaginous tissue over a period of 2–3 years (Brazaitis 1981).

1.2 Significance of Tail Regeneration in Lizards: Zoological Background

It is not clear why only lizards among reptiles (squamates, lepidosaurians) and amniotes, in general, have such a remarkable capability to regenerate a large organ such as the tail, made of many complex tissues. Most of the other reptilian groups, chelonians and crocodilians, have a lesser ability to regenerate large organs, like in birds and mammals, in general not even in the tail. What makes the lizard tail such a remarkable organ for the process of regeneration?

We start to address this problem by citing recent studies on the evolution of the scarring process in amniotes that have indicated the following considerations on the biological significance of wounds (Ferguson and O'Kane 2004). Large wounds such as limb loss are often fatal and therefore not subject to selective pressure for regeneration. Small wounds are instead subjected to a strong selective pressure for walling-off the penetration of microbes by a strong inflammatory reaction leading to rapid healing and then to scarring. Wounds of intermediate size, e.g., large stubs or partial loss of stromal tissue compatible with survival, are those more

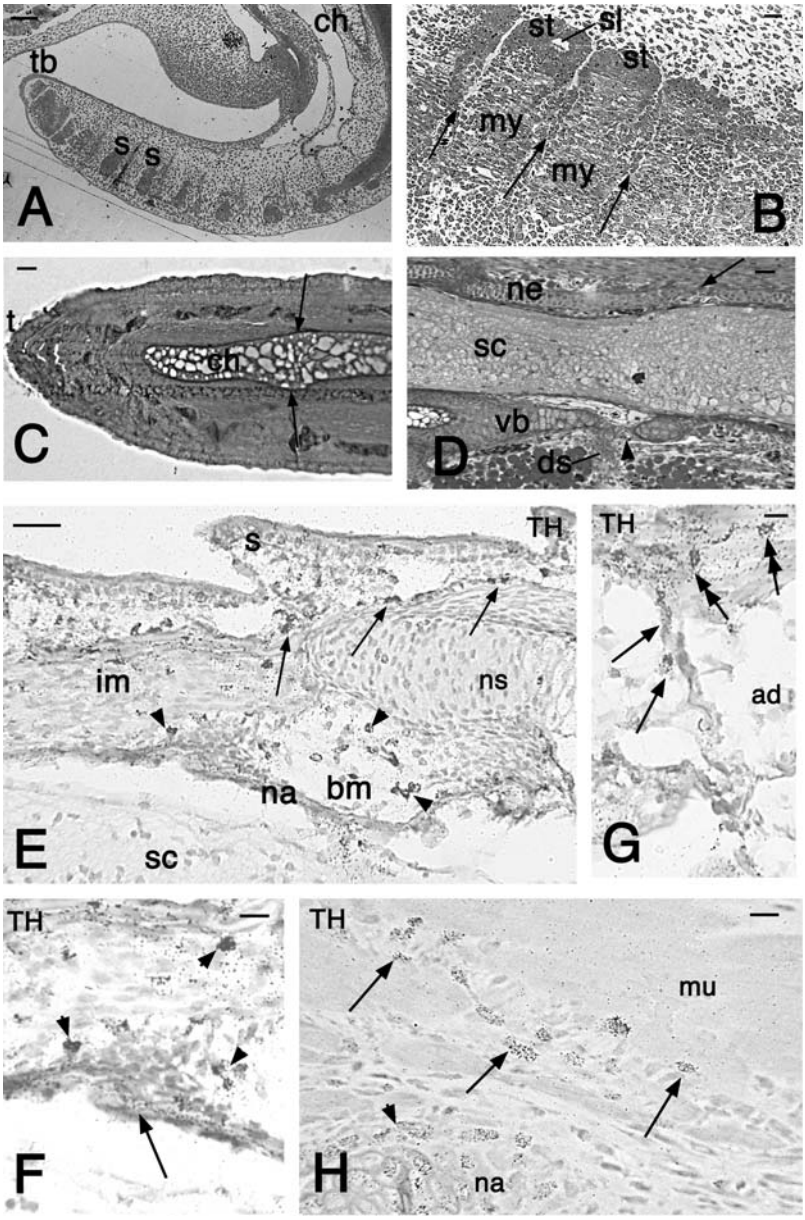

Fig. 1.3 Embryonic development of the tail and vertebral column in *Lampropholis guichenoti* at embyonic stage 29 (**a, b**) and in *P. sicula* at embryonic stage 30 (**c**) and embryonic state 34 (**d**) according to Dufaure and Hubert (1961). **e–h** Autoradiography images of *Anolis lineatopus* at stage 35, derived from a single injection (pulse) of tritiated thymidine (**c–h**; see details in Alibardi 1996c). **a** Elongating tail with the terminal bud made of

exposed to selective pressure. The latter condition applies for the tail loss of lizards, an important but not always essential organ.

Lizards constitute about 3,300 species of tailed, medium-small diapsid-derived reptiles, and represent the largest groups of modern reptiles, the Squamata, together with snakes and amphisbaenids (Evans 2003). Lizard progenitors (fully diapsid eosuchians) evolved from the Mid Triassic into different lineages, but complete lizard characteristics are fully present in the fossil record only from the early Jurassic. More or less elongated tails with numerous vertebrae have been a constant characteristic for lizards since their early history (Bellairs and Bryant 1985; Evans 2003). It seems that a basic group of lizard-like eosuchians (Paliguanidae) from the Triassic, from which possibly various lizard families later evolved, did not possess autotomy planes in their tail vertebrae. Autotomy planes are prefracture planes, laminar regions of tissues along which the fracture of the tail can occurs under various stimuli (grabbing, biting, or simply scaring the lizard that behaviorally releases the tail). Osteological indications of autotomy planes, however, have been detected in some fossils of lepidosaurians and mesosaurs (large aquatic lizard-like reptiles), suggesting that autotomy evolved independently in some lizard groups but was absent in other lizards of the Jurassic. The lack of autotomy planes in some extant lizards supports this notion (Arnold 1984).

One reason for the successful tail regeneration in lizards might be linked to the process of autotomy (Vitt 1983; Reichman 1984; Goss 1987; Arnold 1990; Maginnis 2006), a preadaptative antipredatory device of tail release that can be associated with the need to regenerate the tail. The tail is an organ derived from the tail bud of the embryo, a growing organ with an unknown capability to preserve a reservoir of stem cells left from the embryo. In fact, recent studies seem to indicate that stem cells are indeed retained in the tail (Alibardi, personal observations; see Fig. 1.3 and the later description).

Fig. 1.3 (continued) mesenchyme. Numerous tail somites (*arrows*) are present. *Bar* 100 μm. **b** Detail of caudal sclerotomes of the autotomous region among which a fissure is present (*arrows*) that will form the autotomy planes. *Bar* 25 μm. **c** Tip of the tail with the axial cord and a condrifying intercentrum (*arrows*). *Bar* 25 μm. **d** Longitudinal section of developing, cartilaginous vertebra showing a detail of the gaps in the neural arch (*arrow*) and the vertebral centrum (*arrowhead*), from which the intravertebral slits will be formed. *Bar* 15 μm. **e** Thymidine-labeled cells localized along the dorsal intermuscular plane (*arrows*). Labeled cells are also seen along the periosteum (*arrowheads*) along the vertebral body. *Bar* 40 μm. **f** Detail of thymidine-labeled cells (*arrowheads*) near the vertebral splitting (*arrow*). *Bar* 10 μm. **g** Detail of the interadipose septum with thymidine-labeled cells (*arrows*) and intermuscular labeled cells (*double arrows*). *Bar* 10 μm. **h** Detail of labeled cells (*arrows*) within the intermuscular connective tissue of tail muscles. The *arrowhead* points to labeled cells of the perichondrium of the neural arch. *Bar* 10 μm. *ad* adipose tissue, *bm* bone marrow, *c* cord, *ft* fat tissue (adipomeres), *mu* muscles, *na* neural arch, *ns* neural spine (cartilaginous), *s* scale, *sc* spinal cord, *sl* sclerocele (celome), *st* somite, *TH* thymidine autoradiography, *v* vertebral bone

In some cases regeneration occurs from autotomy planes (intravertebral regions) but also intervertebral fractures allow for tail regeneration. The process of tail regeneration is even believed to have evolved from a primitive, intravertebral autotomy plane (Arnold 1984, 1990). Some studies in geckos and lacertids have reported that, even when the tail is sectioned at a different and nonautonomous level, the stump is soon ablated at the closest autotomy plane (Werner 1967b). The latter author showed that there is a latent period after tail injury and before the formation of the blastema in which one quarter of the distal vertebra close to the stump surface was ablated along an autotomy plane from which the process of regeneration of the tail is started. In other lizard species, however, tail regeneration can also start after sectioning the tail tissues outside autotomy planes. Also, the possibility to regenerate a tail from a previously regenerated tail (devoid of autotomy planes) demonstrates that tail regeneration does not only have to begin from autotomy planes. In other species of lizards, intervertebral regeneration is also possible. Autotomy planes have not been described in other reptilian groups, such as in snakes, turtles, and crocodilians, which are unable to regenerate (Bellairs and Bryant 1985).

Various indications suggest that a rapid regeneration is associated, to autotomy, and probably evolved in small lizards, in conjunction with tail behavior and autotomy for avoiding or escaping predation (Congdon et al. 1974; Arnold 1984, 1990). Tail regeneration is absent or rare in species of large size or where autotomy does not take place (Werner 1968; Vitt 1983; Bellairs and Bryant 1985; Fitch 2003; Maginnis 2006). Although prevalent among lizards, tail regeneration does not occur in all lizard species, and the final output can be limited, producing sort tails, 20–30% of the original tail length, medium-sized tails (50–60% of the original tail length), or long tails, nearly 80–90% of the initial tail length. A systematic analysis has been presented (Arnold 1984; Bellairs and Bryant 1985; Maginnis 2006), and it shows the numerous variations of regenerative potential in the different lizard families analyzed. In the following discussion, we only cite some representative examples.

It is known that many agamid lizards and *Sphenodon* can regenerate short, often stubby tails (Fig. 1.1d), anguids form short tails over a long period (more than 1 year in the blindworm), and scincids and iguanids regenerate medium-long tails (Fig. 1.1e, f). Also, teiid lizards regenerate short tails (Vitt 1983). Long regenerated tails are formed in many geckonids and lacertids (Fig. 1.1c, g, h, j). Numerous variations in the size and length of regenerated tails, however, also occur among different genera within lizard families (Arnold 1984; Bellairs and Bryant 1985; Maginnis 2006).

In general, large lizards such as varanids or specialized arboreal species such as chameleontids show a limited or even absent regeneration capability. In scincids, tail regeneration is completely absent in the Australian fence skink, *Chryptoblepharus virgatus*, which does not drop the tail, whereas it is common in the sympatric garden skink, *Lampropholis guichenoti*, which can shed its tail if provoked (Alibardi, unpublished observations).

The iguanid lizard *Crotaphytus collaris* does not regenerate the tail after amputation, whereas other species living in the same area but with different ecological adaptations are capable of regenerating the tail (Fitch 2003). Another case is the agamid *Calotes versicolor*, which cannot regenerate the tail in natural conditions (Woodland 1920). A further case of an iguanid lizard with poor or absent tail regeneration is *Polychrus acutirostris* (Vitt 1983). In all nonautotomous species, the scaling pattern and tail muscles show a lack of preadaptation to autotomy, and then likely to tail regeneration. Whereas in geckos and many autotomous lizards tail scales are arranged in rings, scales are alternated in nonautotomous lizards such as *C. versicolor*. Likewise, long, inner muscles are present around the vertebral column in *C. versicolor*, impeding tail breakage and no tail regeneration will follow. Conversely, short or even degenerated muscles are present in geckos, allowing tail breakage, and these are anatomical preadaptations to autotomy and, likely, to tail regeneration. The autotomy planes extend from the vertebrae to intermuscular connective tissue, and even to the dermis (Quattrini 1952a, b, 1953a, b, 1954, 1955; Furieri 1956; Bellairs and Bryant 1985). In fact, not only tail muscles and adipomeres, but also vertebrae until the spinal cord present autotomy planes. The spinal cord in *Podarcis sicula* is thinner at the same level of autotomy planes of the autotomous region of the tail (located after the fifth distal vertebra), otherwise in nonautotomy planes (more proximal region of the tail) no periodic thinning of the spinal cord is present. The blood vessels such as the caudal artery and veins are broken after the valves so that bleeding is impeded after autotomy.

The above zoological indications suggest that autotomy in lizards evolved as a means to escape predators and then regeneration evolved to replace the autotomous tail, and such a remarkable power of regeneration may have evolved later by a positive selective pressure, maybe in the Jurassic or the Cretaceous (Bellairs and Bryant 1985). If the premises are roughly correct, this means that tail regeneration was a derived characteristic of lizards, and that the cellular mechanisms that allow this broad regenerative capability are relatively recent in the history of lepidosaurians (150 million to 180 million years ago).

Variability in regeneration is not exclusive to lizards, and has also been found in the "champions" of regeneration, the salamanders (Scadding 1977). Out of seven species analyzed, two species are not capable of limb regeneration and two others are poor regenerators. Also, the tail has different capabilities, according to the presence or absence of a basal constriction in the tail where the autotomy plane can allow tail release (Wake and Dresner 1967; Mufti and Simpson 1972). Therefore, also in amphibians there seems to be a correlation between tail autotomy and regeneration, and in general larger species cannot lose and regenerate their tails (Scadding 1977; Reichman 1984). The limb in larger species takes longer to regenerate (Gianpaoli et al. 2003).

Also, the selection of the social status given by the tail during lizard evolution might have favored the selection of a rapid process of tail regeneration. Some lizard species that drop the tail also lose their social rank but can regain it after tail

regeneration, like in the lizard *Uta stonsburiana* (Fox and Rostker 1982). In the agamid lizard *Agama agama*, where the tail is used for whipping other individuals during agonistic events, tail loss results in the regeneration of a partial tail terminating in a club-like fashion (Fig. 1.1d), very effective when the tail is whipping other individuals (Schall et al. 1989). In the similar and sympatric species *Agama stellio*, where whipping behavior is absent, the regenerated tail is short and tends to taper without forming a club-like ending.

In lizards the tail also represent a storage organ for fats (sometimes more than 50% of the body fat), and this is even more so in a regenerated tail (Congdon et al. 1974; Daniels 1984). The evolution of a rapid process of tail regeneration has, in general, permitted a better survival chance for lizards, and no doubt it represents an adaptive mechanism for the survival of many species (Arnold 1990; Fitch 2003; Clause and Capaldi 2006). The regeneration of the tail, although it is imperfect in comparison with the original tail, represents a positive trait selected during adaptation of some species to their specific environment. The understanding of the events that have reactivated the remarkable morphogenetic process of tissue regeneration in adult amniotes such as lizards would provide useful information for the understanding of processes that can reactivate the regenerative capability in mammals.

According to the above descriptions, it appears that in lizards capable of tail regeneration, the remarkable process of regeneration of a nonvital organ has been selected to favor metabolic survival, speed of movement, prehensility, reproductive behavior, social status, etc. The regenerated tail is a large organ relative to the rest of the body of the animal, up to 40–45% of the body mass in some species. On the bais of the above discussion, the following hypothesis on the evolution of tail regeneration in lizards can be proposed.

Initially, basic eosuchian lepidosaurians were not capable of autotomy and regeneration. In the case of attack by a predator, or interspecific competition or accidental injury, these lizards either perished or survived by more or less extensive loss of part of the tail (aside from other damage). Because the loss of the tail was compatible with survival, the recovery of the tail needed a rapid process of wound healing, probably leading to scarring, like in mammals. As compatible with survival, the loss of the tail was subject to evolutionary pressure acting on the selection of an autotomous organization of the tail, which led to the selection of connective autotomy planes. The latter minimized injuries while smaller or larger parts of the tail were lost.

The origin of the relatively fragile connective planes among tail fat tissue and muscles (originating from myotomal connective tissue) occurred by the localization of poor fibrogenic fibroblasts, not secreting a high number of collagen fibrils. Among these cells, true stem cells with a mesenchymal-like aspect and some pluripotentiality in their differentiation were probably present, as indicated from recent studies (see the later discussion). The break of the tail along the connective planes allowed extensive tissue damage to be avoided, especially in the vertebrae and muscles, and resulted in little inflammation and minimized

scarring. A mesenchymal population of cells present in the septa could also accumulate on the surface of the autotomy plane under a wound epithelium that rapidly covered the stump. When the mesenchymal population reached a certain, critical, mass underneath the wound epithelium, the establishment of a trophic dermal–epidermal interaction (a sort of Apical Epidermal Ridge, AER or apical epidermal cup, AEC) was reached. This led to the distal growth of the mesenchymal mass (the blastema) and then to tail regeneration.

The hypothesis presented above can explain why no limb regeneration could evolve in lizards. Because the limb cannot be lost without having a great effect on survival (lizards cannot escape fast and cannot run away with high speed without a limb), injury to the limb is generally fatal in the wild for a lizard. If the animal survives, the limb stump is rapidly turned into a scar. Whereas selection acted positively in lizards with autotomy planes for tail regeneration, this was not the case for the limb, a more essential and vital organ even than the nonautotomous tail. Limbs therefore do not regenerate in all lizards, in particular the distalmost part, the autopodium (arms and feet).

We can now compare the limb failure in lizards with limb regeneration in aquatic amphibians (urodeles). In the latter, the loss of a limb is not so essential for survival as the loss of the tail (often with autotomy planes), which is more essential for swimming away than limbs (Scadding 1977; Reichman 1984). Differently from lizard limbs, the urodele limb (and the tail) had the chance to succumb to an evolutionary pressure leading to limb regeneration. Among the main preadaptations for the selection of limb regeneration in urodeles was the neotenic state of adult urodeles (embryonic characteristics in sexually mature individuals), which suggests the presence of numerous stem cells in the limb. Another factor is the high innervation (mainly sensory) of the limbs in urodeles (higher than in lizards; Zika and Singer 1965). In urodeles, limbs are perhaps more useful for the sensorial exploration of the environment than for walking in water. Therefore, limb loss in urodeles is not so vital as in lizards, and the limb can be subject to evolution for regeneration. Also, limbs in urodele amphibians have a nervous dependence for their regeneration (Singer 1978).

Another favorable characteristic for regeneration in amphibians is that the wounded epidermis seals the stump in a few hours over the small stump surface of these small vertebrates. In fact, reepithelialization takes 4–6 h in tadpoles, 12 h in adult newts in contrast to 5–8 days for the lizard tail stump, and 15–20 days or more to seal the stump of the lizard limb. The rapid reepithelialization of small stumps of amphibians minimizes the penetration of microorganisms and the consequent inflammation or infection, favoring the formation of a regenerative blastema. Some of the largest amphibians cannot regenerate their limbs, another indication that the size of an organ is also important in the selection of a regenerative process (Scadding 1977). The above discussion has indicated the basic biological requirements for an organ to evolve a process of regeneration. However, the cell and molecular processes that govern organ regeneration, even in urodeles, remain largely undiscovered (Mesher 1996; Odelberg 2005).

1.3 Regeneration in Lizards: Growth Rates

The growth rate for tail regeneration varies according to environmental conditions, and fluctuates with daily temperatures and different seasons. Under controlled parameters (temperature and photoperiods), as obtained in laboratory conditions, regeneration rates are more constant and optimal. Some growth curves for tail regeneration in different species of lizards and in *S. punctatus* are presented in Fig. 1.1r and s. Further information on the growth rates for tail regeneration in other species are indicated in the following examples. The latter are meant to give a general idea on the length and stages for tail regeneration in lizards. More and systematic details on the rate of regeneration in several lizard species are summarized in Bellairs and Bryant (1985).

Under temperate environmental conditions (around 30–32°C when basking to 15–17°C at night in summer), the gecko *Hoplodactylus pacificus* showed a growth rate of 0.23–0.26 mm/day, and the skink *Leiolopisma zelandica* showed a growth rate of 0.16–0.37 mm/day in different individuals (Brawich 1959). The eastern dragon agamid, *Physignatus leusueuri*, under natural conditions showed a variable increase in the length of the regenerating tail from 0.21 to 0.77 mm/day (Hardy and Hardy 1977). Other rates of growth can be found in different accounts (Werner 1966; Bellairs and Bryant 1985).

Growth rates also vary according to the level of amputation, and are higher in tails lost in the proximal (autotomous) part of the tail (Bryant and Bellairs 1967a; Tassava and Goss 1966; Baranowitz et al. 1979). Low temperatures (below 22°C) delay the process of wounding and blastema formation. The growth is also faster from the conic blastema stage (Fig. 1.1g) to the prescaling elongated tail phase (Fig. 1.1c). In *Anolis carolinensis* under laboratory conditions, the fastest growth rate occurs during the seventh and the eighth weeks after amputation. In *P. sicula* the maximum rate of growth occurs between 2.5 and 3.5 weeks after amputation under summer conditions (over 32°C in the sun and not less than 22°C during the night; Alibardi, personal observations). Growth rates have been better quantified under laboratory conditions for *A. carolinensis* (Maderson and Licht 1968). In this species the growth rate is 1.5 mm/day from 14 to 28 days after amputation (the fastest period of tail regeneration in this species) at constant 32°C, but falls to 0.15 mm/day at 21°C from 28 to 45 days after amputation, and even less after this period.

The amputation of the tail at very rostral levels (preautotomous tail region present in some species) is followed by the formation of smaller regenerates or no regenerated tail at all, so the lizard remains with a scar or a short stub. Although this was initially associated with the lack of the regenerative territory for the tail (Guyenot 1928), more recent information suggests another explanation. As previously indicated for the lack of tail regeneration after tail amputation in embryonic lizards, also in the case of the elimination of the tail it is likely that also the entire

reservoir of stem cells contained in the tail is probably eliminated. This condition may lead to the lack of regeneration, but further studies are needed on this point.

1.4 Embryos of Lizards Fail To Regenerate Limbs and Tail

In mammalian embryos, tissue regeneration and organ regeneration appear more efficient than in adults (Adzick 1992; Nodler and Martin 1997). This is not the case for lizard embryos, where not only the limbs but also the tail cannot regenerate after amputation (Marcucci 1915a; Moffat and Bellairs 1964; Bryant and Bellairs 1967b, 1970).

The lack of tail regeneration in embryos occurs when the embryos are operated on at relatively early embryonic stages according to Dufaure and Hubert (1961). The amputation of the tail at stages 30–33 (palette stage, when digits are forming and the tail bud is elongating) produces hatchlings without the tail. Also, amputation at later stages (stages 34–37, when digits are growing, the interdigital membrane is resorbed, and the tail is elongating) results in tail loss in hatchlings (no tail regeneration). Conversely, the partial amputation of the tail in the last embryonic stages (stages 37–40 with a long tail and limbs largely scaled) often leads to the regeneration of the tail (Moffat and Bellairs 1964; Bryant and Bellairs 1970). The lack of tail regeneration in the embryo has been associated with mechanical inhibition of the extensive blood clot or with the injury produced after the surgery that stimulates cicatrization (Marcucci 1914). Another interpretation has indicated that the coverage or even the constriction of the amniotic membranes over the tail stump of the embryo often results in autoamputation of the tail and inhibition of tail regeneration (Bryant and Bellairs 1967b).

Knowledge of the modality of formation of vertebrae in the tail of lizards during embryogenesis can give important clues to the process of tail regeneration, especially in relation to the possible presence, proliferation, and accumulation of stem cells in the tail during embryonic development. The anatomical planes of autotomy are formed during late embryogenesis (from stages 33–36 according to Dufaure and Hubert 1961) as myomeres, lipomeres, and sclerotomes are formed with a segmental organization along the notochord (Quattrini 1954; Werner 1971; Bellairs and Bryant 1985; Fig. 1.3a, b). The first authors to analyze the formation of autonomous vertebrae in lizard embryos considered the origin of the vertebral split as secondary and occurring during ossification of the cartilaginous vertebra (Bellairs and Bryant 1985). According to these authors, the split originates from the widening of the bone marrow contained in the center of vertebrae or from the nonossification and resorption of the cartilage along the splitting line. Some mesenchymal (stem?) cells present in the vertebral split may therefore derive from bone marrow elements and migrate to the peridural space of vertebrae (Quattrini 1954; Alibardi, unpublished observations). Some studies have indeed reported that in samples of lizard embryos studied at the cartilaginous stage of

vertebral morphogenesis, the intravertebral splitting line is not yet formed but appears only after ossification of the vertebra (Bellairs and Bryant 1985).

More recent authors, however, have considered the presence of autotomy planes within vertebrae (vertebral splits) as a primitive character of these vertebrae among most lizards. The splitting process has been lost in few families of lizards and has been conserved in most families (Werner 1971; Bellairs and Bryant 1985). In fact, in some species (iguanids) the split is initially present but is later lost when presclerotomes and postsclerotomes merge to form the mature vertebra. According to the latter studies most trunk and nonautotomous tail vertebrae derive from the fusion of the hemisclerotomes, so the postsclerotome of one somite merges with the presclerotome of the following somite. However, in the autotomous caudal region, the two hemisclerotomes remain separated by the somite epithelium, and this split gives rise to the vertebral split after the cartilage has become ossified (Fig. 1.3a, b). The interadipose and intermuscular autotomy planes also derive from the fusion of the cutaneous lamina of two successive somites (Quattrini 1954).

After the axial notochord has been replaced by cartilage, a discontinuity remains in the cartilaginous verbal body and neural arch at the same level where the autoitomous planes (Fig. 1.3c, d). Studies after administration of tritiated thymidine or 5-bromodeoxyuridine (5BrdU) in lizard embryos during late vertebral morphogenesis have indeed shown that the cells that retain the labeling for a long time (12–20 days) are often present along the autotomy planes of the dermis, intermuscular connective tissue, and around the vertebral split (Fig. 1.3e–h). These cells are likely slow-cycling cells, a typical characteristic for stem cells. Cells of other tissues where rapid cell proliferation takes place (epidermis, dermis, muscles, etc.) show most nuclei with diluted silver grain density or are completely unlabeled after 12–20 days from the injection of the DNA precursors (Alibardi, unpublished observations).

At the end of development, the intravertebral plane split contains a loose mesenchyme with some cartilaginous cells (Quattrini 1954; Werner 1967a, b, 1971). Vertebrae of the caudal autotomous regions are held together by the cartilage and the elastic sheath of the cord, and by the cartilage rim surrounding the body of the vertebrae. Between the two surfaces of the vertebral split, a loose mesenchyme remains, and it is a continuation of the mesenchyme of the peridural space, located between the periosteum and the dura mater (Quattrini 1954). It is likely that this embryonic tissue contains stem cells, and it probably participates in the formation of the regenerative blastema after tail loss, in particular supplying cells that give rise to the cartilaginous tube of the regenerated tail.

Mesenchymal cells essentially remain in the dermal, intermuscular, and perivertebral connective septa, and have also been noted between the anterior and the posterior parts of each autotomous vertebra (Quattrini 1954). Among these mesenchymal elements, stem cells are probably present as indicated by long-retention studies utilizing thymidine autoradiography and 5BrdU immunodetection (Alibardi, unpublished observations; Fig. 1.3). If these preliminary

observations are confirmed in future analyses, a new explanation for the lack of embryonic tail regeneration can be proposed. The presence of stem cells in autotomy planes more than the inducement of cicatrization/mechanical constriction from amniotic membranes may therefore explain the failure of tail regeneration after amputation of the tail bud. In fact, the amputation of most of the tail at early stages of development, when stem cells may still be localized in the apical bud, completely depletes the tail region of its stem cell reserve, therefore making tail regeneration no longer possible.

It is known that regeneration also does not occur when the adult tail is amputated at its base, in the nonautotomous region (Misuri 1910; Woodland 1920; Guyenot 1928; Alibardi, unpublished observations). This phenomenon was interpreted according to the "territories of regeneration" by the fact that the basal amputation completely eliminates the tail territory. This phenomenon can now be reinterpreted as due to the depletion of likely stem cells after the basal amputation of the tail. This intervention may completely remove the reserve of stem cells dislocated in the autotomy planes of the adult tail so that the formation of a regenerative blastema is impeded. The first indications of the presence of stem cells in the tail are still being analyzed, and more detailed studies are still needed to confirm the hypothesis.

1.5 Histological and Histochemical Aspects of Tail Regeneration

The present account briefly describes the main histological and histochemical events leading to tail regeneration. This information has been previously illustrated by detailed histological studies of different species representing many lizard families (Fraisse 1885; Misuri 1910; Woodland 1920; White 1925; Guyenot and Matthey 1928; Boring et al. 1948–1949; Hughes and New 1959; Simpson 1961; Bryant and Bellairs 1967a, b; Werner 1967a, b; Shah and Chakko 1966; Cox 1969a; Simpson 1965; Mufti and Iqbal 1975; Purvis 1979; Alibardi and Sala 1983; Alibardi 1986, 1993a, b, 1994a–c, 1995a–c, 1996a, b, 2009a; Alibardi et al. 1993a, b; Alibardi and Toni 2005).

The histochemical and biochemical changes of proteins, nucleic acids, glycogen, enzymes involved in glycidic or lipid metabolism, and small metabolites during progressive stages of tail regeneration have been reported (Shah and Chakko 1966, 1972; Radhakrishnan and Shah 1973; Shah and Hiradhar 1974, 1975; Magon 1977, 1978; Kinariwala et al. 1978; Chakko and Mariamma 1981).

The histological studies have been well summarized in a previous, extensive review on reptilian regeneration (Bellairs and Bryant 1985), and will not be treated in detail here. More cytological details of the process of tail and limb regeneration, unreported in the available literature, will be given in the Chapters 2 and 3 on the ultrastructural characteristics of wound healing and regeneration. In warm–hot conditions (above 25°C) the rate of tail growth is optimal in most species, and the

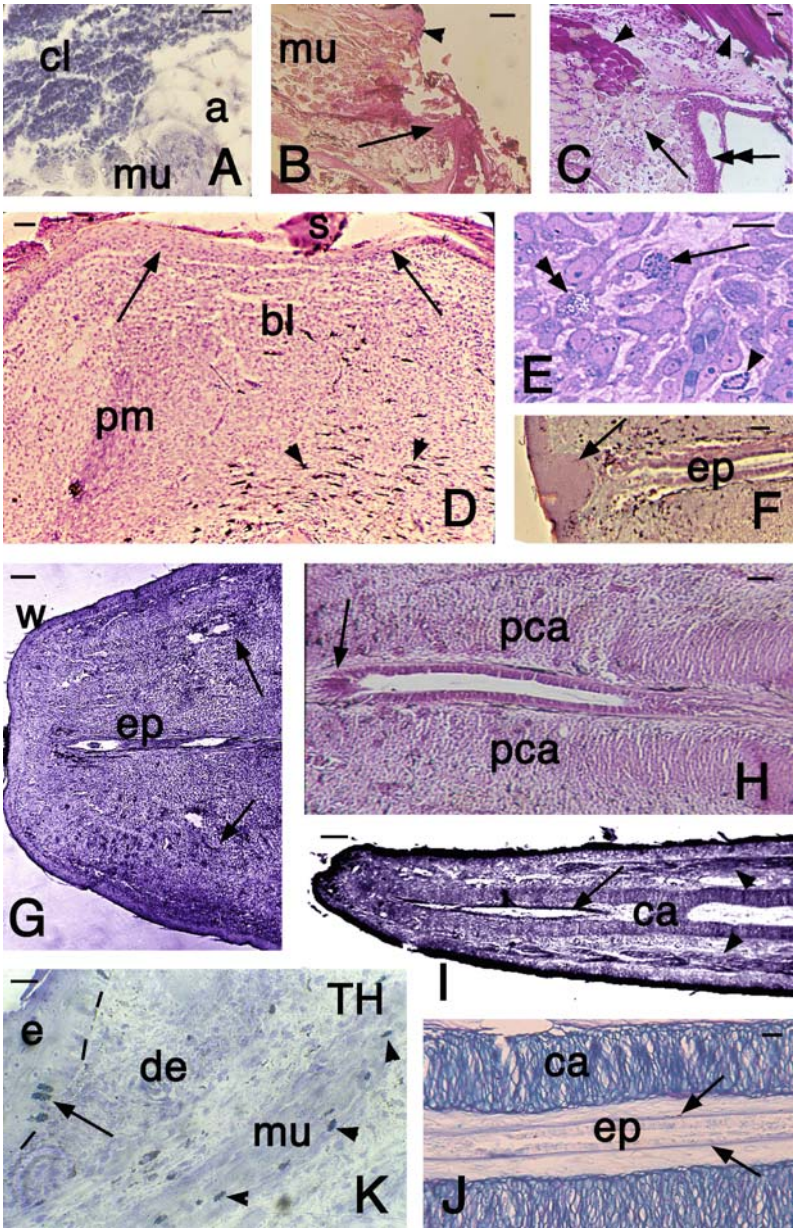

Fig. 1.4 Main histological features of tail wound healing and regeneration in *P. sicula* (**a–j**) and *Anolis carolinensis* (**k**). **a** Detail of the superficial clot covering the stump at 1 day after the amputation. Toluidine blue stain. *Bar* 20 μm. **b** Detail of sectioned and degenerating stump muscles (*arrowheads*) and vertebra (*arrow*), at 2 days after cutting. Periodic acid–Schiff stain (PAS) reaction. *Bar* 20 μm. **c** Detail of stump covered by the wound epithelium

process of tail regeneration can be subdivided into four stages: (1) wound healing (0–10 days of regeneration); (2) blastema-cone formation (10–15 days); (3) tail growth (15–25 days); (4) maturing and scaling tail (25–60 days).

1.5.1 Wound Healing and Blastema Formation

During the wound healing stage following lizard tail amputation, a weak or limited inflammatory response is elicited, a condition that in conjunction with other factors, such as tissue dedifferentiation and stem cell availability, results in a successful regeneration. Compared with autotomy, the amputation of the tail using a cutting blade results in some bleeding and the stump is covered by a blood clot in a few hours (Fig. 1.4a). The transected muscles show the degeneration of the terminal part of their fibers in the first week after amputation (Fig. 1.4), which, after debridement of the phagocytes, are repaired within 3–4 weeks after amputation. The myofibers lose their glycogen content, as evidenced from the disappearance of their periodic acid–Schiff stain positivity (Fig. 1.4b, c). In an autotomized tail, the new muscles that will be formed in the regenerating tail are independent (are not a continuation) of the old muscles of the stump (Brunetti 1948; Simpson 1970; Mufti and Iqbal 1975).

In some species, the amputation at an intervertebral level by a blade delays regeneration in comparison with amputation along autotomy planes (Jamison 1964). This was explained by the scarce number of connective cells (mesenchymal) present in amputated tails in contrast to the numerous connective cells

Fig. 1.4 (continued) at 5 days after injection. Whereas intact muscles fibers are PAS positive (*arrowheads*), most lesioned muscle fibers (*arrow*) have lost PAS reactivity (glycogen). The *double arrow* indicates the PAS-positive (glycogen) wound epithelium. *Bar* 10 μm. **d** Early blastema at 10 days after amputation showing the wound epithelium with still elongating (migrating) keratinocytes (*arrows*) and the mesenchymal blastema. A promuscle aggregate is present. *Arrowheads* on melanophores. Hematoxylin–eosin stain. *Bar* 30 μm. **e** Detail of mesenchymal cells of the blastema with granulocytes (*arrows*), macrophage (*double arrowhead*), and a basophil/mast cell (*arrowhead*). Toluidine blue stain. *Bar* 10 μm. **f** Detail of apical ependymal ampulla terminating near the apical peg (*arrow*) of the tail tip. Papanicolaou stain. *Bar* 20 μm. **g** Conic blastema with an axial ependymal tube and a thick wound epidermis. Toluidine blue stain. *Bar* 40 μm. **h** Detail of an ependymal ampulla (*arrow* on the apical front) surrounded by the precartilaginous aggregates. *Bar* 25 μm. **i** Apical region of an elongating tail featuring the ependyma (*arrow*) inside the cartilaginous tube, and the external muscles (*arrowheads*). *Bar* 100 μm. **j** Detail of the cartilaginous tube with ependyma (*arrows*) in the medial region of the regenerated tail. *Bar* 20 μm. **k** Detail of the lateral part of the regenerating tail with tritiated thymidine labeled cells in the epidermis (*arrow*; *dashes* outline the basal part of the epidermis) and muscles (*arrowhead*). *Bar* 10 μm. *a* adipose tissue, *bl* blastema, *ca* cartilaginous tube, *cl* clot, *de* dermis, *e* epidermis, *ep* ependymal tubule, *mu* muscles, *pca* procartilaginous aggregates, *pm* promuscle aggregates, *w* wound epidermis

present in the autotomy planes. These mesenchymal cells are believed by many authors to be the main sites of the origin of cells contributing to formation of the regenerative blastema (Quattrini 1954; see the résumé in Bellairs and Bryant 1985). Despite the location or extent of injury after tail amputation (by sectioning, ripping, or autotomy), regeneration initiates and eventually results in the reformation of a new tail in most lizards.

In *P. sicula*, *Podarcis muralis*, *Lacerta viridis*, and other species, cells of the autotomy plane, from the dermis (with the exception of the inner compact dermal layer) to the muscle myoseptum, participate in the formation of the blastema (Brunetti 1948; Quattrini 1954; Simpson 1965, 1970). No injured muscles contribute to the blastema cell population, but only from cells of the intermuscular septum. The periosteum of vertebrae and the adipose tissue also appear to give rise to blastema cells, so these tissues are roughly a direct continuation of the blastema where the new cartilage and fat will be reformed. Finally, the bone marrow at the injured sites of vertebrae or near the intravertebral split can give rise to low cycling cells (likely stem cells) that colonize the stump and may participate in the formation of the regenerative blastema.

After the initial, preblastema or wound healing phase, in which each of these tissues gives rise to dedifferentiated cells with the phenotypes of fibroblasts or mesenchymal cells, each cell type is believed to redifferentiate into the same tissue of origin. This has also been observed using autoradiography after tritiated thymidine injection (Simpson 1965; Cox 1969a), and was later confirmed by more detailed ultrastructural studies (Alibardi, unpublished observations, but see later). The specific contribution of each injured tissue to the formation of the blastema is, however, still undetermined, and it seems that each single tissue of the tail stump contributes to the formation of the mesenchymal-like cell population of the blastema (Alibardi and Sala 1988a, b).

During wound healing, vascularization is not very efficient and mesenchymal cells draw their energy from glycogen degradation through phosphorylase activation, the derived glucose is metabolized through glycolysis, and the oxidative metabolism through the Krebs cycle is lowered (Shah and Hiradhar 1974; Magon 1978). Blastema cells utilize glucose to produce other monosaccharides and uronic acids through the pentose phosphate shunt, and these metabolites are utilized to produce ribose, deoxyribose, and acid mucopolysaccharides of the extracellular matrix (Shah and Chakko 1972; Shah and Hiradhar 1975). The presence of lipids in blastema cells and the increase of some lipogenic enzymes such as α-glycerophosphate dehydrogenase, β-hydroxybutyrate dehydrogenase, and esterases indicate that lipids are also utilized to sustain the prevalent anaerobic metabolism of the blastema (Shah and Hiradhar 1975; Magon 1977; Kinariwala et al. 1978; Chakko and Mariamma 1981).

The presence of acid phosphatase activity increases in wounded tissues and remains high in the regenerating blastema and in more distal tissues of the regenerating tail in comparison with normal or more proximal tissues of the regenerating tail (Shah and Chakko 1966; Alibardi 1998). This suggests that

degradation of the intercellular matrix of the stump takes place, a process that together with the production of glycosaminoglycans such as hyaluronate favors cell migration (Alibardi and Sala 1983).

Keratinocytes proliferate from the living layers of the epidermis of proximally damaged scales, and migrate over the injured stump tissues, beneath the scab (Fig. 1.4c, d; Alibardi and Toni 2005; Alibardi 2009a). Normally, the stump is covered between 6 and 10 days after injury at temperatures above 25°C in many species of lizards, and a mesenchymal tissue accumulates underneath, forming the bulk of the future blastema (Fig. 1.4d, e). After migrating keratinocytes have covered the central part of the stump, the epidermis becomes stratified and thick, forming a wound epithelium. The latter, in the central region of the stump, often shows an apical peg contacting the terminal ependymal ampulla of the regenerating spinal cord (Fig. 1.4f, g).

The wound epithelium, especially at the apex of a regenerating tail, remains essential for the continuous growth of the tail, and its destruction leads to failure of tail regeneration (Bellairs and Bryant 1985; Alibardi, unpublished observations). When the scab has completely fallen off (10–12 days in *P. sicula*), a small mound covered by a shiny and pigmented skin covers the stump: the regenerating blastema (Fig. 1.1a, b, k). The latter elongates into a coniform blastema (Fig. 1.1e, g, h) in the following 2–5 days, and the rapid lengthening continues in the following 2 weeks until a smooth regenerating tail has formed (Fig. 1.1c, f). During this period the tail regenerates most of the connective and adipose tissues, numerous nerves, and blood vessels, but in particular axial organs that sustain and address most of its growth. Axial organs are represented by muscle myomeres with a simple but extensive organization, whereas the vertebral column is replaced by a cartilaginous tube enclosing a simple spinal cord mostly made of an ependymal tube (Figs. 1.1l–q, 1.4).

1.5.2 The Blastema Grows into a Cone

Whereas a mesenchymal cell population is present underneath the wound epidermis, the ependyma continues to growth in the central position of the blastema. Mesenchymal cells forming the regenerative blastema belong to four main concentric layers, corresponding to the location of the old skeleton, the submuscular fat, the muscles, and the dermis (Quattrini 1954). The cartilaginous tube derives from the vertebral periosteum, from the mesenchyme of the intervertebral splitting region, and from the subperiosteal space. The regenerated fat and muscles derive from the mesenchyme of the interadipose and intermuscular septa (autotomy planes). The new dermis derives from the dermis of the stump.

At about 100 μm from the wound epidermis, around the ependyma a mass of mesenchymal cells becomes more fusiform, forming the precartilaginous aggregation from which the cartilaginous tube will be formed (Fig. 1.4h–j).

Chondrocytes of the hyaline type rapidly differentiate and completely surround the regenerating spinal cord, forming a cartilaginous cylinder. The ependymal tube therefore remains isolated inside the cartilage and a few holes are sometimes formed along the mature cartilage, mainly containing blood vessels.

More externally, between the procartilaginous aggregates and the external dermis, also promuscular aggregates are formed (Fig. 1.4g, i). The latter derive from the aggregation of groups of myoblasts that give rise to myotubes organized in segmental myomeres (Fig. 1.1n). When the regenerating tail is viewed in cross section, it shows that the myomeres form a complete belt of muscles underneath the regenerating dermis. Their number can vary in different species, but there are generally 16 muscle bundles in *P. sicula*, *Tarentola mauritanica*, and *Gonatodes ocellatus* (Terni 1920; Quattrini 1952b; Furieri 1956). Details of muscle differentiation will be given later in the ultrastructural description (Section 2.2.3).

In the third stage (elongating cone to growing tail, 2–4 weeks after amputation in *P. sicula*), the connective tissue located between the forming muscle bundles and the cartilaginous tube contains a heterogeneous population of connective cells, pigment cells, nerves, and small adipose cells. The latter increase their amount of lipids in a few days, varying from species to species, and form the new adipose layer. This is clearly segmented at the beginning of tail growth, but the segmentation becomes less apparent after about 4 weeks of regeneration when these cells increase in size, forming an apparently continuous submuscular adipose mass (Alibardi 1995d; Fig. 1.1m).

The growth of the blastema into a cone and then rapidly into an elongating tail depends on the proliferation of different tissues, especially the axial tissues (cartilage, muscles, and spinal cord). Autoradiography studies (Simpson 1965; Cox 1969a) have indicated that the initial blastemal population shows little proliferative activity, whereas most proliferation occurs in promuscle aggregates, precartilaginous and cartilaginous cells, and the ependymal tube formed from the stump of the spinal cord. These axial tissues therefore are the main contributors of cells to the elongation of the new tail (Fig. 1.5). The detail of the blastema, beneath the apical wound epidermis, shows few labeled cells (Fig. 1.5, inset), a condition that differs from that of amphibians. In fact, the regenerative blastema of amphibians is a collection of proliferating embryonic cells that have originated through a dermal–epidermal interaction and that possess an intrinsic morphogenetic blueprint. Instead, the limited cell proliferation of apical mesenchymal cells suggests that the lizard blastema is not a true blastema like that of amphibians (Cox 1969a). The latter author considered the lizard blastema as an apical accumulation of mesenchymal cells located in front of proliferating regions for the growth of individual tissues such as the spinal cord, muscles, and cartilage.

As the vascularization of the growing cone improves, the metabolism of differentiating tissues changes in comparison with that of the blastema and the oxidative metabolism of glucose through the Krebs's cycle gradually returns to preamputation levels, and lipids become less important as an energy source (Shah and Hiradhar 1975; Magon 1977). In fact, lipids and their key metabolic enzymes

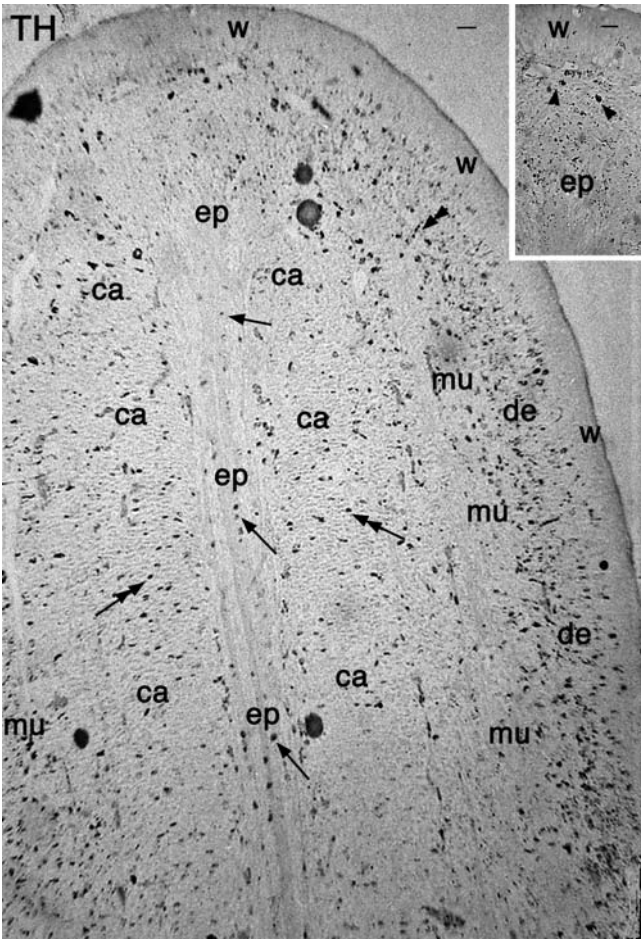

Fig. 1.5 Autoradiography (4 h after injection of tritiated thymidine) view of a regenerating cone in *A. carolinensis*. *Dark spots* are mainly labeled cells (aside from in the dermis, where melanophores can be confused with labeled cells at this low magnification). In particular, note labeled cells in the central ependyma (*arrows*), in the axial cartilage (*double arrowheads*), and in the lateral muscles (*double arrowhead*). *Bar* 20 μm. The *insert* (*bar* 10 μm) shows that a few labeled cells (*arrowheads*) are present in front of the ependymal ampulla and beneath the apical wound epidermis. *ca* cartilaginous tube, *de* dermis, *ep* ependymal tube, *mu* regenerating muscles, *TH* tritiated thymidine autoradiography, *w* wound epidermis

such as β-hydroxybutyrate, α-glycerophosphate dehydrogenase, and esterases decrease in this phase, whereas lipids are turned into deposits, especially in fat cells of the pericartilaginous connective tissue.

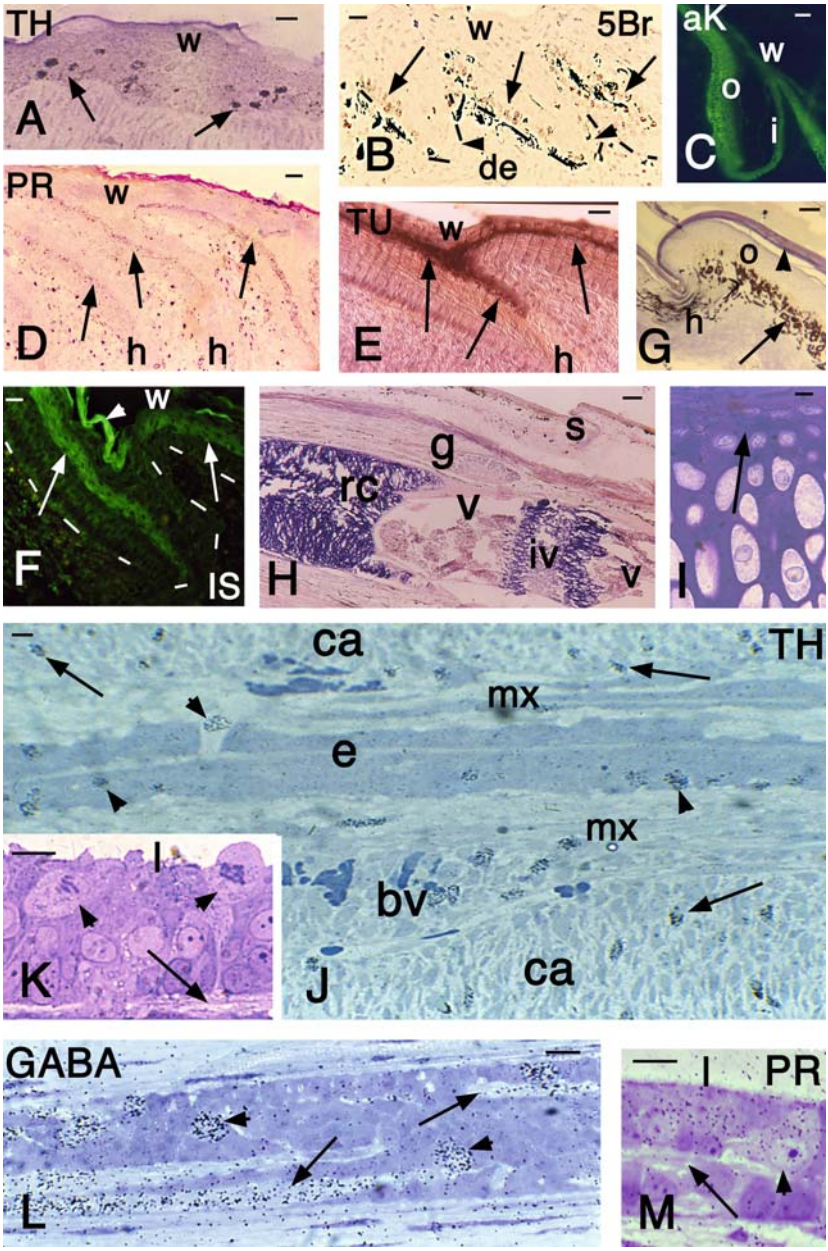

Fig. 1.6 Microscopic features of regenerating scales (**a–g**), cartilaginous tube (**h**, **i**), and spinal cord (**j–m**) in growing cones (18–25 days of regeneration). **a** Tritiated thymidine labeled cells (4 h after injection in *A. carolinensis*, *arrows*) in the basal and suprabasal layers of the waved wound epidermis. *Bar* 10 μm. **b** Asymmetric epidermal pegs with a row of

Also the apical wound epidermis shows relatively infrequent thymidine-labeled cells, which increase in number in the basal layer of the more lateral, wound epidermis (Alibardi 1994a; Figs. 1.5, 1.6a). Scale regeneration (or neogenesis; Liu and Maneely 1969a; Maderson et al. 1978) is initiated in more proximal regions of the wound epithelium, corresponding to the level where myomeres are forming (Alibardi 1994a, b, 1995c; Fig. 1.1m–o). The epidermis forms pegs, initially symmetric but that rapidly become asymmetric and penetrate deeply into the dermis forming variably long epithelial tongues (Fig. 1.6b–d). Labeling studies have shown that the initial symmetric epidermal peg later becomes asymmetric as most proliferating cells are localized in the rostral side of the elongating peg, under which numerous melanosomes are present (Fig. 1.6b). Keratinocytes produce mostly acidic keratins and they actively incorporate tritiated histidine and proline, the latter mainly in the forming β-keratin layer that is formed in the

Fig. 1.6 (continued) labeled cells (*arrows*) in the rostral (outer) side of the peg 3 h after injection of 5-bromodeoxyuridine in *Podarcis muralis*. The shorter caudal (inner) side (*arrowhead*) of the peg has few labeled cells. *Bar* 20 μm. **c** Immunofluorescent asymmetric peg for AE1 (acidic) keratin in *P. sicula*. *Bar* 20 μm. **d** Elongated pegs showing autoradiographic labeling along the forming, inner β-layer (*arrows*) 3 h after injection of tritiated proline in *L. delicata*. *Bar* 10 μm. **e** Terminal dUTP nick end labeling reaction to detect apoptosis in forming scale of *P. muralis*. The dark signal (*arrows*) stains nuclei and some cytoplasm remnants along the shedding line. *Bar* 10 μm. **f** In situ hybridization using a complementary DNA probe for β-keratin messenger RNA on a peg in *P. sicula*. The fluorescent signal is localized in cells of the forming β-layer (*arrows*). *Bar* 10 μm. **g** Regenerated (neogenic) scale after loss of the capping wound epidermis along the newly formed β-layer (*arrowhead*) in *A. carolinensis*. The *arrow* indicates the pigmented cells located underneath the epidermis of the outer scale surface. Toluidine blue stain. *Bar* 20 μm. **h** Proximal region of regenerated tail in *P. sicula* featuring the transition between the cartilaginous tube and the proximal vertebra. Toluidine blue stained chondrocytes. *Bar* 40 μm. **i** Detail of toluidine blue stained proximal chondrocytes and outer perichondrion (*arrow*) in *P. sicula*. *Bar* 10 μm. **j** Detail of a tritiated thymidine autoradiography (4 h after injection) section of regenerating ependyma with labeled cells (*arrowheads*) in *A. carolinensis*. *Arrows* indicate labeled chondrocytes in the surrounding cartilaginous tube. *Bar* 10 μm. **k** Detail of dividing cells (*arrowheads*) contacting the lumen of the ependyma in *P. muralis*. The *arrow* indicates the region occupied by descending axons. *Bar* 10 μm. **l** Autoradiographic detail of labeled cerebrospinal fluid contacting neurons (CSFCNs) (*arrowheads*) and axons (*arrows*) 3 h after injection of tritiated GABA in *Scincella lateralis*. *Bar* 10 μm. **m** Other autoradiographic detail of labeled CSFCNs (*arrowhead*) 3 h after the injection of tritiated proline in *L. delicata*. The *arrow* indicates the region of descending axons. *Bar* 10 μm. *aK* α-keratin immunolabeling, *bv* blood vessel, *ca* cartilaginous tube, *de* dermis, *5BrdU* 5-bromodeoxyuridine immunolabeling, *e* ependyma, *g* spinal ganglion, *GABA* tritiated GABA autoradiography, *h* hinge region between scales, *i* inner (ventral) scale surface (side) of the following scale, *IS* in situ hybridization, *iv* intervertebral cartilage (intercentrum), *l* ependymal lumen, *o* outer (dorsal) scale surface (side) of the previous scale, *PR* tritiated proline autoradiography, *rc* proximal regenerated cartilage, *s* scale; *TH* tritiated thymidine autoradiography, *TU* terminal dUTP nick end labeling reaction, *v* vertebra, *w* wound epidermis

middle of the peg (Alibardi 1994a, b, 2000, 2001; Alibardi et al. 2000; Fig. 1.6d). Among keratins produced in keratinocytes, some low molecular mass forms (40–44 kDa) of embryonic type are produced, and also keratin markers of mammalian epidermal regeneration such as keratins6, 16, and 17 (Alibardi et al. 2000; Alibardi and Toni 2005, 2006).

Both immunocytochemistry and in situ hybridization using β-keratin complementary DNA as well as complementary RNA probes have indicated that proline-rich β-keratins are formed along the medial area of regenerating scales (Alibardi and Toni 2006). These hard keratins restore the mechanical resistance of neogenic scales after their complete morphogenesis and maturation. Neogenic scales eventually derive from the split in the middle region of the initial epidermal pegs, where both acid phosphatase and terminal dUTP nick end labeling positive (apoptotic) cells are detected (Alibardi 1998; Alibardi and Toni 2006; Fig. 1.6e, g). Also, specialized scales, utilized for sensory or scansorial activity (adhesive pads), are regenerated in the tail of some geckos (Maderson 1971; Bauer 1998).

1.5.3 Tail Growth and Tissue Differentiation

As the new tail grows over 2 mm in length, the axial cartilaginous tube forms a homogeneous ring (as observed in cross sections of regenerating tails) that is made of fusiform chondroblasts with little intercellular matrix (Figs. 1.4i, j, 1.6h, i). Many thymidine-labeled cells are seen in the procartilage aggregations and in more proximal areas of the cartilaginous tube during the elongation phase. Labeled cells are located inside the inner cartilaginous ring (internal growth) and also in the ring of external chondrocytes (external growth). Cells in these proximal regions of the cartilaginous cylinder become hypertrophic in the central part of the cartilage but remain flat in the outer and inner surfaces of the cartilaginous tube. These regions assume the role of a perichondrium for the continuous diameter growth of the cartilage, especially after the new tail has reached its definitive length (Alibardi and Sala 1981; Alibardi 1995b). In the proximal region of the regenerating tail, the cartilaginous tube merges with the lamellar bone of the last vertebra of the stump (Fig. 1.6h).

Inside the cartilaginous tube the regenerating spinal cord is growing and many proliferating cells are present in the ependymal tube, which mainly consists of epithelial (ependymal) cells (Fig. 1.6j). Most mitoses are seen in cells contacting the central canal and, aside from ependymal cells, some neuronal and glial elements are also produced (Charvat and Kral 1969; Egar et al. 1970; Alibardi and Sala 1988a, b; Alibardi and Meyer-Rochow 1988; Fig. 1.6k). These regenerated neurons appear as larger and pale cells incorporating tritiated GABA or tritiated proline, and they are contacted by labeled axons or produce few axons (Fig. 1.6l, m). Further analysis has identified these scanty neurons generated among ependymal cells as cerebrospinal fluid contacting neurons as they contact the central canal

and the Reissner fibers with their numerous stereocilia (Alibardi 1992, 1993a, b; Alibardi 1993a, b, 1995a–e; Fig. 1.7a). The light microscope has shown that some 100–200 or more axons are present around or between ependymal cells, as indicated by Bodian staining (Fig. 1.7b). Some of these fibers contain cholinesterase early in regeneration, but it becomes rare in older regenerates (Shah and Chakko 1971). The finer resolution of the electron microscope reveals more detail and an increased number of amyelinic axons (over 1,000 per cross section) in the regenerated spinal cord (see Sect. 2.2.5; Simpson 1968, 1970; Simpson and Duffy 1994).

Other cell types present in variable number within the regenerating spinal cord correspond to macrophages, especially seen inside the central canal during early stages of regeneration (Fig. 1.7c). Cell death among cells of the ependyma and also likely apoptotic cells (pycnotic, Fig. 1.7d) is also present in conjunction with the limited neurogenesis within the apical and more proximal ependyma during 2–3 weeks of tail regeneration (Alibardi 1986). This degeneration may explain the decreases of the number of these neurons in the mature, regenerated spinal cord (Marotta 1946; Zannone 1953; Alibardi 1990–1991). Retrograde labeling using horseradish peroxidase or fluorescent tracers injected into the spinal cord of the stump allows staining of the few axons and the nerve cells of the regenerating spinal cord. The tract-tracing technique has indicated that these cells make connections with other regions of the stump spinal cord (Duffy et al. 1990, 1992; Fig. 1.7e, but see the later description on the ultrastructure of the regenerating spinal cord). Immunolabeling of axons with the anti-NF 200 antibody (heavy neurofilament protein) further confirms that these axons surround the growing ependymal tube and contact the few local neurons (Fig. 1.7f, g).

Numerous motor, sensory, and autonomous nerves grow inside the regenerating tail (Terni 1920, 1922; Cox 1969b; Figs. 1.1q, 1.7h–j). Most of the nerves initially regenerate from the transected nerve roots of the spinal cord and grow distally into the blastema following the elongation of the new tail. The large regenerating nerves mainly enter the pericartilaginous connective tissue that will later become the pericartilaginous adipose tissue of the regenerated tail. Also Schwann cells, apparently mixed with other mesenchymal cells of the blastema, surround the growing nerves and enwrap their axons, beginning a process of myelination (Terni 1920; Hughes and New 1959; Charvat and Kral 1969; Cox 1969a, b; Alibardi 1990–1991; Alibardi 1995a–e). Most peripheral nerves become myelinated with the progression of regeneration (more than 1–2 months from the amputation).

In cross section of the proximal regions of the regenerating tail, the regenerating nerves appear as nine to 12 bundles in the right quadrant and nine to 12 bundles in the left quadrant of the tail (in the lizard *G. ocellatus*; Terni 1920). The number of regenerated nerves is reduced to four symmetric pairs (left and right) in more apical regions of the regenerated tail. This reduction is seen after the nerves surrounded by Schwann cells have innervated the large, proximal regenerated muscles and have formed neuromuscular junctions (Hughes and New 1959)

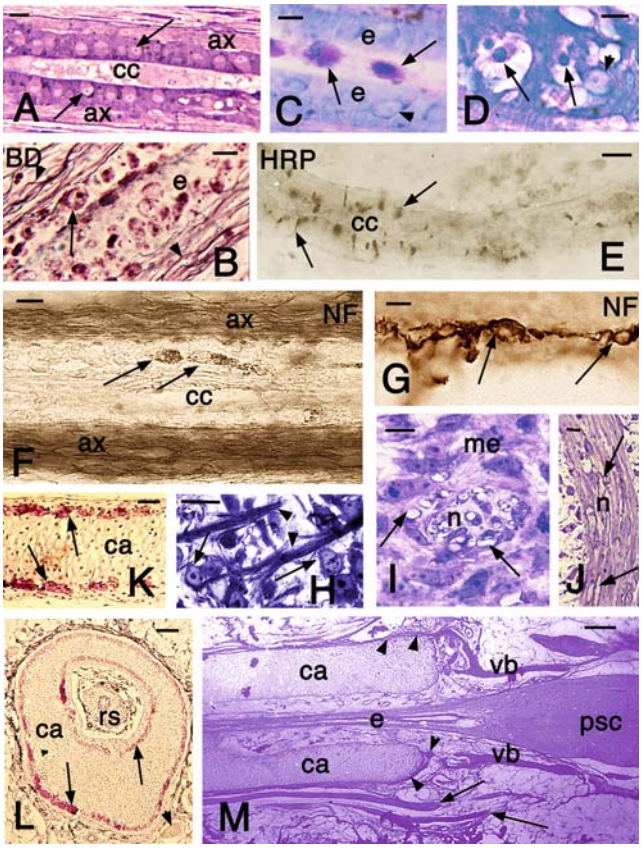

Fig. 1.7 Microscopic features of regenerated spinal cord (**a–g**), peripheral nerves (**h–j**), and cartilage (**l**, **m**) in elongated regenerated tail (3–7 weeks of regeneration). **a** Numerous CSFCNs (*arrows*) are present in the regenerated spinal cord of a GABA-treated lizard (*P. sicula*). Toluidine blue stain. *Bar* 15 μm. **b** Bodian stain of neurons (*arrow*) and axons (*arrowheads*) in the regenerating cord of *P. muralis*. *Bar* 10 μm. **c** Detail of macrophages (*arrows*) inside the ependymal lumen in *T. mauritanica*. Paraldehyde fuchsin stain. *Bar* 10 μm. **d** Detail of pycnotic cells (*arrows*) among ependyma where also a neuron is present (*arrowhead*) in *P. muralis* at 3 weeks of tail regeneration. *Bar* 10 μm. **e** Horseradish peroxidase retrograde labeled CSFCNs (*arrows*) in ependymal tube of *A. carolinensis*. *Bar* 20 μm. **f** Immunostaining for neurofilament 200 kDa (NF) showing immunoreactive axons and few neuronal cells (*arrows*) in *L. delicata*. *Bar* 15 μm. **g** Detail of NF-immunolabeled neurons (*arrow*) among ependymal cells in *L. delicata*. *Bar* 10 μm. **h** Regenerating nerves (*arrowheads*) among blastema cells (*arrows*) of *P. sicula*. Toluidine blue stain. *Bar* 15 μm. **i** Cross-sectioned nerve bundle within the blastema with amyelinic axons (*arrows*) in *T. mauritanica*. Toluidine blue stain. *Bar* 15 μm. **j** Longitudinal section of the proximal part of a myelinic nerve (*arrows*) in *P. sicula*. Toluidine blue stain. *Bar* 10 μm. **k** Detail of a proximal cartilaginous tube of *P. sicula* at about 2 months of regeneration featuring the external regions of calcification (*arrows*). Hematoxylin stain. *Bar* 25 μm. **l** Cross-sectioned

or sensory terminations (muscle spindles; Liu and Maneely 1969b). Because neither motor neurons nor ganglia are reformed in the new tail, the entire sensory and motor innervation of the regenerating tail derives from the proximal segment of the spinal cord and from the last three spinal ganglia (Terni 1920; Fig. 1.1q). Both motor and sensory neurons become hypertrophic because their field of innervation is increased to the previous area of competence and the regenerated tissues (Zannone 1953; Pannese 1963; Duffy et al. 1990, 1992; Geuna et al. 1992).

Aside from the motor and sensory axons, also the two large autonomous nerves (sympatic) grow into the regenerating tail in the form of two amyelinic bundles, each located lateral to the regenerated ventral artery present ventrally to the cartilaginous tube (Terni 1922). These nerves are amyelinic and reach the most apical regions of the regenerating tail. The main blood vessels, the caudal artery and two veins, regenerate as a continuation of the preexisting vessels, although no valves appear to be reformed in the new veins (Quattrini 1954).

1.5.4 Tail Scalation and Maturation

In the fourth, maturing stage of tail regeneration, the regenerated tissues continue their differentiation (Hughes and New, 1959; Simpson, 1965; Shah and Chakko 1966; Cox, 1969a; Mufty and Iqbal, 1975; Alibardi and Sala, 1983) in the more distal regions of the new tail, within 1–2 mm from the tip. A small amount of tissue continues to be formed by the small apex at the tip of the regenerated tail where a tiny mass of mesenchymal cells is still seen beneath the wound epidermis.

At this stage (after 5 weeks of tail regeneration in *P. sicula*), most of the new tail appears covered with well-cornified scales, although their dimension is smaller than that of those of the original tail. Regenerated scales form a simpler pattern of scalation with respect to that present in the normal tail (Woodland 1920: Quattrini 1952a, 1953a, b, 1954). Often at this stage most regenerated scales have undergone one shedding cycle, the cyclical epidermal regeneration with the production of a molt, and most of their histological features are exactly the same as in normal scales.

The full maturation of muscles and their innervation is completed but the diameter of the regenerated myofibrocells remains definitely smaller and more

Fig. 1.7 (continued) cartilaginous tube as in **k** with outer and inner calcifying rings (*arrows*). The *arrowhead* indicates a ventral nerve bundle. *Bar* 40 μm. **m** Transitional region between normal spinal cord (*right*) and the regenerated cord (ependymal tube) in an old regenerated tail. The vertebral bone is a continuation of the periosteum (*arrowheads*) surrounding the cartilage. The *arrows* indicate peripheral nerves. *Bar* 50 μm. *ax* axons, *ca* cartilaginous tube, *cc* central canal of the spinal cord, *e* ependymal cells, *me* mesenchymal cells, *mx* meninx, *n* nerve bundles, *psc* proximal spinal cord of the stump, *rs* regenerated spinal cord, *vb* vertebral body

uniform than that of the original myofibers. At 2 months after amputation, numerous nuclei still remain in the central position within the myofiber and do not move to the periphery along the sarcolemma as in normal myofibers. It is not known whether different physiological forms of muscle myofibres are regenerated, although most of them are probably of the fast contraction type rich in glycogen (Radhakrishnan and Shah 1973).

Among late changes of inner regenerated tissues in various species of lizards, the calcification of the peripheral regions of the cartilaginous tube occurs after 2 months of tail regeneration (Calori 1858; Quattrini 1954; Alibardi and Sala 1981; Alibardi and Meyer-Rochow 1989; Fig. 1.7k, l). The cartilaginous tube remains, however, nonsegmented and stiff in most species. It is likely that the perichondrion becomes osteogenic sometimes after calcification (later than 2 months after amputation), and therefore a true periosteum as a continuation of the periosteum of the proximal vertebra of the stump is formed (Fig. 1.7m). The proximal part of the cartilaginous tube (1–3 mm or more in length) forms a thin ring of bone which is a continuation of that of the body of the proximal vertebra in the tail stump.

The regenerated spinal cord after 2 months from amputation consists of an ependymal epithelium made of thin ependymal cells, often differentiated into typical tanycytes, with a tapering basal region terminating at the external basement membrane (Simpson 1968). Few and hypotrophic cerebrospinal fluid contacting neurons are seen, less than 3% of the entire cell population of the regenerated cord. During these late stages, also an intense myelination of peripheral nerves and of the axons in the regenerated spinal cord as a continuation of the spinal cord of the stump takes place (Fig. 1.7j, m). The central myelination of some larger axons within the regenerated spinal cord occurs by the differentiation of oligodendrocytes from ependymal tanycytes or/and by the penetration of Schwann cells into the regenerated spinal cord (Alibardi 1990–1991; Alibardi and Meyer-Rochow 1990).

In conclusion, the fully regenerated tail resembles the original tail in gross aspect, but the axial skeleton, spinal cord, and musculature (axial organs) are greatly simplified in comparison with the same tissues of the original tail.

1.6 Histological Aspects of Limb Regeneration and Cicatrization

Some phenomena of limb regeneration in lizards have been reported for lacertids (*Lacerta* sp., *Podarcis* sp., Marcucci 1925, 1930a, b; Guyenot and Matthey 1928), iguanids (*Liolaemus* sp., Hellmich 1951; and *Sceloporus* sp., Mather 1978), and under experimental manipulation (*A. carolinensis*, Singer 1961). Other cases were reported for scincids (skinks) under experimental manipulation (*Ablepharus deserti*, Kudokotsev 1960; and *Lygosoma laterale*, Simpson 1961), and in xantusids under experimental stimulation after autoimplantation of ependyma (*Xantusia vigilis*, Bryant and Wozny 1974).

Much less is known and has been documented about the progressive histological stages of the unsuccessful or limited limb regeneration in lizards (Marcucci 1925, 1930a, b; Kudokotsev 1960; Bellairs and Bryant 1985). Although numerous connective tissues, muscle tissues, and nerves are regenerated, the limb remains small and never forms autopodial elements such as fingers or toes. In the limb, the extensive tissue damage and the slow removal of the axial bones (humerus or femur) results in the infiltration of white cells and the inflammatory reaction is therefore enhanced, leading to scarring. Also the wound epidermis is rapidly turned into a typical differentiating epidermis (Alibardi and Toni 2005). However, when the hindlimb is amputated half way along the femur and also the tail is amputated in *P. sicula* or *P. muralis*, a variably long (2–5-mm) stump is formed in numerous cases within 1 month, even in 60% of cases in some experiments (Alibardi, unpublished observations). During this period the tail has broadly regenerated over 2 cm in length. In other species of lizards, the power of limb regeneration may be less, as is also the case for the variability previously reported for tail regeneration among different lizard families (see Sects. 1.2, 1.3).

The amputation of a limb leads to some bleeding, which stops after about 5–10 min, leaving a clot on the stump surface (Fig. 1.2a). The clot evolves into a scab in 1–2 days, but a protruding bone is generally present unless the bone is trimmed with scissors. The scab remains present in the following 1–2 weeks after amputation. In amputated *P. sicula* and *P. muralis* kept at 27–30°C, the amputation of the hindlimb at proximal levels produces a large stump where the skin flaps remain confined to the lateral borders of the stump. Therefore, in this case little tissue shrinkage takes place on the surface of the stump, like in the tail stump. Under these conditions, 60–70% of outgrowth formation (2–4 mm long) is obtained within 35–40 days after amputation in *P. sicula* or *P. muralis* (Alibardi, personal observations; Fig. 1.2b–d). Initially, from 2–3 weeks after amputation, the limb stump resembles the blastema of the tail and it has domelike shape (mound), is soft, and is covered by smooth epidermis. However, most of these outgrowths in the following week become paler, indicating that the vascularization is decreasing and a scarring process is taking place beneath the wound epithelium. The growth of the initial outgrowths is consequently blocked and they rapidly form intensely cornified scales.

In a few cases (5–10% in *P. sicula* or *P. muralis*), the outgrowths can elongate to produce filiform (tail-like) regenerates, linear or articulated over 5 mm in length, that also rapidly become scaled at 40–50 days after amputation (Fig. 1.2e). Despite the length of the outgrowth, the formation of an autopodium with digits is never observed in amputated lizard limbs. Some regeneration can also take place from these tail-like outgrowths, but no autopodium is, however, reformed (Marcucci 1925, 1930a, b).

The histological examination of some cases of regenerating limb outgrowth shows that 1–2 days after limb amputation the surface of the stump is reduced by the contraction of the sectioned tissues and is covered with a blood clot (Barber 1944; Kudokotsev 1960). Injured muscles and the bone (humerus or femur) appear to be degenerating and infiltrated with numerous leukocytes (Fig. 1.8a, b).

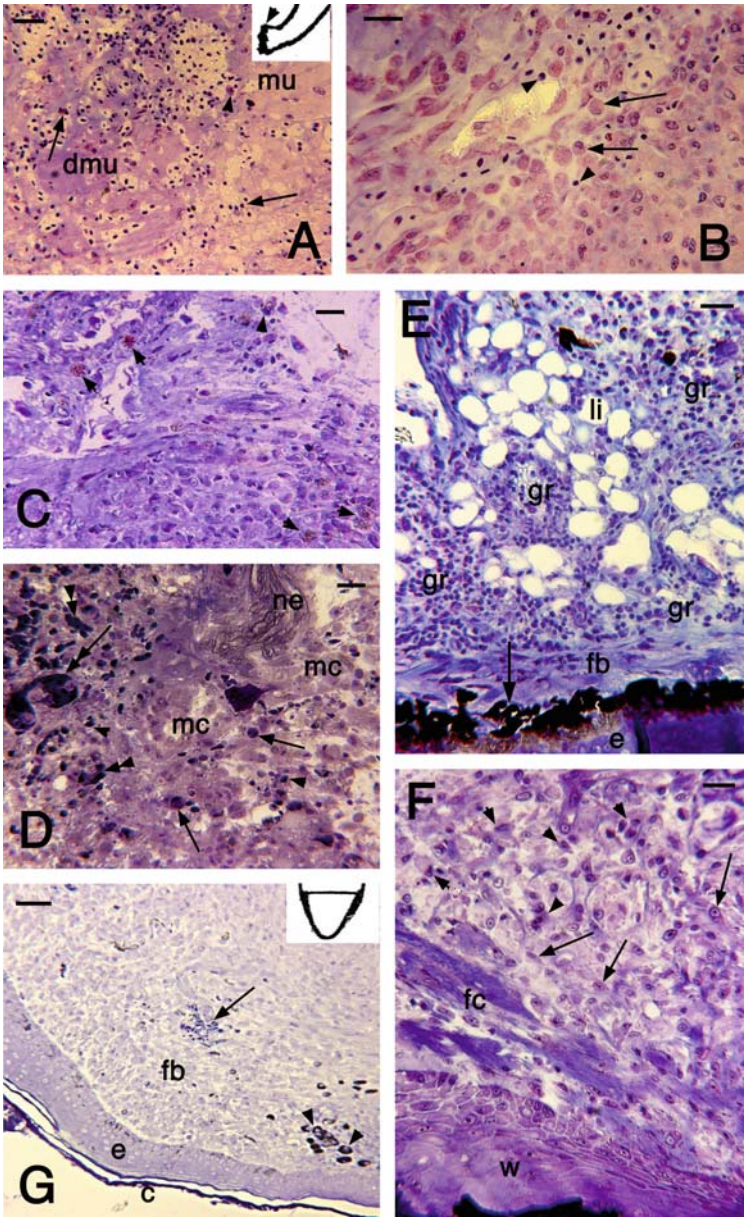

Fig. 1.8 Microscopic features of the early tissue reaction in the limb stump in *P. sicula* (toluidine blue stain). **a** Detail of injured connective and muscle tissues at 2–3 days after amputation (location indicated by the *arrowhead* in the *inset*). Numerous leukocytes (*arrows*) are seen among injured tissues, including larger eosinophil phagocytes, probably macrophages (*arrowhead*). *Bar* 25 μm. **b** Detail of the leukocyte population (*arrowheads*)

Muscle degeneration extends in the following few days to proximal regions of the limb stump. This strong inflammatory cellular response persists for over 10–14 days after amputation at 27–30°C in *P. sicula*, or for over 20–30 days after amputation when the femur or the humerus is protruding from the stump surface, impeding the complete reepithelialization of the stump (Kudokotsev 1960; Alibardi 2009a). Among leukocytes present in the stump tissues, most are represented by heterophil granulocytes in the first 10 days after lesion, whereas macrophages become more abundant later (Fig. 1.8c, d). Granulocytes often form granulomes surrounded by fibroblasts or macrophages (see the later ultrastructural description), and some degenerative spaces containing cell debris or exudates are formed giving rise to cavities underneath the scab.

Epidermal cells from the living epidermis of proximal scales of the stump migrate toward the center of the stump, but the complete reepithelialization depends on the extent of tissue damage, and in particular on the presence of a protruding femur or humerus on the stump surface. The reepithelialization takes 12–18 days in the case of bone protrusion (Alibardi 2009a) or even longer (Kudokotsev 1960). Osteoclasts erode the protruding bone that is eventually excised from the stump surface. Beneath the wound epithelium in those stumps where the bone does not protrude, mesenchymal cells (irregularly shaped cells) or fibroblasts (more-fusiform-shaped cells) accumulate after 7–10 days after amputation and at 15–16 days a blastema-like mound is formed (Fig. 1.8e, f). In typical 1–2-mm-long mounds, the cell population is made of loose fibroblasts and irregular mesenchymal cells, among which numerous blood vessels are seen (Fig. 1.8g). Most mesenchymal cells, however, disappear at 18–20 days after amputation, and are replaced by typical fibroblasts (elongated and flat cells) surrounded by a dense extracellular matrix, and from leukocytes and macrophages.

Fig. 1.8 (continued) among injured tissues 4 days after amputation, which includes larger macrophages (*arrowhead*). *Bar* 20 μm. **c** Detail at 6 days after injury. *Arrowheads* indicate phagocytes with numerous lysosomes (metachromatically stained in red). *Bar* 30 μm. **d** Area beneath the scab at 7 days after amputation. Clusters of leukocytes (mononucleates, *double arrowheads*) and single leukocytes (*arrowheads*) are seen near dilated capillaries (*double arrow*). Larger granulocytes are also present (*arrows*) among mesenchymal cells. *Bar* 20 μm. **e** Detail of the lateral area near the stump epidermis (the *arrow* points to the pigmented layer of the dermis) at 12 days after amputation. Numerous dark leukocytes are still present among the granulation tissue. *Bar* 30 μm. **f** Detail of the healing tissue beneath the wound epidermis at 16 days after injury. Numerous fibroblasts (*arrows*) are present with sparse phagocytes/macrophages (*arrowheads*). Beneath the wound epidermis fibrocytes are depositing blue-stained collagen bundles. *Bar* 20 μm. **g** Aspect of the fibroblast population beneath the wound epidermis of a regenerating mound (indicated in the *inset*) at 18 days after amputation (similar to Fig. 1.2b). The *arrow* indicates a large capillary. *Arrowheads* show melanophores. *Bar* 40 μm. *dmu* degenerating muscles, *fb* fibroblasts, *gr* granulation tissue, *li* lipocytes; *mc* mesenchymal cells; *mu* muscles; *ne* nerve; *w* wound epidermis

In the skink *A. deserti*, an epidermal cup has been reported to be initially formed in the center of the wound epidermis (Kudokotsev 1960). However, in both *A. carolinensis* and *P. sicula* or *P. muralis*, the wound epidermis becomes thicker but no AEC is, however, formed (Barber 1944; Alibardi 2009a). In these lizards, beneath the wound epidermis some mesenchymal-like cells accumulate during the first 15–20 days after the amputation, forming a blastema-like outgrowth.

Scale regeneration (neogenesis) occurs as in the tail, by the initial formation of epidermal pegs (see the previous descriptions for the tail; Fig. 1.2i).

Some myotubes and later muscle bundles are formed in the proximal regions of the elongating limb mound, from 10 to 20 days after amputation. At 20–30 days after amputation, new muscle bundles are formed in limb outgrowths, as a continuation of or completely separated from the bundles of muscles present in the stump (Fig. 1.2h, i). In small outgrowths no muscles and bone are regenerated, but only connective tissue, blood vessels, and probably nerves are present (Fig. 1.2f, i). The bone remains underneath the keratinized epidermis, and is repaired by a callus of cartilaginous and fibrous tissue at 35–40 days after amputation. Although mesenchymal cells persist in the tail, the small number of mesenchymal cells initially accumulated over the limb stump do not persist and the cells are transformed into fibroblasts (Barber 1944; Alibardi 2009a). Whereas in the tail apical mesenchymal cells stimulate the AEC to proliferate and the AEC probably maintains the distal mesenchymal population (like in the amphibian blastema, see Han et al. 2005), this does not occur in the limb of lizards. The analysis of the ultrastructural details of the apex of the mounds helps us to better understand the failure of distal growth in the limb (see later).

The study of 1–2-cm-long regenerated limbs resembling tails shows that in the proximal region of the limb a regular scaling pattern is formed, but the scales become more irregularly arranged in the distal, thinner part of the limb (Marcucci 1925, 1930a). The proximal stump of the femur is repaired by a cartilaginous and fibrous callus, and extends as a cartilaginous rod for most of the length of the regenerated limb (Fig. 1.2n–r).

From numerous observations (Marcucci 1915a, b, 1930a, b; Alibardi, unpublished studies) it appears that the increase of the stump surface and the reduction of the contraction of the skin over the stump surface stimulate limb regeneration. In fact, when the old skin is folded over the stump of the limb and also of the tail, regeneration is inhibited. In the most remarkable cases of limb regeneration described so far (Marcucci 1925, 1930a, b; Guyenot and Matthey 1928), a noteworthy formation of muscles and even long bones was observed. Numerous nerves and blood vessels were also present in the proximal part of the limb. Nine muscle fascicles were present in some of the tail-shaped limbs in *Lacerta* (presently *Podarcis*) *muralis*, and they were wrapped by the epimysium to form four groups of limb muscles. In some cases, aside from the dense connective tissue, also a large mass of fat tissue was regenerated inside these tail-like outgrowths. The muscle bundles extended distally and were inserted into various segments of the regenerated bones (Marcucci 1930a;

Fig. 1.2n–q). The larger, proximal part of the limb bones corresponded to the femur and was interconnected with the two intermediate bones, indicated as regenerated tibia and fibula. The small distal bones corresponded to the tarsus, metatarsus, and possibly the phalanges of one digit (the second according to Marcucci 1925; Fig. 1.2q, r).

The contraction of muscles of these long regenerated limbs, which might have represented the flexor muscles of the limb, could lead to some limited movement of the tail-shaped regenerated limb. Muscles and the other tissues within the regenerated limb appeared vascularized by two arteries and one large vein, which derived from the femoral artery. Two to three large nerves also extended down into the exceptionally long, tail-like limbs that further showed the potential regenerative capability of the limb in lizards. The number of axons innervating the forelimb in lizards is about half that in the limb of the newt and it is believed that nerves have little neurotrophic influence on limb regeneration (Zika and Singer 1965). Other studies have indicated that only the regenerating ependyma, when implanted in the limb stump, can actually stimulate limb regeneration, whereas nerves alone with no ependyma appear to have little influence on the process (Bryant and Wozny 1974; Cox 1969b). This is also the case for the tail, where it is the lack of ependyma, not nerves, that influences tail regeneration (Cox 1969b). In conclusion, it appears that the lack of an AEC, the lack of a critical mass of blastema cells, and the lack of autotomy planes are the main limiting factors for limb regeneration in lizards.

1.7 Single Tissue Regeneration in the Lizard Tail

The previously reported studies on the tail and limb have indicated that in lizards tissues can regenerate by an autonomous or by an epimorphic modality. The first modality refers to the possibility of an independent regeneration of each lesioned tissue, muscular, nervous, dermis, and is treated here in some detail. The second modality, epimorphosis, indicates a morphogenetic process that starts from an apical, undifferentiated mass of mesenchymal cells, which reorganize new tissues that grow to reform a new organ (limb or tail). The two processes appear to operate during tail regeneration, when an apical mesenchyme interacts with the apical wound epidermis (AEC).

Previous studies have indicated a high degree of tissue regeneration in lizards (Werber 1905; Marcucci 1930a, b, 1932; Brunetti 1948; Pritchard and Ruzicka 1950; Quattrini, 1953a, b, 1954; Furieri 1957; Mufty and Mahmood 1970; Maderson and Roth 1972; Maderson et al. 1978). The analysis of the pattern of cell proliferation in the lizard blastema (Simpson 1965; Cox 1969a) and the heterogeneous ultrastructure of blastema cells (Alibardi and Sala 1988a, b, 1989; Alibardi 1994b, 1999) have suggested that the lizard blastema is a collection of mesenchymal cells of different origin. These cells contact a wound epithelium with a discontinuous

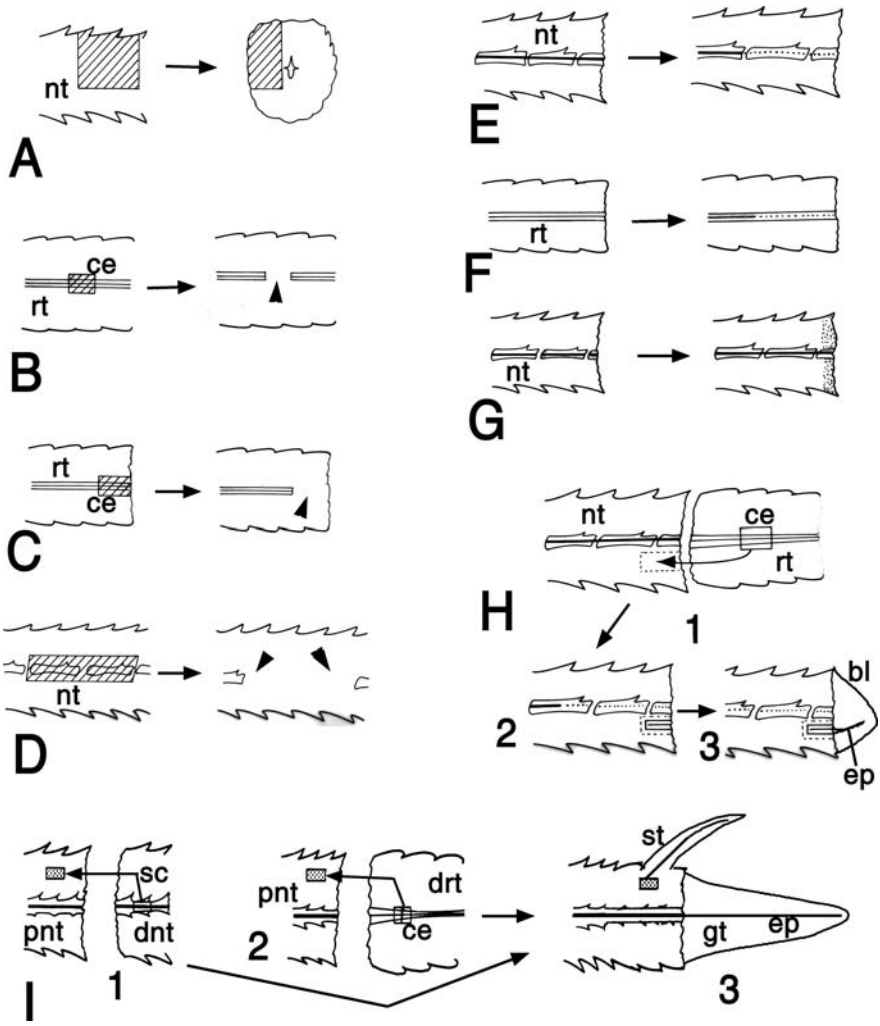

Fig. 1.9 Experimental intervention to test single tissue regeneration (see the text). **a** The area removed (*shadowed*) in longitudinal (*left*) and cross (*right*) view. **b** The removal of the cartilage-ependyma in the intermediate region of a regenerated tail (the *arrowhead* indicates the gap). **c** The removal of the cartilage-ependyma on the stump surface of a tail (the *arrowhead* indicates the gap). **d** The removal of two vertebrae in a normal tail to produce a gap (*arrowheads* indicate the gap). **e** The cauterization of the spinal cord (*dots*) inside the last two to three vertebrae of the stump. **f** The cauterization of the ependymal tube (*dots*) inside the regenerated cartilage of the stump. **g** The cauterization of stump tissues, aside from the spinal cord. **h** The result of the autoimplantation of the cartilage-ependyma into the stump (*arrowed square* in *1*), the following cauterization of the normal spinal cord (*dots* in *2*), and the following regeneration of the ependymal tube (in *3*). **i** The formation of supernumerary tails (*3*) after autoimplantation (*square*) of the distal spinal cord of the tail

basement membrane through which an exchange of trophic material (among which is fibroblast growth factor 2, see later) that maintains an apical growing site may take place. Most cells in the blastema redifferentiate into the same type from which they were derived, so the meninx, ependyma, cartilage, adipose connective tissues, nerves, and muscle tissues grow by the apical addition of cells of the same type, like in the root apex of a plant. In lizard blastema, cell transdifferentiation is probably either absent or limited (e.g., mesenchymal cells of the intermuscular septa give rise to new myoblasts). The reorganization and patterning of blastema cells into a new organ, typical for the amphibian blastema, is absent in the blastema of the lizard limb. This is also the case for the blastema of the tail, which has a more limited organogenesis capability than the bud blastema of the embryonic tail (Woodland 1920; Bellairs and Bryant 1985; see Sect. 1.4).

Several experiments, summarized in Fig. 1.9, have further indicated that the lizard tail has an intrinsic regenerative capability in single tissues, such as muscles, cartilage, bone, and the spinal cord (Alibardi et al. 1988; Alibardi, unpublished observations). It is probably this individual tissue regeneration that, together with the formation of an apical blastema-like growing front, allows the regeneration of long tails.

To test the autonomous muscle regeneration, the normal tail of some geckos (*T. mauritanica*) and wall lizards (*P. muralis*) underwent a massive removal of tissue, mainly represented by muscles (5–8 mm × 3–5 mm; Fig. 1.9a). Between 2 and 7 days after the operation, about half of the animals also lost the tail distal to the lesion, and the remaining stump with the tissue gap became covered by a clot, and later by a scab. In the remaining half of the experimental lizards, the distal part of the tail instead remained, and the gap was also covered by a clot and then by a scab. After 25–30 days after removal at 27–32°C, the scab eventually dropped of, leaving underneath new skin covering a bulk of muscle tissue mixed with connective and adipose tissue (Fig. 1.10a). Muscles fibers of different diameter were present in the area removed, occupying most of the regenerated volume in some cases (Fig. 1.10b). However, in other cases dense connective tissue and adipose cells were prevalent over regenerated muscle fibers. Interestingly, regenerated muscles formed myotomes like in the regenerating tail (Fig. 1.10c, d). Two months after amputation, the regenerated fibers were still thinner than the fibers of the original tail and they were organized in circular bundles, like in a regenerated tail (Fig. 1.10a, b, e).

Fig. 1.9 (continued) into the dorsal part of the tail stump (*1*), or of the cartilage-ependyma from the regenerated tail (*3*). *bl* regenerative blastema, *ce* cartilage-ependyma, *dnt* distal normal tail (is lost), *drt* distal regenerated tail (is lost), *et* ependymal tube, *gt* growing (regenerating) tail, *nt* normal tail, *pnt* proximal normal tail (remains as stump), *rt* regenerated tail, *sc* spinal cord, *st* supernumerary tail

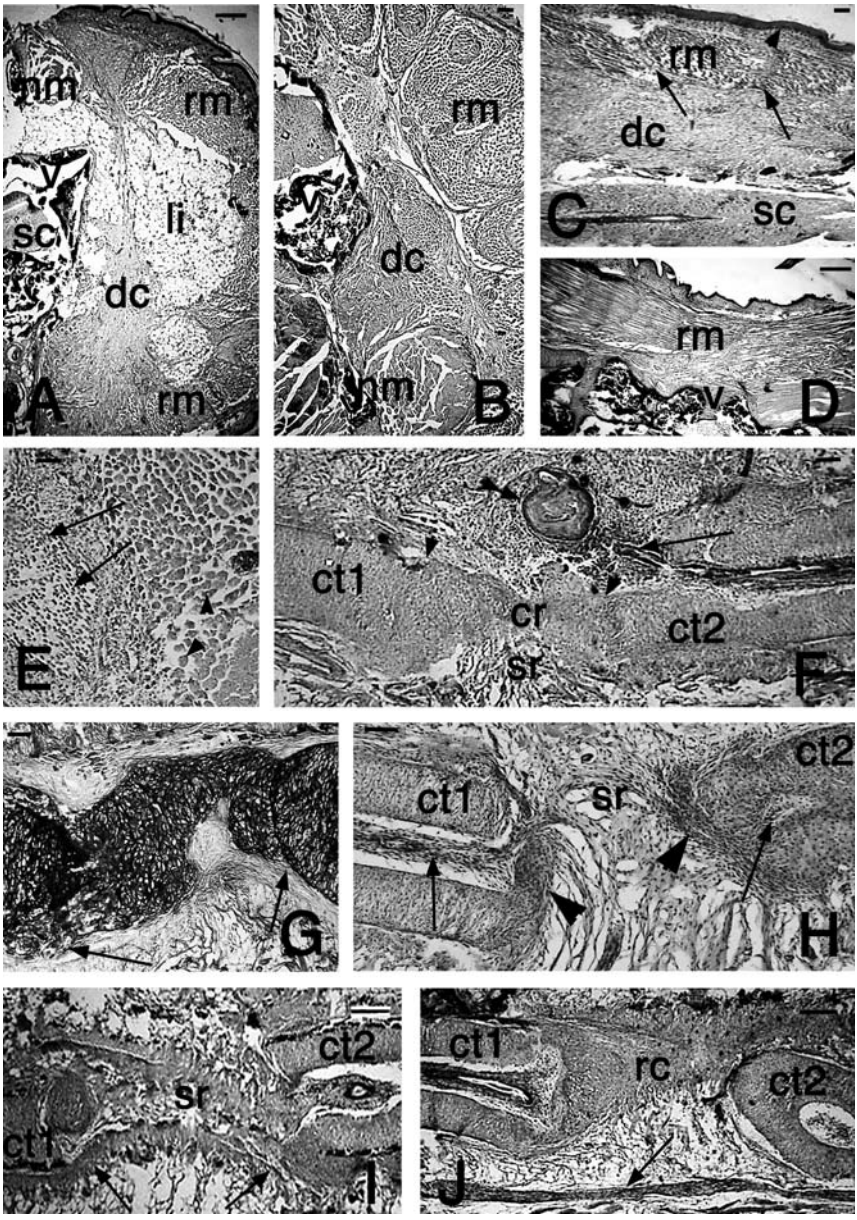

Fig. 1.10 Regeneration of muscles (**a–e**) (see Fig. 1.9a) and cartilage (**f–j**) (see Fig. 1.9b) in *P. muralis* (hematoxylin–eosin stain in all cases, except in **g**, for which toluidine blue stain was used). **a** Cross section 35 days after the lesion showing large bundles of regenerated muscles around the adipose and inner dense connective tissues. *Bar* 200 μm. **b** Detail of the regenerated muscles, the fiber diameter of which is still much less than that of some muscle

Another experiment on geckos (*T. mauritanica*) and wall lizard (*P. sicula*), designed to detect the autonomous capability of cartilage regeneration, is shown schematically in Fig. 1.9b. An intermediate segment of 2–3 mm of cartilage containing the regenerated ependymal tube was removed from the central axis of a regenerated tail. In about half of the cases studied, the gap between the proximal and the distal cartilaginous segments was filled with a compact rod of cartilaginous tissue in 30–40 days (Fig. 1.10f, g). Often, the regenerated cartilage did not form a cylinder like in the regenerated tail. In the remaining 50% of cases, the two cartilaginous stumps were reconnected by the proliferation of a bridge of dense fibrous tissue, in which cartilaginous cells were scarce (Fig. 1.10h, i). The ependymal tubes within the two cartilaginous stumps appeared to be trapped by the dense connective tissue (Fig. 1.10i, j), and the more advanced cartilaginous bridge did not surround any ependymal tube. Therefore, unless the ependymal tube had degenerated before the histological analysis, cartilage regeneration seems to be independent of the influence of the ependymal tube (Simpson 1964). This independence of chondrogenesis from the presence of the regenerating ependyma is also indicated by the results obtained in the experiments described next.

The following experiment, also performed to detect cartilage regeneration, is shown schematically in Fig. 1.9c. Regenerated tails of *P. muralis* were amputated and about 2–3 mm of the cartilaginous cylinder containing the ependymal tube was removed from the stump surface. Generally the tail did not regenerate, and only a coniform scar was produced in most cases after this operation. The histological analysis at 3–4 weeks after amputation showed that the ependymal tube had regenerated for a small distance but was apparently trapped inside the fibrous, scar tissue produced on the stump surface (data not shown). An irregular

Fig. 1.10 (continued) fibers of the original muscle group (*bottom*). *Bar* 50 μm. **c** Longitudinal section showing the segmental organization of the regenerated muscles at about 30 days after amputation (*arrows*). *Bar* 40 μm. **d** A case with long regenerated myofibers that are inserted into the perivertebral connective tissue. *Bar* 50 μm. **e** Detail comparing the thinner regenerated myofibers (*arrows*) with the original fibers (*arrowheads*). *Bar* 50 μm. **f** Cartilaginous bridge formed between the two cartilaginous stumps (the original gap is indicated by *arrowheads*). The ependymal tube (*arrow*) has partially grown near an incorporated epidermal cyst (*double arrowhead*). *Bar* 40 μm. **g** Detail of regenerated cartilage filling the initial gap between the two cartilaginous stumps (*arrows*). *Bar* 50 μm. **h** In this case mainly fibrous tissue has formed between the two cartilaginous stumps, which are sealed by fibrocartilaginous tissue (*arrowheads*). The ependyma has remained inside the cartilaginous tubes. *Bar* 100 μm. **i** A case where dense connective tissue has bridged the two cartilaginous stumps (*arrows*). *Bar* 50 μm. **j** A case where the bridge tissue is made of cartilage surrounded by dense fibrous connective tissue. The *arrow* points to a peripheral nerve. *Bar* 50 μm. *cr* regenerated cartilaginous tissue, *ct1*, *ct2* cartilaginous stumps, *dc* dense connective tissue (scar), *li* lipid tissue, *nm* normal muscles, *rm* regenerated muscles, *sc* spinal cord, *sr* scar tissue, *v* vertebra

cartilaginous rod of cartilage (1–2 mm long) surrounded by fibrous tissues regrew apically in the absence of an ependymal outgrowth (Fig. 1.11a). Also in this case, unless the ependyma had initially regenerated and then degenerated before the histological analysis, this experiment also suggests that there is no influence of the ependyma on cartilage regeneration.

The experiments indicated in Fig. 1.9d tested the regenerative potential of the vertebrae in the tail. Two vertebrae in the proximal region of the tail were removed, including the inner spinal cord, as indicated in the drawing. Two to 3 days after surgery, about 60% of the animals also lost the distal part of the tail, which was probably dropped by autotomy, leaving the damaged vertebrae initially in contact with the stump and later with a regenerating blastema. In the remaining animals, the distal tail remained in place, so vertebral recovery was observed. Broad parts of the missing bone of the vertebrae were repaired by cartilage at 25–30 days after injury (Fig. 1.11b–e). The cartilage was either a continuation of the periosteum of the vertebral body or of cartilaginous cells of the intervertebral cartilage (intercentra). Fibrous connective tissue was also seen, and this connective tissue was mixed or surrounding the cartilaginous tissue. In the case of the continuity of the vertebrae with the regenerating tail, the cartilage tended to form a tube, so vertebrae were replaced with an irregular cartilaginous tube, like in the regenerating tail (data not shown).

Further experiments were conducted on geckos (*T. mauritanica* and *Hemidactylus turcicus*) and lizards (*P. sicula*). These studies aimed to test the capability of the tail to regenerate after cauterization and destruction of the spinal cord remaining in the stump of a normal tail, using a hot needle (Fig. 1.9e). Other experiments involved the cauterization of the ependymal tube present in the stump of a previously regenerated tail (Fig. 1.9f). The histological analysis of both cases showed that 13 days after injury, the normal spinal cord (or the regenerated ependymal tube) was totally or partially missing inside the last vertebrae or the cartilaginous tube (Fig. 1.11f). In the normal spinal cord, most neurons degenerated, and numerous phagocytes invaded the surrounding meninges or even the nervous tissue.

Following this operation, the process of wound healing was retarded and a scar or an outgrowth resembling a blastema was formed much later, after 15–20 days instead of 8–10 days as in normal controls. In some cases the initial outgrowth formed short, stubby scaled tails at 35–40 days after trauma (Figs. 1.11g, h). These short, scarred tails (1–3 mm in length) were invaded with fibrous connective tissue (Fig. 1.11i). In a few cases however, long regenerated tails were also produced. The histological examination of the latter regenerated tails showed that they contained numerous muscle bundles and large nerves (Fig. 1.11j). In some short scars, the surface of the stump contained a dense and fibrotic connective tissue instead of a mesenchymal blastema (Fig. 1.12a). Eosinophilic granulocytes and some large areas of eosinophilic fibrils (collagenous, keloid-like material) were sparse among fibrocytes in these flat scars or in the short scarred tails.

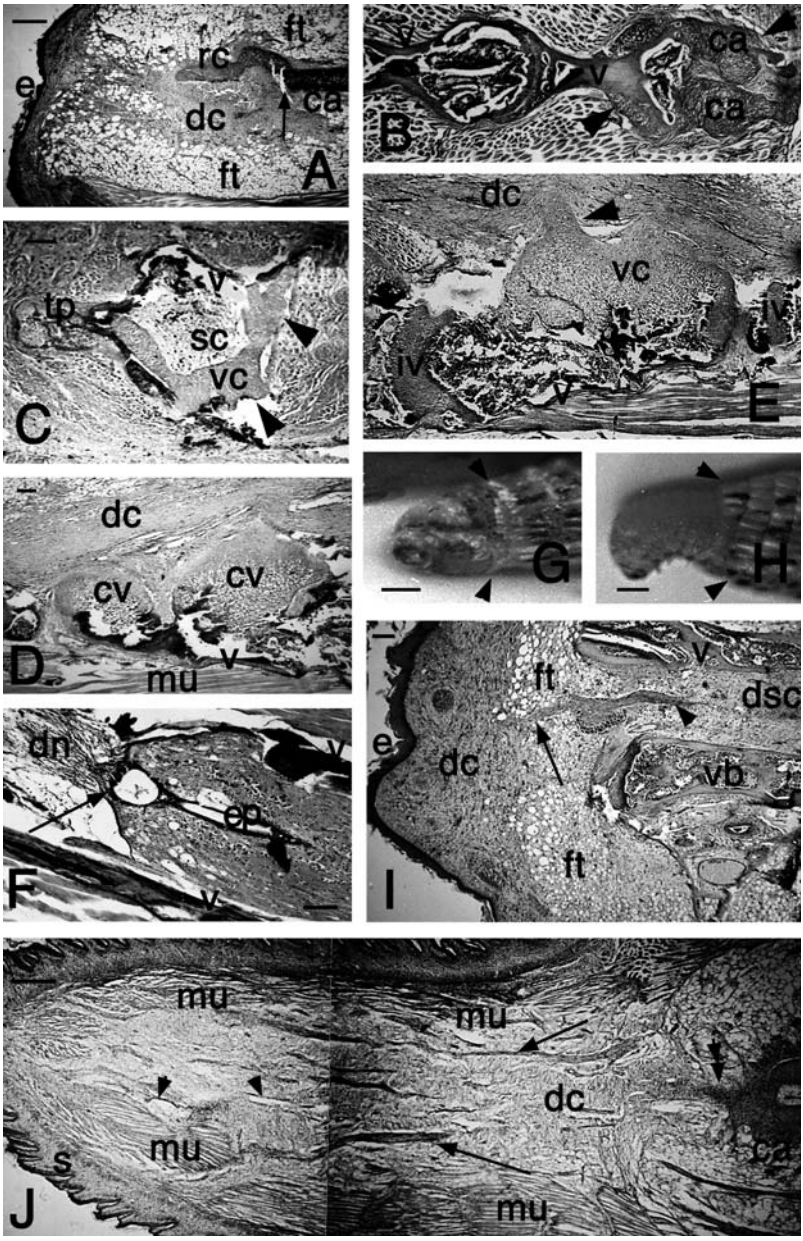

Fig. 1.11 Autonomous regeneration of cartilage (**a**) (see Fig. 1.9c), bone (**b–e**) (see Fig. 1.9d), connective tissues, fat, and nerves after cauterization of the spinal cord (**f–j**) (see Fig. 1.9e). **a–i** *P. sicula*. **j** *T. mauritanica*. **a** A rod of cartilage is seen among connective tissue and fat cells in front of the level of amputation (*arrow*). *Bar* 50 μm. **b** Frontal section of a damaged

The results of the experiments after normal spinal cord cauterization (Fig. 1.9e) are summarized as follows. In many cases (about 63%), tail regeneration was abolished, producing 0.05–0.2-cm-long, scaled scars after 45–50 days after injury. These scars were mainly constituted by fibrous connective tissues with few blood vessels, nerves, and traces of muscles. In about 28% of cases, shorter but irregular tails (0.3–0.9 cm in length) were produced. Some of these short regenerated tails possessed an axial cartilaginous rod without an ependymal tube (Fig. 1.12b–d). In other cases there was a single or even a double ependymal tube associated with or completely surrounded by a cartilaginous rod (Fig. 1.12e). In a few other cases, the outgrowth did not contain any cartilaginous tube at all, but instead fibrous connective tissue that was surrounded by muscle bundles with the typical circular pattern, and by connective and adipose tissue (Fig. 1.12f, g). Nerves were often large and abundant in these outgrowths, whereas muscles appeared organized in myotomes.

Finally, only 9% of cauterized animals in the experiments reported in Fig. 1.9e and f possessed longer regenerated tails at 50 days after amputation (0.6–1.9 cm long), and contained a cartilaginous tube surrounding a central ependymal tube, like in normally regenerated tails. Also, the cauterization of the regenerated spinal cord (essentially an ependymal tube; Fig. 1.9f) resulted in the formation of scars or short tails, like those illustrated in Fig. 1.11g and h.

These types of variation in the anatomical structure of regenerated tails, namely, tails containing an ependymal tube that was not completely surrounded by cartilage, or tails lacking a cartilaginous axis and ependyma, or tails with a single rod of

Fig. 1.11 (continued) vertebra (*arrowheads*) which has been largely replaced by cartilage after about 1 month after injury. *Bar* 50 μm. **c** Cross section of damaged vertebra with proliferated cartilaginous tissue (*arrowheads*). *Bar* 40 μm. **d** Longitudinal section showing that most vertebral bone is replaced by cartilage. *Bar* 40 μm. **e** Detail of damaged vertebra with formation of a cartilaginous neural arch (*arrowhead*). *Bar* 50 μm. **f** Detail showing the completely degenerated spinal cord inside the vertebral canal about 20 days after cauterization. The *arrow* indicates the reactive ependymal ampulla contacting the distal fibrous scar. *Bar* 40 μm. **g** Cicatrix outgrowth of about 40 days after spinal cauterization (*arrowheads* indicate the level of tail amputation). *Bar* 1 mm. **h** Another curved scar outgrowth at 50 days after cauterization of the spinal cord (*arrowheads* indicate the point of amputation). *Bar* 1 mm. **i** Longitudinal section of a short cicatrix at 25 days after cauterization. Beneath the epithelium, scar tissue is present which is contacted (*arrow*) by a nerve derived from an intact ganglion. The latter contacts the degenerated spinal cord through a nerve root (*arrowhead*) after cauterization. *Bar* 50 μm. **j** Long and scaled outgrowth produced about 35 days after cauterization of the ependyma at the point of amputation (*double arrowhead*, see Fig. 1.9f). Numerous nerves (*arrows*) and large blood vessels (*arrowheads*) are present together with segmented muscle bundles but no axial cartilaginous tube or bones are present. *Bar* 200 μm. *ca* cartilage, *dc* dense connective tissue, *dn* degenerated nervous tissue replaced by a fibrous scar, *dsc* degenerated spinal cord (scar), *e* epidermis, *ep* ependyma, *ft* fat tissue, *mu* muscles, *sc* spinal cord, *tp* transverse process of the vertebra, *v* vertebral bone, *vb* vertebral body, *vc* cartilaginous vertebra

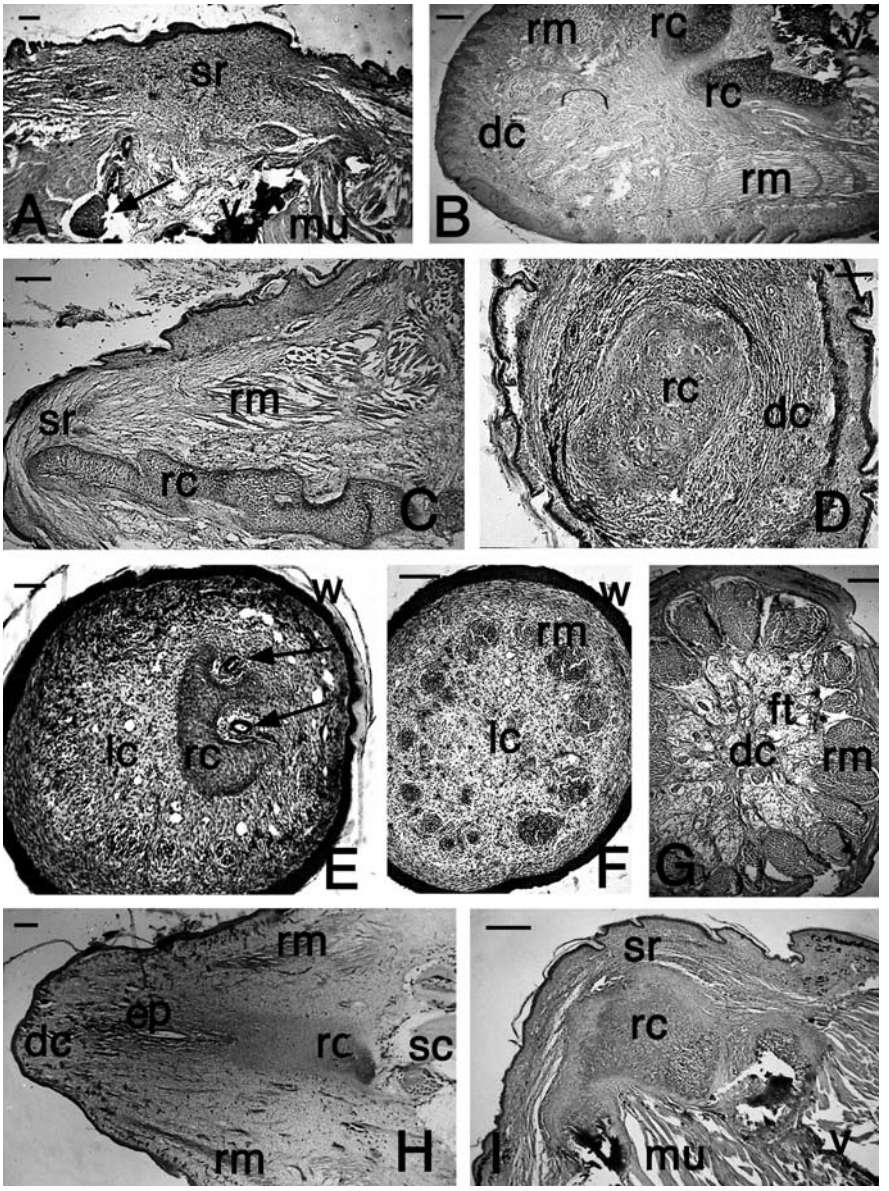

Fig. 1.12 Effects on tail regeneration after cauterization of the spinal cord (**a**–**g**) (see Fig. 1.9e) or after the cauterization of the stump with the exception of the spinal cord (**h**, **i**) (see Fig. 1.9g). **a**, **c**–**i** *P. sicula*. **b** *H. turcicus*. **a** Scar with almost no regeneration (the *arrow* points to a spinal ganglion). *Bar* 200 μm. **b** Short regenerated cone of about 30 days of regeneration where only dense connective tissue and segmental muscles are present, whereas the cartilage has only recovered the injured vertebra. *Bar* 200 m. **c** Irregular

cartilage but not ependyma, have also been described in regenerated tails found in natural conditions (Bellairs and Bryant 1985). In both experimental conditions and naturally occurring anomalous outgrowths, it is unknown whether the ependymal tube was initially absent or had degenerated for physiological reasons after the regeneration of the tail. This possibility, however, remains unlikely as other experiments indicate that the implanted ependyma either degenerates rapidly or survives beyond 30 days (Simpson 1964; Alibardi et al. 1988; Fig. 1.9h, i).

A further experiment tested the ability of caudal tissues to regenerate after cauterization of the superficial tissues of the stump, with the exception of the spinal cord (Fig. 1.9g). After this operation, in 30% of cases short regenerated tails (0.3–1.2 cm) were produced where a cartilaginous tube with ependyma was present (Fig. 1.12h). However, in 70% of cases no tail regeneration occurred. In the latter cases, the cauterized stumps initially produced softer mounds which became scars of 1–3 mm in length at 30 days after cauterization, sometimes containing large masses of cartilage (Fig. 1.12i). Also in this case, as in the experiments where the cauterization of the ependymal tube was performed (Figs. 1.9f, 1.12e), the ependymal tube was sometimes bifurcated or was connected to nerves carved inside the cartilage (Fig. 1.13a–d). The connective tissue formed after stump cauterization was composed of fibroblasts containing large amounts of banded collagen and the intercellular matrix appeared densely fibrous, not like the loose mesenchyme formed in the normal blastema (Fig. 1.13; Alibardi and Sala 1988).

The final experiments were designed to determine the capacity of the spinal cord or the ependymal tube (autotransplant from the amputated distal regenerated tail) to grow and sustain tail regeneration after cauterization of the normal spinal cord (Fig. 1.9h). It is known that the implantation of a cartilaginous tube containing the ependyma on dorsal incisions of a tail can induce the formation of additional tails (Guyenot 1928; Singer 1961; Simpson 1964; Whimster 1978; Alibardi et al. 1988; Figs. 1.1, 1.9h, i). This operation was done by the autotransplant of a piece of the cartilage-ependyma tube into the tail stump where the spinal cord was cauterized by a hot needle (Fig. 1.9h). This experiment produced

Fig. 1.12 (continued) cartilaginous rod forming the axis of a conical outgrowth of about 35 days of regeneration. *Bar* 200 m. **d** Cross section of a conical outgrowth showing a central rod of cartilage surrounded by dense connective tissue. *Bar* 200 μm. **e** Cross-sectioned elongating cone of about 3 weeks of regeneration with two ependymal tubes (*arrows*) not completely surrounded by cartilage. *Bar* 100 μm. **f** Cross section of a coniform tail at 3 weeks after injury showing only muscle bundles but not cartilage-ependyma in the center. *Bar* 100 m. **g** Cross section of regenerated tail about 1 cm long (about 40 days of regeneration) with muscle bundles but not axial cartilage-ependyma. *Bar* 200 μm. **h** Regenerating cone at about 3 weeks with ependyma-cartilage but few muscle bundles. *Bar* 50 μm. **i** Coniform scar at 1 month after cauterization mainly occupied by cartilage. *Bar* 100 μm. *dc* dense connective tissue, *ep* ependyma, *ft* fat tissue, *lc* loose connective tissue, mu muscle, *rc* regenerated cartilage, *rm* regenerated muscles, *sc* spinal cord, *sr* scar tissue, *w* wound epidermis

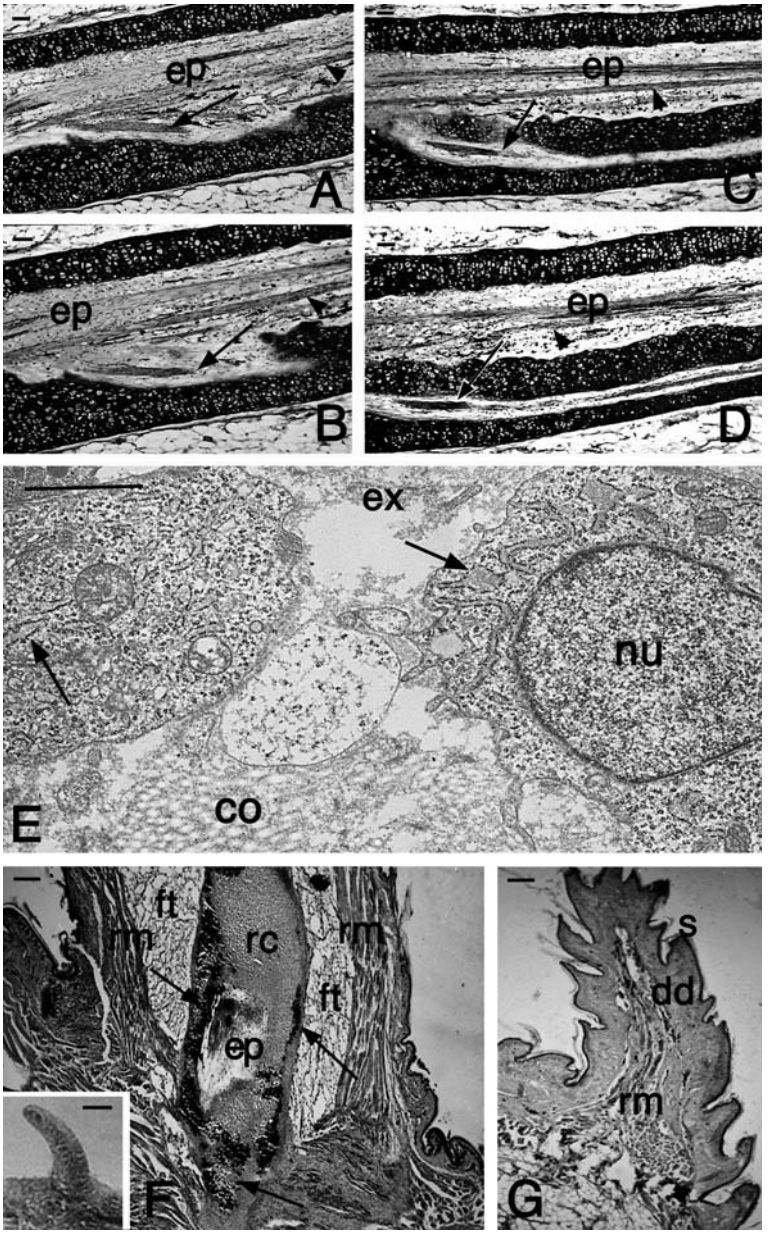

Fig. 1.13 Effect on tail regeneration of cauterization of the regenerated ependyma (**a**–**d**) or the stump (**e**), or of implants of cartilage-ependyma (**f**, **g**). **a**–**d** Longitudinal sections of the same cartilage-ependyma of regenerated tail. **a** Beginning of the bifurcation of a nerve (*arrow*) from the ependyma. Another nerve (*arrowhead*) runs parallel to the ependyma. *Bar* 50 μm. **b** The bifurcated nerve insinuates (*arrow*) into the cartilage wall. Another nerve

in 37% of the cases scar outgrowths of 0.2–0.3 cm in length, which contained neither cartilage nor ependyma (probably the transplanted tissues had degenerated). In the remaining 62.5% of cases, the implanted tissues remained viable, and normal regenerated tails (0.6–1.7 cm) were produced after 40 days after the operation. The latter contained a cartilaginous tube with ependyma. Also, the autotransplant of spinal cord or cartilage-ependyma in the dorsal part of the tail stump often resulted in the formation of adjunctive (supernumerary) tails after 30–60 days after the operation (Fig. 1.9i). The production of supernumerary tails of 3 mm to over 1 cm in length varied from 27% of the cases after spinal cord implantation to 28–41% of the cases after cartilage-ependyma implantation. Some of the induced tails contained a cartilaginous-ependymal axis surrounded by muscle bundles as in normal regenerated tails (Fig. 1.13f). In other cases where shorter and smaller supernumerary tails were induced, these supernumerary tails did not contain a cartilaginous tube with ependyma but instead dense connective tissue, with nerves, blood vessels, and thin muscle bundles (Fig. 1.13g). It is not known whether the implanted ependyma in the latter cases had degenerated before the histological examination. The potential of tissue regeneration is, however, expressed only when the connective tissue surrounding the above-mentioned tissues slowly turns into a scar. In contrast, the rapid formation of scar connective tissue halts the regeneration and elongation of the ependymal tube and of the cartilaginous cylinder, limiting the regeneration of a new tail and leading to the formation of flat scars or short tails.

In conclusion, the experiments described above have indicated that in lizards many of the axial tissues of the normal tail (cartilage, bone, muscles, spinal cord, and large nerves) can express a large regenerative capability, higher than in other amniotes (Tsonis 2002). From a zoological point of view, these experiments further suggest that the broad autonomous tissue regeneration in lizards was probably a preadaptative characteristic for the evolution of the regeneration of a large organ such as the tail (Sect. 1.2). What was needed for the regeneration of the tail was the formation of a thin mesenchymal mass interacting with an apical

Fig. 1.13 (continued) (*arrowhead*) runs parallel to the ependyma. *Bar* 50 μm. **c** The bifurcated nerve grows into a cavity (*arrow*) carved in the cartilage. The other nerve (*arrowhead*) runs parallel to the ependyma. *Bar* 50 μm. **d** The nerve runs inside a channel carved in the cartilage. The other nerve (*arrowhead*) merges with the ependyma. *Bar* 50 μm. **e** Ultrastructural detail of the fibroblasts with developed ergastoplasm (*arrows*) present in an outgrowth at 15 days after cauterization. Numerous collagen fibrils are seen in the extracellular space. *Bar* 0.5 μm. **f** Induced tail regeneration after 25 days from the implantation of the cartilage-ependyma (experiment reported in Fig. 1.9h; *bar* 1 mm in the *inset*). The longitudinal section of a supernumerary tail of about 50 days shows that a central cartilage-ependyma surrounded by fat tissue and muscles is present like in a normally regenerated tail. *Arrows* indicate the beginning of calcification of the cartilage. *Bar* 100 μm. **g** In another, short outgrowth at 45 days after implantation, only dense connective tissue and a few muscles are regenerated. *Bar* 200 μm. *co* collagen fibrils, *dd* dense dermis, *ep* ependyma, *ex* extracellular matrix, *ft* fat tissue, *nu* nucleus, *rc* regenerated cartilage, *rm* regenerated muscles, *s* scale

wound epidermis, the epidermal cup, capable of maintaining a soft growing apex where mesenchyme and epithelial cells communicate through the incomplete basement membrane. The type of molecules possibly operating in this epidermal–mesenchymal interaction still remains to be discovered in the lizard system, but studies on the inhibition of tail regeneration will help in future molecular analysis of the process.

1.8 Failure of Tail Regeneration and Cicatrization

Many internal and external factors control tail regeneration in lizards, and they operate at the molecular and cellular level (growth factors, neurotrophic factors, signaling molecules) or at a physiological and more systemic level (endocrine and immune systems).

Although the regeneration of the tail occurs in most lizards under warm or hot conditions, the process of tail regeneration is retarded or completely inhibited when the temperature falls below 20°C. For instance, in *A. carolinensis* the rate of tail regeneration falls to one tenth when the temperature is lowered from 31 to 21°C (Maderson and Licht 1968). The rate of regeneration is so low at 18–20°C in *P. sicula* and *P. muralis* (Alibardi, personal observations) that tail growth is virtually stopped. This process very likely occurs because the metabolism is too low to sustain tissue growth. The effect of the temperature on the general metabolism is however nonspecific since it does not affect the molecular mechanism that induces the regenerative response. More specific cellular process that are needed for tissue regeneration include the presence of a wound epithelium, the presence of stem cells in the tail and limb, the degree of inflammatory reaction after wounding, and even the participation of the immune system to limit the formation of a new proliferating tissue such as the regenerative blastema. Finally, the influence of the nervous system on the regenerating tissues is also a key factor controlling the process (Simpson 1970, 1983; Bellairs and Bryant 1985).

The destruction of the apical wound epidermis of the tail blastema stimulates scarring (Alibardi, personal observations). It is, however, not known whether the apical wound epidermis forming the epidermal papilla localized in front of the regenerating ependymal ampulla (Fig. 1.4e) corresponds to the apical epidermal ridge of the newt blastema (Mesher 1996; Harty et al. 2003). An apical epidermal papilla is absent in the wound epidermis of the wounded limb, although the keratinocytes express wound keratins like those of the epidermis in the tail (Alibardi and Toni 2006). The presence of a complete basement membrane in the mounds of a healing limb very likely stops the morphoregulatory communication between dermis and epidermis, leading to the stoppage of growth and therefore to scarring. In contrast, in the tail blastema the basement membrane is incomplete, at least in the more apical and central part, and dermal–epidermal interactions (and perhaps also epithelial–mesenchymal transformation) take place

(Alibardi 1994b, 2009a). When the tail stump is covered with old skin taken from the side of the stump (where a basement membrane is well formed), tail regeneration is inhibited (Marcucci 1915a, b; Quattrini 1955).

The process of regeneration in lizards is sensitive to other natural or experimental conditions, directly or indirectly stimulating a strong inflammatory reaction. In fact, as we have previously reported, one way to inhibit tail regeneration or produce variably irregular tail scars is through the cauterization of the amputated stump or of the single spinal cord (Fig. 1.9e, f). Another intervention aiming to block the process of tail regeneration is carried out by making a few incisions in the tip of the blastema where the apical epidermal papilla is located. A further operation that retards or inhibits tail regeneration is through the use of irritating chemical agents such as beryllium and cadmium nitrate, which block limb or tail regeneration in amphibians (Carlson 1970). Similar treatments on the stump of the lizard tail retard tail regeneration or sometimes result in the formation of scars (Alibardi, unpublished observations). All the above-mentioned effects seem to induce the stimulation of a chronic inflammatory response in tail tissues, similar to the intense inflammation of the wounded limb (Alibardi 2009a, b).

Also, repeated amputations of the tail in a close temporal sequence lower the rate of tail regeneration and eventually abolish it (Hughes and New 1959; Bryant and Bellairs 1967a, b; Maderson and Licht 1968; Werner 1968; Alibardi, personal observations). This operation, after the third amputation, leads to the formation of shorter tails or even blunt scars. This effect can derive either from the depletion of hormones from endocrine glands sustaining regeneration (hypophysis and thyroid) or from the enhancement of the inflammatory reaction to infection, or even from immune reactions due to the chronic wounding stimulation. The latter may evoke the sensitization to autoantigens, but molecular data are missing. In lizards that have formed a tail scar instead of a regenerated tail, the monocyte content in the blood is abnormally high (Sabrazes and Muratet 1924; Alibardi, personal observations). The inflammatory reaction can turn the blastema into a fibrotic granulation tissue that prevalent on the healing process and forms a scar. The molecular processes operating during lizard inflammation are not known.

Endocrine effects on the process of tail regeneration and, in general, of tissue regeneration are indirect, and their molecular action in lizards remains poorly known. The hypothalamus is probably involved since the supraoptic and paraventricular nuclei show the maximum secretory activity during the highest rate of growth of the regenerating tail in the gecko *Hemidactylus flaviviridis* (Desai et al. 1977). Also, the thyroid is more active during tail regeneration, sustaining the metabolism and the growth of the regenerating ependyma (Turner and Tipton 1971; Magon 1975).

The hormonal supply for tail regeneration is essential for sustaining the process, e.g., maintaining an active protein synthesis and metabolism (Licht and Howe 1969; Turner 1972). Hypophysectomy delays the formation of a regenerative blastema and the growth of the regenerating tail as it retards the differentiation and growth of the main elongating tissues, muscles, cartilage, and probably

the nervous system (ependymal tube). The administration of the growth hormones prolactin, gonadotrophin, and/or of thyrotropin recovers tail regeneration in hypophysectomized lizards. Thyroxine stimulates regeneration and the formation of promuscle cell aggregates, procartilaginous condensation, and the growth of the ependymal tube (Turner and Tipton 1971; Turner 1972).

The spinal cord is important for stimulating the regeneration of the tail as its removal results in inhibition of tail regeneration (Guyenot 1928; Kamrin and Singer 1955; Simpson 1961, 1970; Whimster 1978; Alibardi et al. 1988). The implantation of spinal cord stimulates the regeneration of supernumerary tails (Fig. 1.9i). In most cases of tail bifurcation or of supernumerary tail formation in natural conditions, the spinal cord appears as the essential element capable of promoting the process of regeneration (Terni 1915; Woodland 1920; Volante 1923; Quattrini, 1953a, b, 1954; Evans and Bellairs 1983). In particular, the regenerating ependyma appears to be the main stimulator of tail regeneration (Simpson 1964; Alibardi et al. 1988), although its specific neurotrophic action remains to be demonstrated. Regenerating nerves appear less important for inducement of the regeneration of the tail or of the limb, and their experimental reduction over the tail stump does not significantly affect tail regeneration (Cox 1969b).

Finally, the role of the immune system in limiting the process of tail regeneration in lizards has still to be assessed. Preliminary studies have indicated that the number of lymphocytes and of γ-globulin fraction of the serum increase with repetitive tail amputations (Alibardi, unpublished data). At the third and fourth successive amputations of the tail, numerous lizards do not regenerate the tail anymore, but tend to form a scar outgrowth or a short tail that rapidly becomes scaled. The histological analysis of the blood at the first, second, third, and forth amputations has shown the presence of a very high level of lymphocytes and lymphoblasts, in particular in individuals with scars instead of regenerated tails (Alibardi, personal observations). It is not clear whether this increase of leukocytes is due to the status of a lasting inflammation and infection resulting from the persisting amputation, or to a specific stimulation of the immune system by new antigens formed in the regenerating blastema.

The stimulation of tail scarring is also obtained in the second continuous regeneration in gecko lizards maintained at a constant temperature of 37–40°C, a condition that resembles that of a mammal (Alibardi, unpublished observations). Only specimens of *T. mauritanica* or *H. turcicus* resist these constant high temperatures, whereas *P. sicula* cannot tolerate them. It is likely that the immune system is more active in these lizards, virtually in homeothermic conditions, and both the lymphocytes and γ-globulin fraction increase in comparison with normal conditions.

Chapter 2
Tail Regeneration: Ultrastructural and Cytological Aspects

Despite the numerous histological studies on regenerating tails, few ultrastructural studies have been conducted on the progressive stages of the process. These studies would allow a better identification of the modification of injured tissues and of the different cell types activated during the process of wounding. No ultrastructural studies are available for the wounding and the limited tissue regeneration of the limb.

Only the regenerating spinal cord has received a detailed transmission electron microscopy (TEM) analysis (Simpson 1968; Egar et al. 1970; Turner and Singer 1973; Alibardi 1990–1991). Other ultrastructural studies have been conducted on the differentiation of the main tissues in the tail (see later). These studies have permitted us to determine precisely the types of cells involved in the formation of the regenerative blastema in lizards and the proliferative potential of cells of the connective, ependymal, muscular, and blood tissues.

The following sections provide a summary of published and unpublished observations on the fine structure of the wounded and regenerating tissues of different species of lizards. More details can be found in specific publications cited in the following sections.

2.1
Wound Healing to Blastema Formation

Despite the extensive injuries following tail or limb amputation in lizards, the animals rarely acquire infections, a phenomenon almost impossible in a mammal. How can lizards cope with microbe penetration across their extensively exposed tissues? Ultrastructural analysis has shown that the injured stump is covered with bacteria of different types (Alibardi 2009a; Fig. 2.1a, b). Despite the contact with a dirty substratum in the terrarium, lizards rarely develop infections. These observations have shown that numerous neutrophils are present among the wound epithelium and are also located beneath the scab, where they actively engulf bacteria.

At about 2 days after amputation, many degenerating endings of sectioned muscles are seen, and numerous white blood cells are infiltrated among the

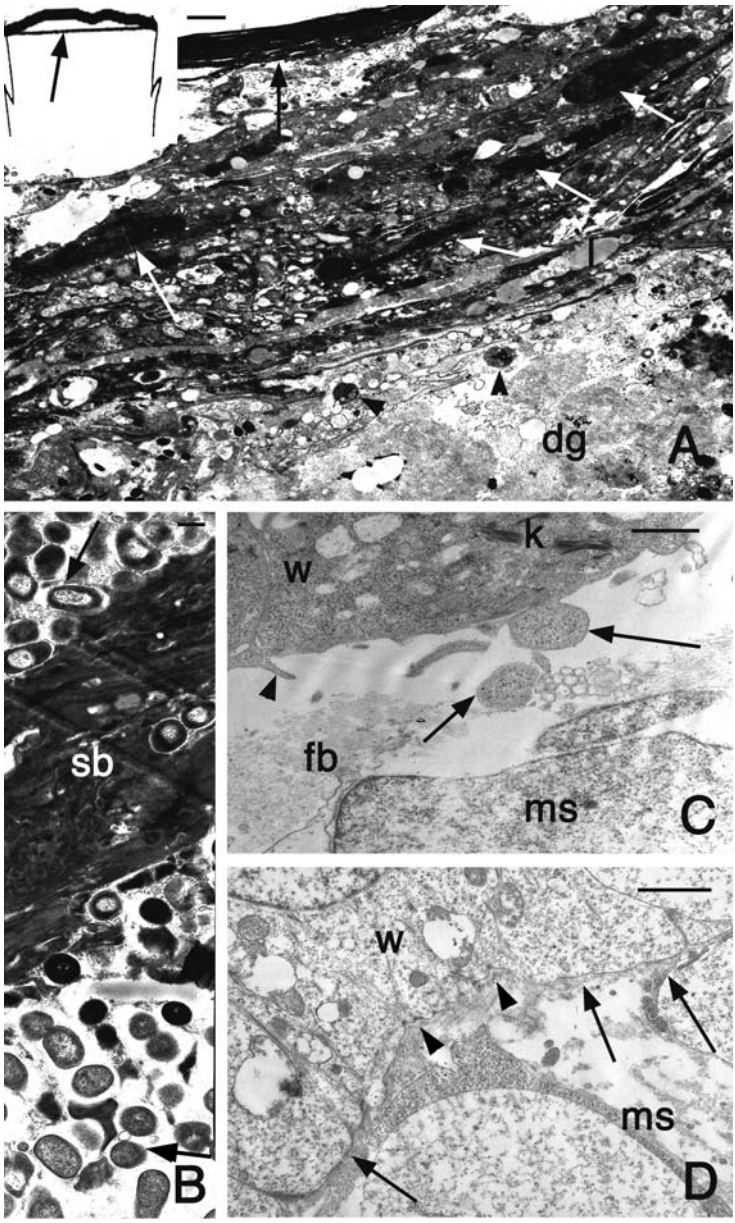

Fig. 2.1 Ultrastructural details of the tail stump (location indicated by the *arrow* in the *inset* in **a**) in *Podarcis sicula* (**a**–**c**) and *Anolis carolinensis* (**d**). **a** Aspect of the scab at 4 days after wounding. Beneath the compact outer stratum (*dark arrow*) numerous degenerating cells (*white arrows* indicated electron-dense nuclei), keratinocytes, and blood-derived cells with numerous vacuoles are accumulating. Degenerating pale cells underneath represent

connective and adipose tissues, for an extension up to 0.2–0.3 mm within the stump. The surface of the stump of the tail is initially covered with a blood clot, derived from the accumulation of blood cells over the sectioned tissues (Figs. 1.4a, 2.1a). At 3–4 days after amputation, the keratinocytes from the last sectioned scales have migrated over part of the stump but do not completely cover the stump surface (Alibardi and Sala 1983; Alibardi and Toni 2005; Alibardi 2009a).

The scab is made of electron-dense, largely amorphous material derived from platelets, and erythrocytes accumulate over injured tissues during the first few hours after lesion. Numerous bacteria (*Bacillus* sp., *Staphylococcus* sp., sometimes also *Mycobacterium* sp. with a capsule) are seen externally, but also within the scab (Fig. 2.1b). Bacteria in the phase of cell division are often seen. The scab contains numerous pycnotic nuclei, 0.1–2.0-μm lipid-like vesicles and degenerating leukocytes with digestive lysosomes, especially in contact with the wounded tissues underneath. The microbes are engulfed in digestive vacuoles of leukocytes localized among the migrating keratinocytes. The leukocytes contain 0.1–0.5-μm dense granules with a "spongy-like" texture that resemble the azurophilic granules of neutrophil granulocytes in mammals. Other dense granules instead resemble the specific granules of eosinophils/heterophils, as they contain denser particulate/polygonal structures among a less dense material.

The phagocytic keratinocytes contain few keratin bundles, desmosomal junctions, and scattered phagosomes or pale digestive vacuoles of 0.2–0.5 μm together with short vesicles of the rough endoplasmic reticulum. Although the plasma membrane of granulocytes and migrating keratinocytes is often apposed one to another, no desmosomal junctions are present between these cell types. At 12–14 days after amputation the wound epidermis comprises six to ten layers of spinous-like keratinocytes with euchromatic nuclei, located beneath a corneous layer made of five to eight layers of thin corneocytes. The flattening keratinocytes of the more external layers contain numerous short keratin bundles that tend to merge together in precorneous keratinocytes (Alibardi 1995c, Alibardi and Toni 2005). Beneath the corneous layers of forming scales, a granulated (clear) layer is formed, which forms a characteristic serrated interface with the next layer produced underneath, called the oberhautchen layer. The granulated and the new oberhautchen layers will form the splitting line for the shedding of the wound

Fig. 2.1 (continued) granulocytes containing dense granules (*arrowheads*). *Bar* 1 μm. **b** Detail of scab at 5–6 days with condensed cell material surrounded by bacteria (*arrows*). *Bar* 200 nm. **c** Detail of the basal part of the wound epithelium contacting the underlying connective tissue at 7–8 days after wounding. Two cytoplasmic blebs (*arrows*) and a microvillar elongation (*arrowhead*) from migrating keratinocytes are seen. *Bar* 1 μm. **d** Detail showing the dermal–epidermal boundary of the blastema at 16 days after amputation. The dense lamella is largely incomplete (*arrowheads*), whereas an amorphous material (*arrows*) occupies most of the incomplete basement membrane. *Bar* 1 μm. *dg* degenerating granulocytes, *fb* fibrin exudate, *k* keratin bundles, *l* lipid vesicle, *msn* mesenchymal cell, *sb* scab material, *w* wound keratinocytes

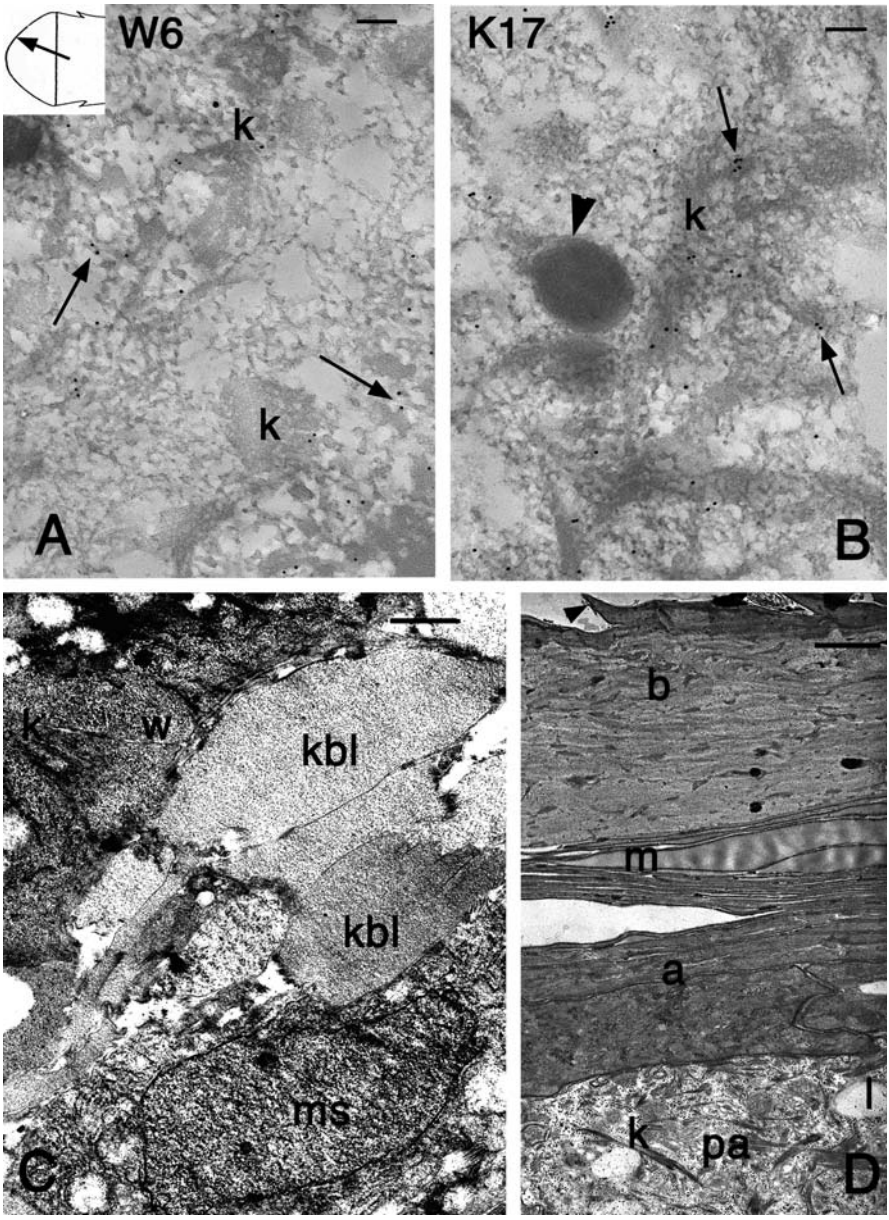

Fig. 2.2 Ultrastructural detail of cells of the wound epidermis (**a**–**c**) in the blastema (*arrow* in the *inset* in **a**) and regenerated epidermis of the new scales (**d**) in *P. sicula*. **a** Diffuse immunogold labeling (*arrows*) for wound antigen 6 among keratin bundles. *Bar* 100 nm. **b** Diffuse immunogold labeling for keratin 17 (*arrows*) among keratin bundles. The *arrowhead* points to a dense granule. *Bar* 100 nm. **c** Cytoplasmic blebs of the basal cells

epidermis (Alibardi 1998, 1999, 2001). The process of shedding is favored by the degradation of cell junctions between granulated and oberhautchen layers as indicated by the activity and localization of acid phosphatase contained in the lysosomes of these cells.

In the tail blastema, the basement membrane of the wound epidermis, in particular the dense lamella appears discontinuous and some cytoplasmic blebs of migrating keratinocytes are seen (Fig. 2.1c, d). Elongating keratinocytes show numerous microvillar extensions contacting the loose exudates and the few collagen fibrils with no banding present in the healing connective tissue.

Wound keratinocytes contain short endoplasmic cisternae, irregular pale vesicles, lipid droplets, and sparse, round, and dense granules of 0.1–0.4 μm. The short keratin bundles of wound keratinocytes are diffusely immunolabeled for wound keratins 6, 16, and especially 17, like in mammalian wound keratinocytes (McGowan and Coulombe 1998; Alibardi and Toni 2005, 2006; Fig. 2.2a). Keratin 17 is a special keratin believed to favor the movement of migrating keratinocytes as it is linked to elastic elements of their cytoskeleton (actin, etc.) Migrating and stratifying keratinocytes of the wound epidermis are also react toward wound antigen 6, a typical cytoskeleton-associated marker associated with the regenerating wound epithelium of amphibians (Estrada et al. 1993; Fig. 2.2b). Immunogold labeling at the TEM level has shown that the antigen is diffuse in the cytoplasm and associated with keratin bundles. The immunogold labeling shows that the keratin 17 antibody tends to label loosely the periphery of the short keratin bundles of lizard wound keratinocytes but not the entire bundle (Alibardi and Toni 2005). The long bundles most likely contain other keratin types. Both these cytoskeletal proteins, wound antigen 6 and keratin 17, are associated with the short keratin bundles of migrating keratinocytes, and are absent in stabilized keratinocytes of normal epidermis (Geraudie and Ferretti 1998).

The basal layer of the wound epidermis often appears irregular, and this is due to the numerous cytoplasmic blebs produced by basal keratinocytes in the initial wound epithelium of the blastema at 8–12 days after amputation (Alibardi 1994b, 1999). Often this part of the epithelium is so irregular and the boundary between epithelial and mesenchymal cells is quite indistinct that some cells may actually detach from the epithelium to move into the mesenchyme through a process known as epithelial–mesenchymal transformation (Hay 1996; Fig. 2.2c).

Fig. 2.2 (continued) of the wound epidermis in contact with mesenchymal cells of the blastema. *Bar* 1 μm. **d** Restored epidermal layer sequence after loss of the wound epithelium in regenerated scale. The *arrowhead* indicates a spinule of the external oberhautchen layer which is merged with the electron-pale β-layer, separated by thin mesoS cells from the differentiating α-layer underneath. *Bar* 0.5 μm. *a* α-layer, *b* β-keratin layer, *k* keratin bundle, *kbl* basal bleb of keratinocytes, *K17* keratin 17 immunolabeling, *l* lipid droplet, *m* mesoS (intermediate) layer, *ms* mesenchymal cell of the blastema, *pa* pre-α (differentiating) cell, *W6* wound antigen 6 immunolabeling, *w* cells of the wound epithelium

Within the wound epidermis a shedding layer is gradually formed. The upper part of the wound epidermis is lost and new cells derived from the basal layer will form the hard, β-keratin layers of the new epidermis (Figs. 1.1o, 2.2d).

The inflammatory process in lizards has some differences from the cellular response present in mammals. In the latter, granulocytes degenerate in 1–3 days and are replaced by macrophages of blood origin in the following days which become the more common phagocytes in wounds (Kovacs and DiPietro 1994; VanDen Boom et al. 2002; Wynn 2008). Differently, in wounded reptilian tissues most leukocytes and only a few macrophages colonize the injured area during the first week, and leukocytes persist in high number in the inflamed area for a long time (Montali 1988; Huchezermayer and Cooper 2000; Tuchunduva et al. 2001; Alibardi 2009a). These cells are recruited from the blood, as is also indicated from some lowering of their number in the blood during the preblastematic and early stages of tail regeneration (Hiradar et al. 1979; Shah et al. 1980). The longer permanence of granulocytes that have migrated into the wound tissues in reptiles in comparison with mammalian wounds (Montali 1988; Smith and Barker 1988; Tuchunduva et al. 2001; Alberio et al. 2005) may also indicate that these cells survive longer than in mammals. Macrophages are less frequent during the first 4–6 days after amputation, and beneath the scab of the stump the second main line of defense is represented by granulocyte heterophils. The numerous azurophil granules, and the specific granules, may contain potent antimicrobial molecules that remain to be specifically identified. However, the cellular and molecular nature of this innate immunity, whether present in regenerating keratinocytes or/and in the underlying white blood cells in lizard wounds, is not known. Can lizards produce antimicrobial molecules responsible for the relatively low and brief inflammatory reaction that favor tissue regeneration? Innate molecules such as defensins and cathelicidins are not known in lizards, but they have been described in amphibians and the chick (Zasloff 2002). The presence of putative, antimicrobial molecules in injured lizard tissues and their potential pharmacological role remain to be discovered.

Beneath the wound epidermis, migrating chromatophores such as lipophores, iridophores, and melanophores are often present. Typical mesenchymal (blastema) cells accumulate beneath the wound epithelium at 12–14 days after amputation, and very little amorphous material (glycosaminoglycans) and scarce, nonbanded thin collagen fibrils are present (Alibardi and Sala 1988a, b, 1989). Around the ependymal ampulla, cells of mesenchymal aspect actively take up tritiated thymidine (Fig. 2.3a) and proline (Fig. 2.3b). Although they are surrounded by numerous collagen fibrils, proliferating fibroblasts are also present in the lesioned meninges and in the regenerating dermis (Fig. 2.3c).

The ultrastructural aspect of blastema cells is essentially summarized in the variation of shape and extent of surface elongation, from fusiform cells (fibroblast-like) toward a more irregular mesenchymal aspect, and in the variable amount of rough endoplasmic reticulum that is present in these cells (Alibardi 1986, 2009b; Alibardi and Sala 1988a, b, 1989). These cytological aspects and the

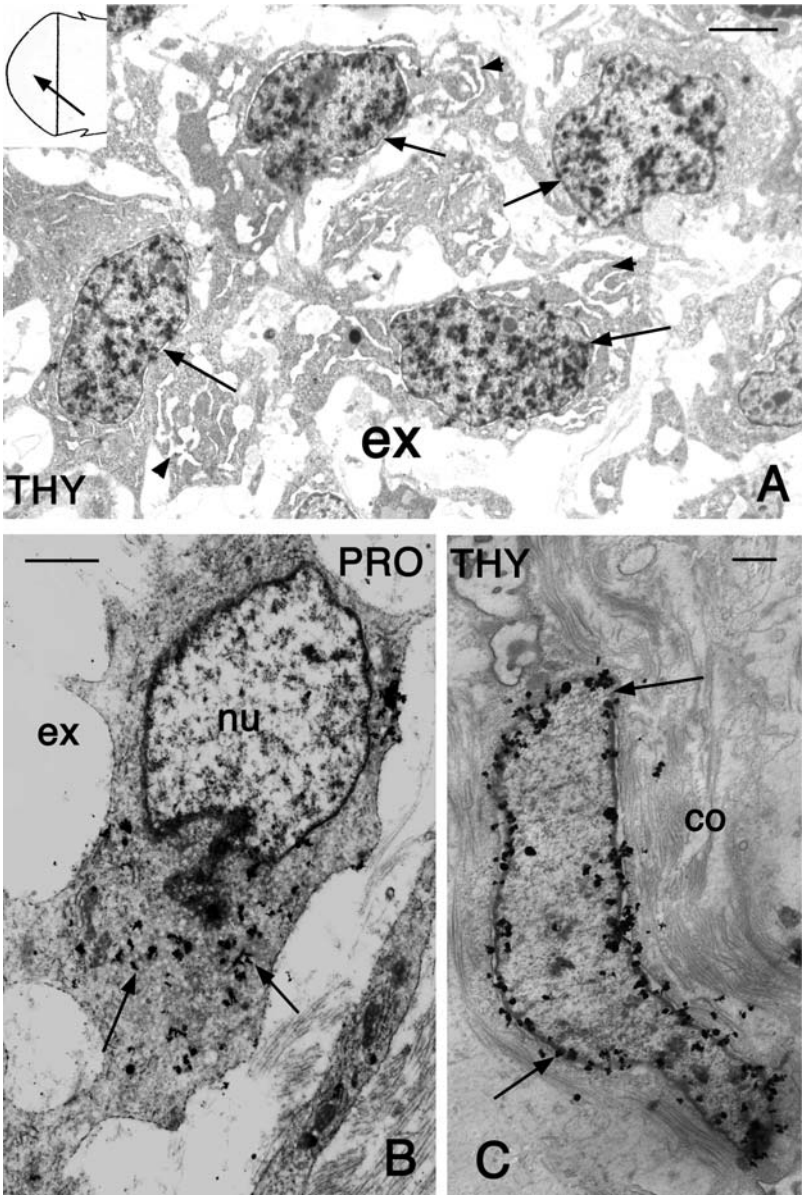

Fig. 2.3 Ultrastructural aspects of cells of the regenerative blastema in *A. carolinensis* (**a**, **c**) and *Lampropholis delicata* (**b**). **a** Mesenchymal cells with tritiated thymidine labeled nuclei (*arrows*) present in the central region of the blastema (*arrow* in the *inset*). *Arrowheads* indicate regions of the cytoplasm with developed ergastoplasmic cisternae. *Bar* 2.5 μm. **b** Labeled cell (*arrows*) 1 h after injection of tritiated proline, located at the apex of the regenerating meninx. *Bar* 2 μm. **c** Thymidine-labeled fibroblast in the more lateral region (dermal) of the blastema. *Bar* 1 μm. *co* collagen fibrils, *ex* extracellular space, *nu* nucleus, *PRO* tritiated proline autoradiography, *THY* tritiated thymidine autoradiography

cell density within the tail blastema and cone are probably related to the tissue derivation. In the center of the blastema, mesenchymal cells have a poorly developed ergastoplasm, but those located around or as a continuation of the apical ependymal ampulla contain numerous endoplasmic cisternae. The latter probably represent meningeal cells or even detached ependymal cells. In the area of promuscle aggregates, mesenchymal cells frequently divide, and appear labeled after 4 h to 1 day after injection of tritiated thymidine. They appear well labeled after injection of tritiated proline, indicating that these cells possess an active metabolism. In the lateral area of the blastema, where the dermis will be formed, some typical fibroblasts surrounded by few collagen fibrils are present, often incorporating tritiated thymidine. In all the regions of the tail blastema however, the extracellular matrix is very scarce and contains mainly amorphous material, probably glycosaminoglycans, and collagen fibrils are scarce and generally do not form banded bundles.

Numerous cell types are present among mesenchymal cells of the blastema, in particular macrophages, hematogenous cells (immature red blood cells or other types of blood cells), and melanophores. In conclusion, it is clear from the above description that a limited inflammatory reaction with a relatively low number of leukocytes and macrophages occurs along the autotomy planes of the tail. This condition favors the accumulation of mesenchymal cells of different origin, and perhaps also the wound epithelium can provide cells of the blastema through an epidermal–mesenchymal transformation. The latter phenomenon and its quantitative contribution to the cell population of the regenerative blastema in lizard regeneration has still to be evaluated. Typical of the tail blastema is the close association between mesenchymal and epithelial cells due to the discontinuous basement membrane, an aspect that indicates an intense dermal–epidermal interaction during these stages.

2.2 Tissue Differentiation

2.2.1 Epidermis

The wound epidermis at 1–2 mm from the tail tip is covered by five to eight layers of mature corneocytes, whereas the living keratinocytes form a waved epidermis (Figs. 1.4k, 1.6a). After the formation of deep epidermal pegs (Fig. 1.6c–e), the epidermis undergoes cell differentiation to produce the typical stratification of normal scales (Maderson et al. 1978; Maderson 1985; Alibardi 1995a, 1998, 2001). The wound epidermis is an immature α-keratin layer and the formation of the granulated layer occurs by the accumulation of keratohyalin-like granules of 0.1–4.0 μm in diameter (depending on the species; see Alibardi 1999, 2001). Numerous dense granules of submicroscopic dimension (0.1–0.2 μm) are

produced in upper wound keratinocytes before they pack into the corneous layer (Fig. 2.2b). When it matures, the granulated layer (known as the clear layer) forms interdigitations with the next layer (the oberhautchen layer), along which the epidermis of the pegs splits into two parts producing new scales (Fig. 1.6e–g). Beneath the oberhautchen layer, all the new epidermal layers of the regenerated (or neogenic) scales are formed, like in normal scales: the hard β-layer, the water-loss-limiting mesos layer, and the flexible α-layer (Fig. 2.2d; Maderson and Roth 1972; Maderson 1985; Alibardi 1995c, 2000).

Both acidic and basic keratins are present in the regenerating epidermis and the molecular mass of these proteins varies from 40 to 63 kDa (Alibardi et al. 2000). When the oberhautchen and β-layers are produced, they accumulate a large amount of a hard type of keratin, termed β-keratin. α-Keratins (soft) remain in the mature β-layer but are the prevalent keratins of the softer α-layers produced underneath the β-keratin layer. The formation of neogenic scales (regenerated) that show the same sequence of epidermal differentiation as in normal epidermis has become an essential model to analyze the molecular biology of corneous proteins in the reptilian skin. In fact, from regenerating scales, the genes coding for epidermal keratins were determined for the first time (Dalla Valle et al. 2005). Since the initial sequences were obtained, it has been easier to clone and sequence these proteins from all reptilian groups.

Few studies on regenerated skin have illustrated the complete differentiation not only of a normal epidermis but also of some epidermal specializations (Maderson 1971). These consist of sense organs (likely mechanoreceptors) or modified scales with pads made of microscopic hairy-like bristles (likely touch-sensorial or capable of adhesion to the substrate), and even some glandular structures. In some climbing geckos, numerous regenerated scales of the central area of the tail reform extensive, pad-like areas of adhesion, which are made of millions of setae, like those present in the original tail. These modified scales help the tail to tightly grasp and adhere to the substratum represented by tree branches and other rough surfaces (Bauer 1998).

2.2.2 Blood Vessels, Fat, and Meninges

After the stage of blastema formation, various tissues differentiate and grow, so sustaining the elongation of the new tail, among which there is a new vasculature, pericartilaginous fat deposits, and, more internally, meninges around the new spinal cord.

The anatomical details of the vascular network that is established in the regenerating blastema and in the elongating tail are not specifically known, but the initial vascularization of regenerating tissues is likely irregular as in the regenerative blastema of the newt (Peadon and Singer 1966). Numerous endothelial cells take up tritiated thymidine in the blastema, giving rise to narrow

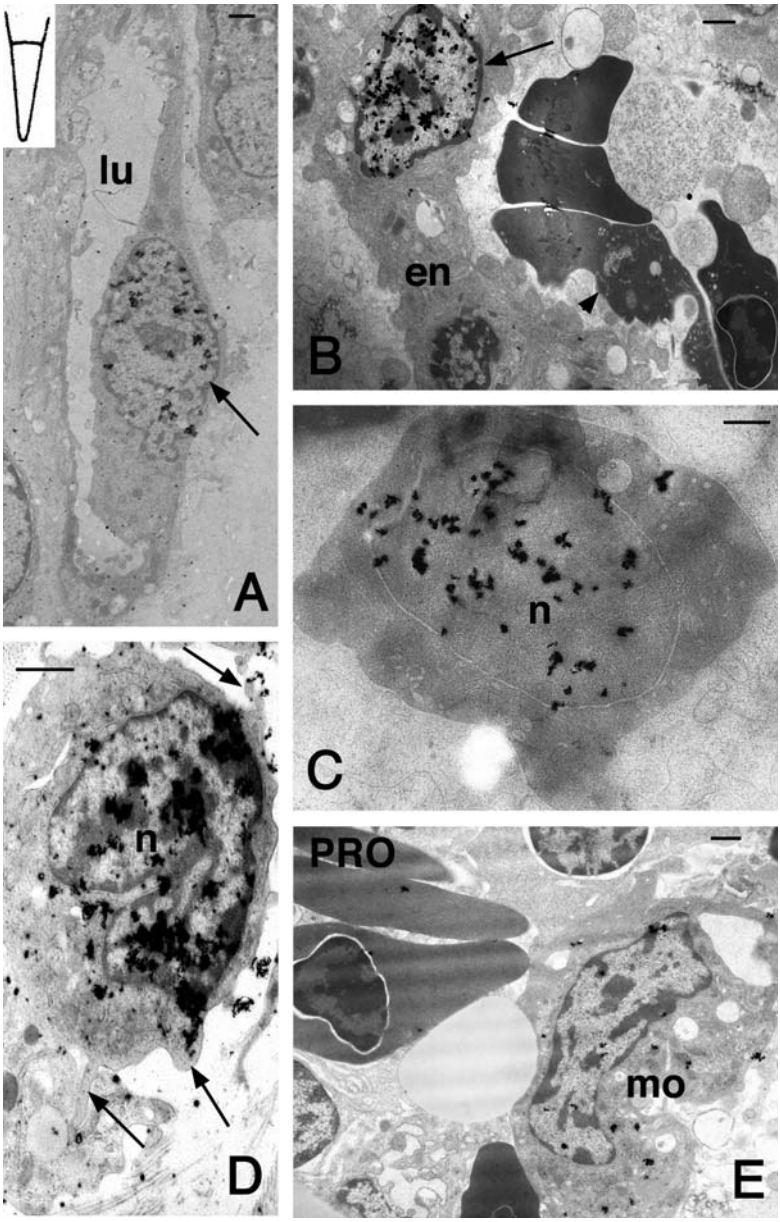

Fig. 2.4 Blood cells in regenerating tail (correspondent stage indicated in the *inset* in **a**) of *A. carolinensis* (**a–d**) and *L. delicata* (**e**). **a** Tritiated thymidine labeled nucleus of endothelial cells (*arrow*) among the blastema of the regenerating tail (the *inset* shows the approximative stage). *Bar* 0.5 μm. **b** Tritiated thymidine labeled, immature blood cells (*arrow*) in a blood island (the *arrowhead* indicates compacted erythrocytes) located at the

capillaries or to the large lacunae initially present (Hughes and New 1959; Alibardi 1993b; Fig. 2.4a, b). The initial blood vessels are of the fenestrated type and form broad lacunae among blastema cells and around the apical ependymal ampulla. Therefore, no tight blood–brain barrier is initially present in the early regenerating spinal cord, and small to medium-sized molecules such as amino acids, and likely also higher molecular weight molecules, may freely move from the blood into the nervous system and vice versa. From the apical sinusoid vessels present in the blastema, mature or immature red and white blood cells can move into the blastema, comprising polychromatophilic and orthochromatophilic erythroblasts and monocytes.

Inside these capillaries or in the larger sinusoids, red blood cells often appear not completely mature and still capable of multiplication, as is indicated by the uptake of tritiated thymidine (Fig. 2.4b, c). The increased hematopoiesis activity, elicited by the process of regeneration (Ramachandran et al. 1983; Shah et al. 1980), has allowed the erythropoietic span in lizards to be determined (Alibardi 1994c). In the lizards *Lampropholis delicata* and *Anolis carolinensis* the erythropoiesis is initiated in the bone marrow and continues during tail regeneration, also in the bloodstream. The stage from erythroblasts to orthochromatophilic nucleated erythroblasts lasts about 14 days, about twice as long as in some homeothermic amniotes (mammals) of the stage from erythroblasts to reticulocytes. It is also likely that both red and white blood cells can divide within the bloodstream during tail regeneration. Monocytes and macrophages incorporating tritiated thymidine have also been seen within the blood vessels and even in the regenerating blastema (Fig. 2.4d), but the importance of extramarrow cell multiplication of blood cells during lizard regeneration is not known. Many monocytes within blood vessels also incorporate high levels of tritiated proline, in relation to their high metabolism in comparison with a lower metabolic activity of immature or mature red blood cells (Fig. 2.4e).

Although they exist in lower numbers than blood vessels, lymph vessels are also regenerated during tail regeneration, as is illustrated for the gecko *Christimus marmoratus* (Daniels et al. 2003). During the first 3 weeks of tail regeneration, the flux of lymph is slower than in the normal tail. Lymph vessels are more actively formed from 3 to 9 weeks of regeneration, as also indicated by the activation of the vascular endothelial growth factor during this period. Most lymph vessels are localized in the subcutis, between the dermis and the underlying regenerating muscles, and carry the lymph to the liver and then to the heart.

Fig. 2.4 (continued) tip of the regenerating tail. *Bar* 0.5 μm. **c** Thymidine-labeled nucleus of proerythroblasts in the blastema. *Bar* 1 μm. **d** Thymidine-labeled nucleus of a macrophage in the blastema (*arrows* indicate cytoplasmic blebs). *Bar* 1 μm. **e** Tritiated proline labeled monocyte migrating into the blastema from a sinusoid blood vessel. *Bar* 1 μm. *cy* cytoplasm, *er* erythrocytes, *lu* lumen of the capillary, *Mo* monocyte (macrophage), *n* nucleus, *PRO* tritiated proline autoradiography

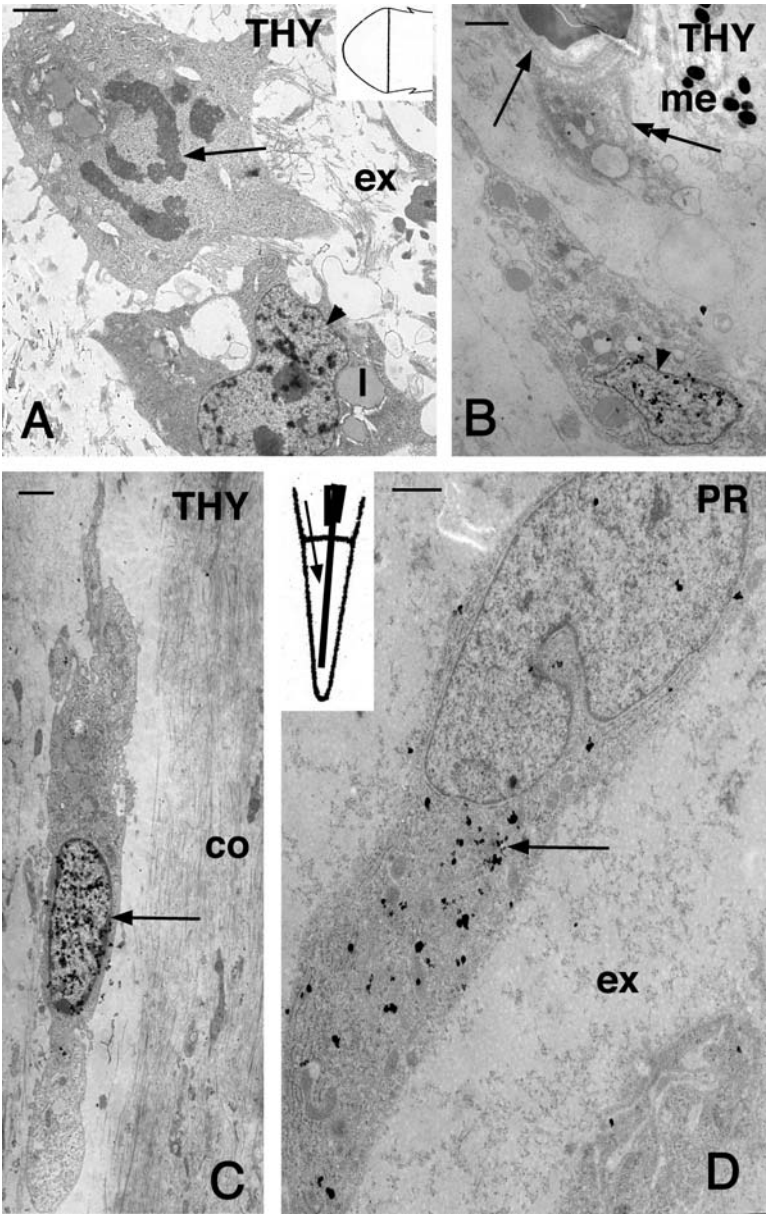

Fig. 2.5 Differentiating lipocytes in pericartilaginous regions (**a**, **b**) and meningeal cells surrounding the regenerating spinal cord (**c**, **d**). **a** Dividing cell (*arrow* on chromosomes) present within the mesenchyme close to a lipoblast with a tritiated thymidine labeled nucleus in *A. carolinensis*. *Bar* 1 μm. The *inset* shows the stage of regeneration. **b** Other thymidine-labeled lipoblasts (*arrow*) with numerous lipid droplets close to a blood vessel

In proximal regions of the elongating tail, capillaries, arterioles, and venules around the spinal cord mature into tight vessels owing to the disappearance of gaps in the endothelium and to the formation of tight junctions between endothelial cells. The latter are completely surrounded by a continuous basement membrane. These changes are observed in regenerated tails after 1 month of regeneration, and the blood vessels then now similar to those of the normal tail. The vessels are connected to the axial, caudal (dorsal) artery, from which they probably originated, and eventually join to the two main caudal veins. The process of angiogenesis appears also related to the formation of the fat tissue in the new tail.

At the stage of the elongating cone (Fig. 1.1l), in the region located between the differentiating muscles and the cartilage (Fig. 1.1m), numerous fibroblast-shaped cells often associated with blood vessels show labeled nuclei after injection of tritiated thymidine (Fig. 2.5a, b). These cells often contain small lipid droplets (0.3–1.0 μm) that indicate they are dividing lipoblasts (Alibardi 1995d). The number of fat cells and their lipid content rapidly increase, and the initial series of metameric adipomers (at least in *L. delicata*) later disappears to be replaced by an apparently unique mass of fat tissue that surrounds the cartilaginous tube. As a result, the adipose tissue is more abundant in the fully regenerated tail than in the native tail. Differentiated lipocytes retain the thymidine label, indicating that they do not frequently multiply when differentiation is under way. However, some lipocytes with large lipid droplets are still capable of taking up tritiated thymidine at 4 h after injection, suggesting that they can still divide.

Aside from the uptake of tritiated thymidine in their nuclei, lipoblasts also take up tritiated proline, which concentrates in the ergastoplasm, indicating not only an active cell division but also protein synthesis at early stages of tail elongation. The burst of cell division mainly occurs in cells of the submuscular connective tissue, 1–2 mm distant from the tip of the regenerating tail. The initial small lipid droplets rapidly merge into large droplets that occupy most of the cell at maturity until a unilocular cell is formed in proximal regions of the regenerated tails around 1 month from the beginning of tail regeneration.

Around the apical regions of the regenerating spinal cord, within 1–2 mm from the tail tip, mesenchymal cells tend to flatten and these cells become surrounded by numerous collagen fibrils (Fig. 2.5c, d). These flat fibroblasts actively take up tritiated thymidine and especially proline, indicating these cells are metabolically more active than the mesenchymal type from which they derive, and are still capable of intense cell multiplication. The numerous, tendentially oriented

Fig. 2.5 (continued) (*arrowhead*) in *L. delicata*. *Bar* 1.5 μm. **c** Flat meningeal fibroblast with a tritiated thymidine labeled nucleus (*arrow*) in *A. carolinensis*. *Bar* 1 μm. **d** Meningeal fibroblast actively synthesizing collagen as indicated by the tritiated proline labeling (*arrows*) in the cytoplasm (*L. delicata*). The *inset* gives the indicative position of this cell around the spinal cord (*arrow*). *co* collagen fibrils, *l* lipid droplet, *ex* extracellular matrix, *me* melanocyte, *n* nucleus, *PR* tritiated proline autoradiography image, *TH* tritiated thymidine autoradiography image

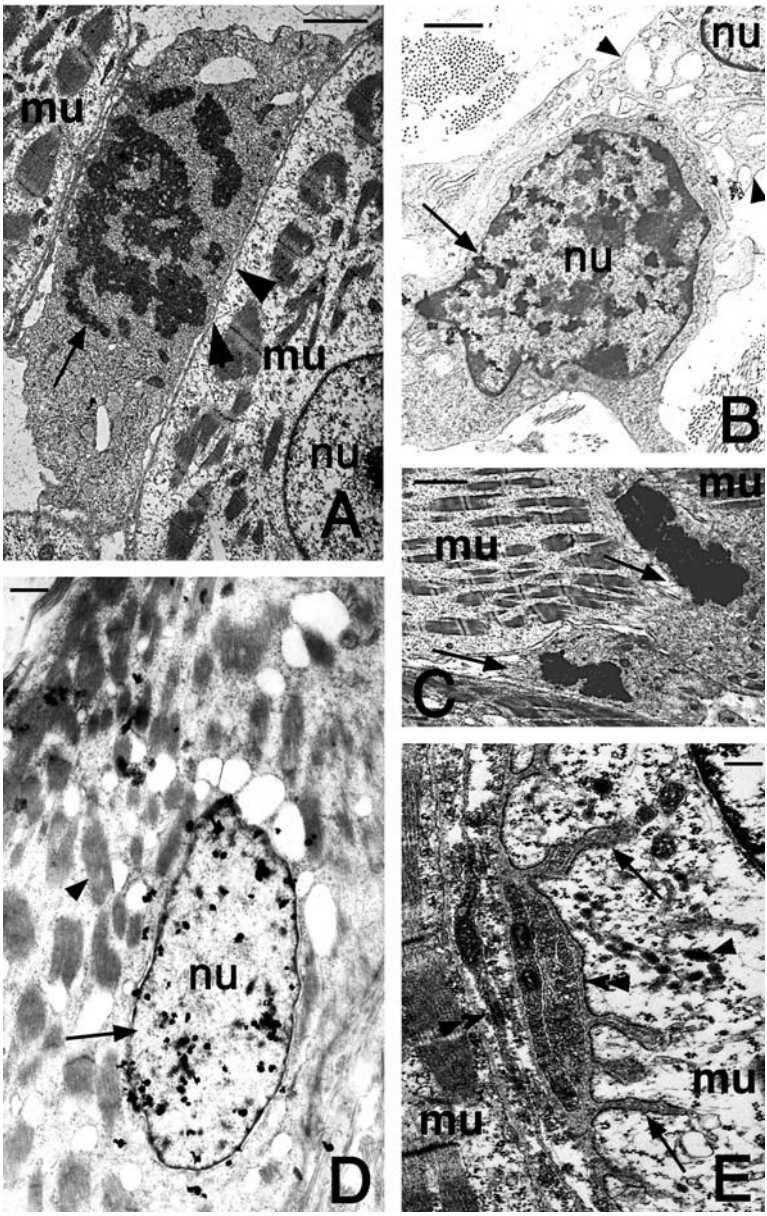

Fig. 2.6 Ultrastructural detail of regenerating muscles in elongating tails of *A. carolinensis* (**a, b**) and *L. delicata* (**c–e**). **a** Dividing cell (*arrow* on forming chomosomes) that is likely merging (*arrowhead*) with regenerating muscle cells. *Bar* 1 μm. **b** Thymidine-labeled nucleus of a myoblast in the phase of fusion (*arrowheads*) with another myoblast (4 h after injection). *Bar* 1 μm. **c** Detail of a dividing cell (*arrows* point to the nuclei in telophase)

collagen fibrils along the axial ependyma form a relatively regular dense connective tissue surrounding the spinal cord (Fig. 2.8b). These fibers are likely involved in mechanically sustaining the new spinal cord during the bending movements of the tail. This hypothesis is also suggested by the case of meningeal regeneration in the New Zealand gecko *Hemidactylus maculates*. In this species, the meningeal fibroblasts of the regenerated spinal cord synthesize a large amount of elastin and are eventually surrounded by numerous and large elastic fibrils in addition to collagen fibrils (Alibardi and Meyer-Rochow 1989). In this species, the regenerated tail is commonly curled up around objects of tree branches. This activity might result in the bending or tearing of the regenerated spinal cord within the cartilaginous tube. The presence of an elastic meninx inside the curling elastic cartilaginous tube in the regenerated tail of this species allows the functionality of the tail without damaging the delicate spinal cord.

2.2.3 Muscles

In case of autotomy, muscle regeneration in the blastema derives from stem cells localized in the autotomy septum, adjacent to satellite cells of the stump muscles (Bayne and Simpson 1977). Therefore, it is likely that myogenic cells derived from satellite cells of old muscles can detach from the fiber after lesion, migrate to the stump, and contribute to the formation of a blastema. Later, these cells reform the new muscles. Although myoblasts merge in vivo, they can still synthesize DNA, and DNA synthesis also seems to occurs in some of the nuclei already incorporated in myotubes (Alibardi 1995e). Tritiated thymidine labeled nuclei and mitotic nuclei are mainly present near the myosepta or in the more external parts of the myotome (Fig. 2.6a–c). This observation suggests that the growth of the regenerating muscle fibers mainly occurs in the area contacting the myosepta. An in vivo autoradiography study has indicated that new myocells penetrate into the myotube in 2–3 days, and that centrally located and labeled nuclei are seen after 12 days from the injection of tritiated thymidine (Fig. 2.6d).

When the regenerating tail is more than 1 cm long, in the lizard *Podarcis muralis*, in the skink *Gonglylus gongylus* (Filogamo and Marchisio 1961), as well as in the gecko *Hemidactylus bowringi* (Liu and Maneely 1969b), the long myotubes are reached by nerves that form ramified neuromuscular junctions (Hughes and New 1959). Thin fibers (0.5–1 μm) are believed to be sensory fibers, whereas thicker axons are believed to be motor fibers. A diffuse distribution of cholinesterases has

Fig. 2.6 (continued) located at the end of an elongating muscle fiber. *Bar* 2.5 μm. **d** Thymidine-labeled nucleus (*arrow*), at 12 days after injection of tritiated thymidine. The *arrowhead* points to a myofibril. *Bar* 1 μm. **e** Detail of a forming neuromuscular junction (*double arrowheads*) with deepening folds (*arrows*). Various dense core vesicles (*arrow*) are present in this end plate. *Bar* 200 μm. *mu* muscle cell/myotube, *nu* nucleus

been detected in myoblasts and also in myotubes, and the enzymes become restricted to the neuromuscular junction of mature regenerated muscles (Filogamo and Marchisio 1961; Sassu and Marchisio 1963; Shah and Chakko 1972). In most myofibers of the nonautonomous part of the tail, the neuromuscular junction (motor plaque) is localized in the medial/central part of the fiber. Conversely, in regenerating muscles the neuromuscular junction is present in the distal extremity of the fiber, close to the connective septa (Hughes and New 1959; Filogamo and Marchisio 1961; Sassu and Marchisio 1963; Gabella 1965). The first neuromuscular junctions are seen in long myotubes, localized by their extremities and more infrequently in the central part (Fig. 2.6d). This pattern of innervations seems to derive from the relatively late period in which the growing nerves reach the regenerated muscles in comparison with the more rapid innervation process that occurs during normal development. In fact, in regenerating muscles the growing nerves derived from the stump spinal cord or ganglia reach the new muscles at the stage of elongating mytotubes, containing various nuclei and numerous myofibrils. The neuromuscular junction is therefore established in the more immature part of the sarcoplasm, namely, at the extremity of the fiber. The late innervations during muscle regeneration explain the flaccidity and lack of contractility of the early regenerated tail, where numerous myotomes are already present

Ultrastructural studies have indicated that the motor end plate is immature at the extremity of regenerating fibers (Bottazzi-Bacchi and Sassu 1973; Alibardi, personal observations). Progressive stages of end-plate maturation have been described. From a small synaptic bouton contacting superficially the muscle fiber, an invaginated bouton is derived where the initial junctional folds are present (Fig. 2.6e). At later stages, the folds become deeper and the bottom surface is more extended in the more deeply located neuromuscular junction.

The process of myogenesis has been reproduced and analyzed in vitro (Simpson and Cox 1967; Cox 1969a, b; Simpson and Bayne 1979) using an initial growth medium for cell survival and proliferation, and later a fusion medium, favoring myotube formation and fiber differentiation. These studies on the lizard model of myogenesis have contributed to detailed knowledge of the process of myogenesis in vertebrates.

Fusiform myoblasts, derived from promuscle aggregates and cultivated for 8–9 days in the first growth medium, become rounded and the postmitotic cells enter the G1/G0 phase of the cell cycle, ready to merge into myotubes. In fact, whereas fusiform myoblasts take up tritiated thymidine, most of the round myoblasts do not take up this DNA precursor. The surface of round and prefusion cells shows numerous blebs or filopodia, and few of these cells have a smooth surface (Bayne and Simpson 1977). Instead, a smooth surface is generally typical of stretching myoblasts and forming myotubes. A specific cell antigen indicating muscle differentiation, indicated as Ag1422, is present in G0 phase and myosin-positive rounded myoblasts, but the antigen is absent in round myoblasts still capable of proliferation and that also appear to be myosin-negative (Marusich and Simpson 1983).

A detailed ultrastructural analysis of prefusion (round) myoblasts has shown the gradual formation of Z-bands, and has indicated that this is a useful system for the molecular analysis of myogenesis in general (Chlebowski et al. 1973; Bayne and Simpson 1977). This analysis has shown that the production of bundles of thin filaments of 7–8 nm (actin) precedes the appearance of the thick filaments of 12–14 nm (myosin). However, an equal number of thick (myosin) and thin (actin) bundles is rapidly produced in these cells as they differentiate, as confirmed by the immunoreactivity for myosin. Also acetylcholinesterase is present in some of the prefusion myoflasts (Simpson and Bayne 1979). This indicates that prefusion myoblasts are heterogeneous, in particular some are likely in G1 phase (acetylcholinesterase negative), whereas other myoblasts are in G0 phase (acetylcholinesterase positive). As these cells merge into myotubes, the immunoreactivity for myosin increases. The filaments assemble into myofibrils delimited by Z-bands forming sarcomeres that are arranged in linear rows, as observed in vivo (Fig. 2.6a, c, d). Some of the myosin-positive cells containing striated myofibrils can take up tritiated thymidine, suggesting that these nuclei may still divide, as observed in vivo.

2.2.4 Cartilage

The more apical 400–1,000 μm of the differentiating cartilaginous tube contains large extracellular spaces rich in acid mucopolysaccharides and relatively scarce fine fibrils of collagen synthesized from fusiform chondroblasts (Shah and Hiradhar 1975; Alibardi and Sala 1983). Initially in the blastema and in the precartilaginous aggregates, neutral or acidic but nonsulfated mucopolysaccharides are present, probably represented by hyaluronate, like in the amphibian blastema and cartilage (Toole and Gross 1971; Shah and Hiradhar 1975; Alibardi and Sala 1983; Alibardi, unpublished biochemical data).

From the precartilaginous aggregate in the regenerating cone until the elongating tail stage, numerous chondroblasts take up tritiated thymidine in both central and external regions of the cartilaginous tube (Figs. 1.6j, 2.7a). Therefore, cartilage growth occurs by both interstitial and appositional cell multiplication, although isogenic islands are rarely observed. The labeling index is higher in the apical regions and decreases in proximal regions of the cartilaginous tube (nearly one fifth of that in apical regions; Cox 1969a; Alibardi 1995b). In more proximal regions of the cartilaginous tube and near the old vertebra of the stump, the intercellular matrix becomes reduced around chondrocytes. In this region, few cells are seen to incorporate tritiated thymidine in both the inner region and the outer (external) region of the cartilaginous tube, suggesting that the growth of this region of the cartilaginous tube takes place slowly for both interstitial and appositional growth within the first month of regeneration (or at least until the new tail is completely scaled).

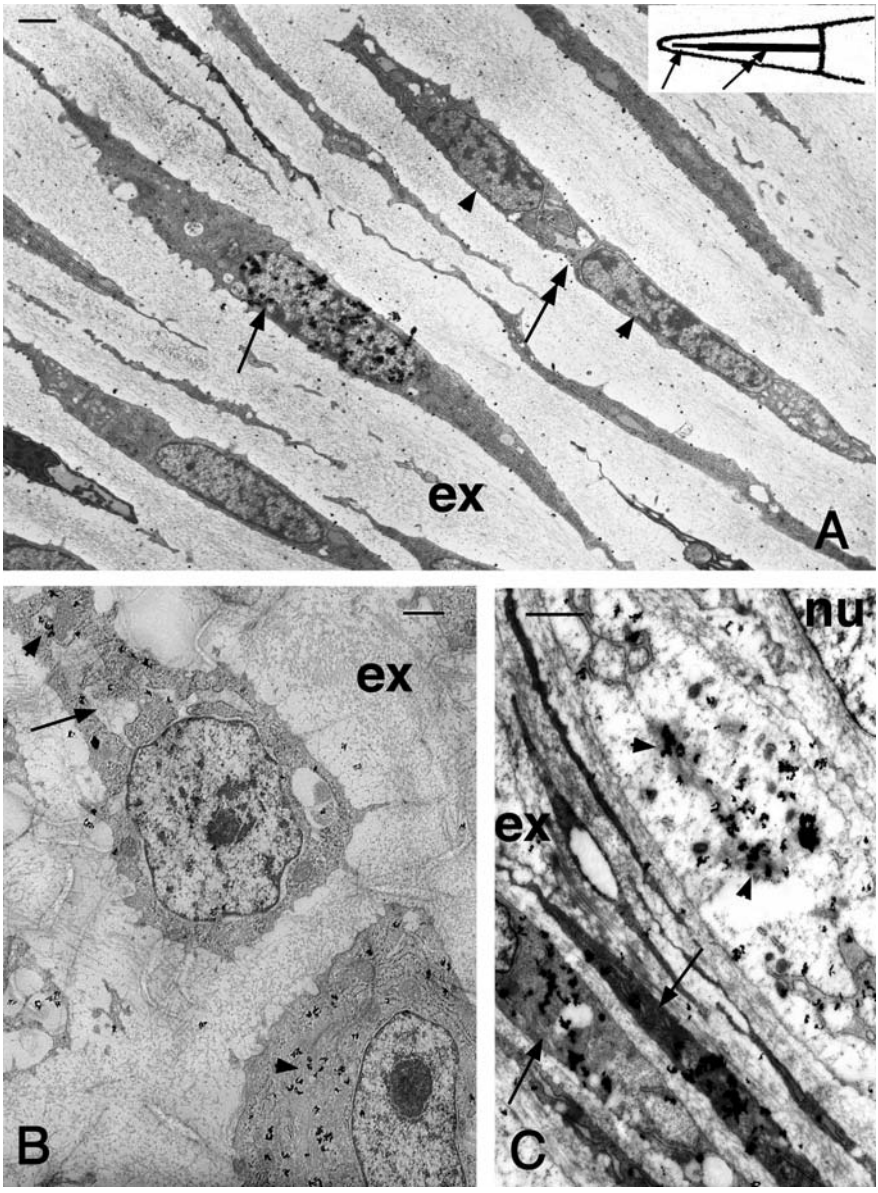

Fig. 2.7 Ultrastructural details of regenerating cartilage in *A. carolinensis* (**a**) and *L. delicata* (**b**, **c**). **a** Apical cartilage (*arrow* in the *inset*) showing a thin cell that has completed division (*arrowheads* on the nuclei; the *double arrow* indicates the separation cytoplasm in telophase). Another cell has a tritiated thymidine labeled nucleus (*arrow*). *Bar* 1 μm. **b** Two chondroblasts in the medial area of the cartilage (*double arrow* in the *inset* in **a**) with large ergastoplasmic cisternae (*arrow*) and incorporating tritiated proline (*arrowheads* on the

The early chondroblasts are metabolically very active cells as they take up tritiated proline in a higher amount in comparison with most epidermal cells, fibroblasts, adipose cells, and endothelial cells (Fig. 2.7b). Half an hour after injection of tritiated proline, the autoradiographic signals (dense curling silver trace grains) are mainly localized over the endoplasmic reticulum and the secretory cisternae (Fig. 2.7b). One hour after injection, the tracer is also abundant in the Golgi apparatus (Fig. 2.7c), but not outside chondroblasts. Three hours after injection, silver granules are also seen in the extracellular matrix and decrease inside chondrocytes (Alibardi 1995b). Therefore, the time of synthesis of collagen and acid mucopolysaccharides in lizard chondrocytes at the optimum temperature is similar to that for mammalian cells (Leblond 1991), although extrusion of labeled proteins appears to take somewhat longer in lizard cells.

When cartilaginous cells become more ovoidal or even rounded (Fig. 2.7b), about 1 mm from the apical tip of the regenerating cartilage in elongating tails, the cartilaginous matrix becomes richer in collagen fibrils and in sulfated mucopolysaccharides. This is indicated by the intensification of the periodic acid–Schiff stain reaction (collagen), by the appearance of metachromasia using toluidine blue, and by the reactivity to acidic alcian blue (indicating acid mucopolysaccharides with pI lower than 3) (Alibardi and Sala 1981, 1983). Other biochemical analyses (Alibardi, unpublished data) confirm the histochemical observations. The mature, mainly cellular cartilage only occasionally forms isogenic groups (two close chondrocytes), and chondroblasts remain isolated from one another.

The regenerated cartilaginous tube in most species so far analyzed is made of hyaline cartilage with a scarce matrix, which is responsible for most of the stiffness of the mature regenerated tail, especially after the cartilage has begun calcify. The formation of a hyaline cartilage with broad intercellular spaces and frequent isogenic groups has been noted in the lizard *Agama agama* (Alibardi and Meyer-Rochow 1989). Therefore, in most species of lizards the new tail is not very functional aside from having a balancing and lipid-storage function.

Differently from most lizards, in the gecko *Hemidactylus maculatus* elastic cartilage is formed instead of a stiff hyaline cartilage (Alibardi and Meyer-Rochow 1989). Chondrocytes become hypertrophic and contain very high amount of glycogen. Their Golgi apparatus produces dense vesicles that contain elastin, and the vesicles are extruded into the extracellular matrix that contains nonbanded collagen of undefined type. In more proximal and mature regions of the cartilaginous tube, the extracellular matrix contains many amorphous elastic bundles. The production of such an elastic cartilage, in conjunction with the

Fig. 2.7 (continued) silver grains) 1 h after injection. *Bar* 1 μm. **c** Detail of a maturing chondroblast contacting the fusiform cells of the external perichondrium (*arrows*). An intense labeling is also present in the Golgi apparatus (*arrowheads*) 1 h after injection of the radioactive precursor. *Bar* 0.5 μm. *ex* extracellular matrix, *nu* nucleus

formation of meninges rich in elastic fibrils (elastic meninges), allows the new tail of this gecko to curl up like the original tail. Therefore, the regenerating tail can be used for grasping and for climbing trees as this species is preferably arboreal.

Like in fractured bones of lizards (Pritchard and Ruzicka 1950), the replacement of cartilage tissue of the cartilaginous tube with bone occurs very slowly in lizards. Details of the process of calcification in mature regenerated tails are partially known (Calori 1858; Alibardi and Sala 1981; Alibardi and Meyer-Rochow 1989). In the more proximal regions of the cartilaginous tube, before calcification chondrocytes become hypertrophic and accumulate much glycogen. The process of calcification starts in the inner and outer cartilaginous rings in contact with the perichondrion (Fig. 1.7k, l). The replacement of degenerating chondrocytes initially occurs through the addition of new chondroblasts from the inner and the outer perichondrium, but later osteoblasts are produced in these ringlike regions where a true periosteum is formed as continuation of that of vertebrae (see the arrowheads in Fig. 1.7m). This process begins at 2–3 months after amputation in *Podarcis sicula* and at 6–8 months after amputation in *Sphenodon punctatus*. Calcium salts are initially deposited over the fine matrix grains, perhaps made of glycosaminoglycans, present among the collagen fibrils of the extracellular matrix in the outer and inner rings of the proximal cartilaginous tube (this occurs after 2 months from amputation in *P. sicula*). As a consequence, the cartilaginous matrix is destroyed and chondrocytes degenerate. Mineral deposits rapidly obscure the initial glycoprotein–collagenous network of the intercellular matrix. A true lamellar bone tissue slowly replaces the calcified cartilage and the inner and outer laminae.

2.2.5 Spinal Cord and Central Nerves

Aside from the apical ependymal ampulla where migrating cells seem to be loosely arranged (Fig. 1.4f, h), in more proximal regions ependymal cells form a close epithelium owing to the presence of numerous desmosomes (Simpson 1968; Egar et al. 1970). Ependymal cells are polarized with a relatively developed ergastoplasmic reticulum, Golgi apparatus, and numerous microvilli contacting the central canal during 2–4 weeks of regeneration. Numerous granules and vesicles containing glycoprotein material are secreted into the lumen (Turner and Tipton 1971; Alibardi and Sala 1986, 1989). Ependymal cells differentiate in more proximal regions of the spinal cord, at 2 mm from the tip and in regenerated tails over 4 weeks from the amputation. These cells initially terminate onto the basement membrane with a large base (Fig. 2.8a), but their basal part becomes thinner and branched as they mature. The latter cells present broad lateral spaces (tunnels in three-dimensional perspective) that are occupied by

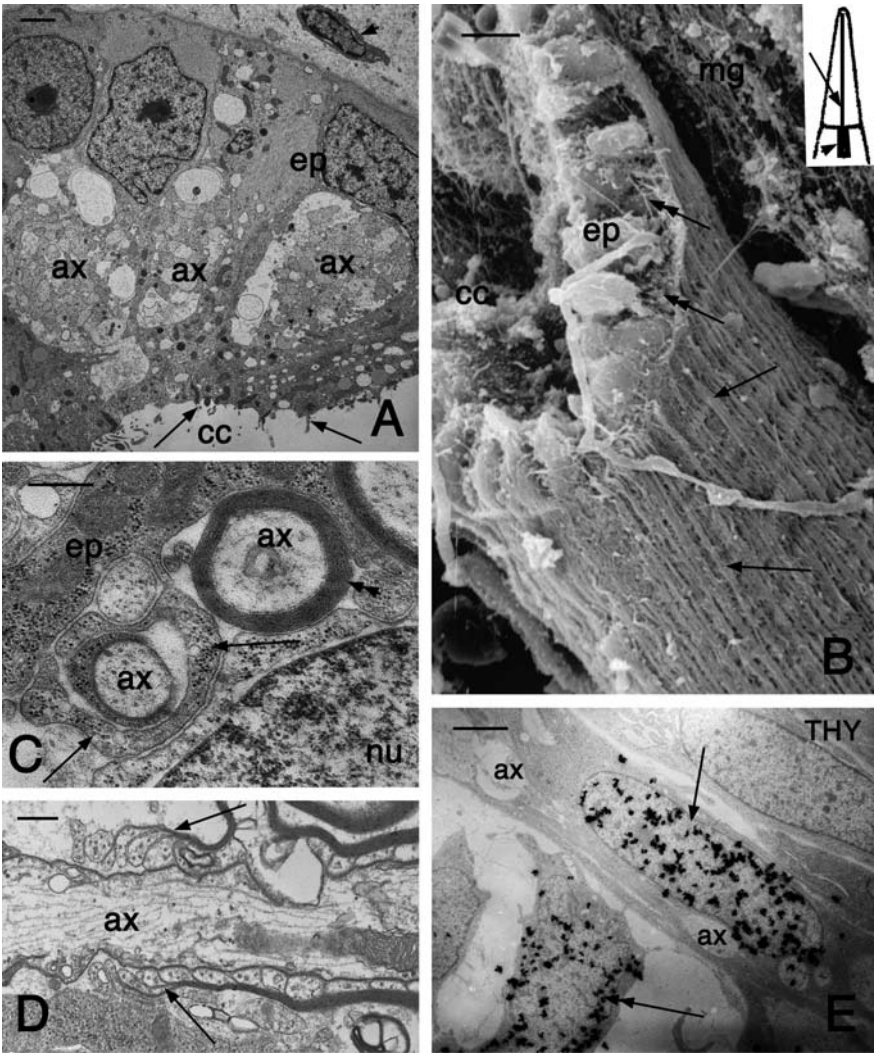

Fig. 2.8 Ultrastructural aspects of the regenerating spinal cord (**a**–**d**) and peripheral nerve (**f**). **a** Regenerated spinal cord of *P. sicula* in medial regions (see the indicative position in the *arrow* in the *inset* in **b**). The *arrow* indicates the luminal face and the *arrowhead* indicates the meninges. *Bar* 1 μm. **b** Scanning electron microscopic view of medial regenerated spinal cord in *A. carolinensis*. The *arrows* indicate collagen fibrils of the meninges. *Double arrows* indicate subpial spaces where the regenerating axons are located. *Bar* 10 μm. **c** Cross sections of two axons at the beginning of myelination (*arrowhead*) from elongation of ependymal tanycytes (*arrow*; 2 months of tail regeneration in *P. sicula*). B*ar* 250 nm. **d** Detail of a myelinating axon showing the terminal pedicels (*arrows*) of the oligodendrocyte in *Hemydactilus maculatus*. *Bar* 250 nm. **e** Two thymidine-labeled Schwann cells (*arrows*, 4 h after injection of the DNA precursor) surrounding a regenerating axon of *A. carolinensis*. *Bar* 1 μm. *ax* axons (located in among ependymal cells), *cc* central canal, *ep* ependymal cells, *nu* nucleus, *THY* tritiated thymidine labeling image

bundles of axons or axonal sections. Initially, ependymal cells act as a guide for the descending regenerating axons derived from the spinal cord stump (Simpson 1970, 1983). After 2 months of regeneration, ependymal cells tend to produce a narrow elongation containing bundles of intermediate filaments that terminate on the basement membrane, and are termed ependymal tanycytes (Simpson 1968; Alibardi 1990–1991). The basement membrane is in contact with regenerated meningeal cells and fibers, and the latter become numerous in regenerates over 2 months of age (Fig. 2.8b). From tanycytes, small elongations grow toward the axons and begin to enwrap the axons, so amyelinic or eventually truly myelinic axons are formed (Fig. 2.8c). In regenerates older than 2 months, numerous axons become myelinated from cells that have lost the epithelial organization and are recognizable as oligodendrocytes (Fig. 2.8d, e). Some of the myelinating cells are likely Schwann cells that have probably migrated into the regenerating spinal cord from actively dividing cells present around the growing nerves of the blastema (Fig. 2.8e) or from intracartilaginous nerves (Fig. 1.13a–d). Other glial cells are indicated as astrocytes, mainly owing to their pale cytoplasm and their elongation, that are rich in intermediate filaments, and by the lack of an axon and synaptic boutons.

The neuronal component of the new spinal cord is scarce and limited to specialized cerebrospinal fluid contacting neurons (CSFCNs). These small neurons are metabolically more active than ependymal cells, as indicated by their higher uptake of tritiated GABA and proline, which can probably circulate through the fenestrated blood vessels that surround the early regenerating spinal cord (Alibardi 1993b; Alibardi et al. 1993a, b). Neural nitric oxidase, the enzyme forming the neurotransmitter nitric oxide, is particularly abundant in these neurons innervating the growing blastema (Cristino et al. 2000a, b), but its role is not clear. Recent ultrastructural analysis has shown that CSFCNs are also regenerated in the reactive ependyma of the injured lumbar spinal cord before the ependyma becomes trapped with a glial scar. This observation indicates an intrinsic neurogenetic potential of the reactive ependyma of lizards at both tail and more rostral levels (Alibardi, unpublished observations).

CSFCNs have a pear-shaped body (12–18 μm), an electron-pale cytoplasm, sparse endoplasmic cisternae that sometimes form short Nissl bodies, and few axosomatic synaptic boutons (Fig. 2.9; Alibardi and Sala 1986, 1989; Alibardi and Meyer-Rochow 1988). These cells produce growth cones during their differentiation among ependymal cells. The presence of 90–120-nm-diameter large dense core vesicles, derived from the Golgi apparatus, indicates that these cells store and utilize catecholamines or, more likely, neuropeptides. CSFCNs possess a tuft of 2–6-μm-long stereocilia that contact the central canal and are more or less continuously regenerated. With use of tritiated thymidine autoradiography, it has been established that these cells derive from a few pale elements present among ependymal cells, and that they completely differentiate into CSFCNs in about 20 days (Alibardi et al. 1992; Alibardi 1993b). These neurons represent 5–10% of the entire cell population of the regenerating spinal cord at about

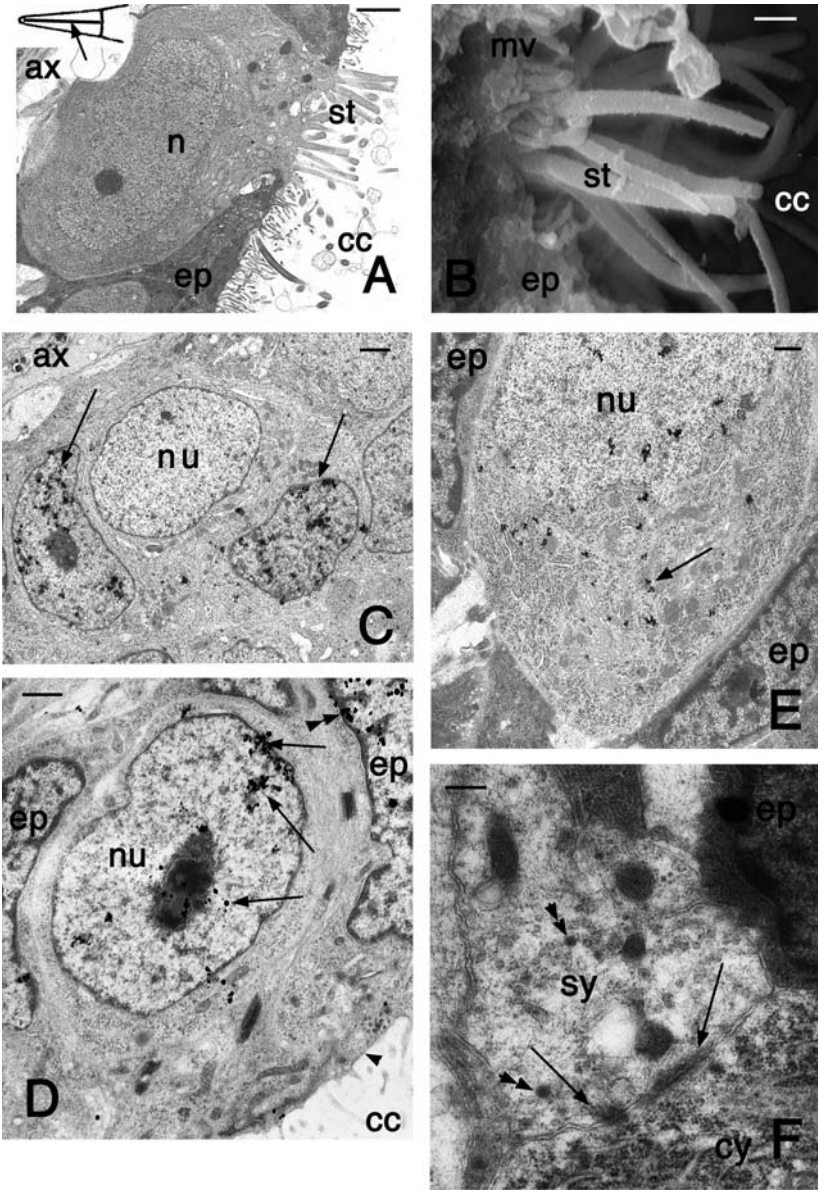

Fig. 2.9 Characteristics of regenerated cerebrospinal fluid contacting neurons (CSFCNs). **a** Pale CSFCN with tufts of stereocilia in the lumen of the central canal in *Leiolopisma nigriplantare maccanni*. The *inset* indicates the position of this cell in the regenerated spinal cord (*arrow*). *Bar* 2 μm. **b** Scanning electron microscope detail of the tuft of stereocilia of a CSFCN in *A carolinensis*. *Bar* 0.5 μm. **c** Differentiating CSFCNs between two tritiated thymidine labeled cells (*arrows*; 2 days after injection of the DNA precursor) in

1 month of tail regeneration (Fig. 2.10a): however, their number later decreases, probably owing to the isolation of the regenerated spinal cord inside the cartilaginous tube. During the tail elongation and maturation stages, neurons degenerate and are resorbed by ependymal phagocytes or by macrophages that have migrated into the spinal cord (Alibardi 1986). The number of CSFCNs increases after treatment with GABA, which seems to retard their degeneration (Alibardi et al. 1987). This suggests that under appropriate stimulation of the spinal cord, more CSFCNs may survive (see the later discussion).

The scarce numbers of axons present in the regenerating spinal cord mainly belong to descending axons and few axons form ascending pathways (Duffy et al. 1990, 1992). The ascending projections mainly derive from the few regenerated CSFCNs and appear to terminate on neurons present in the more proximal spinal cord in the stump (Duffy et al. 1992, 1993; Alibardi 1993a, b). Only a few long descending projections, largely originating from few a rhomboencephalic nuclei, reach down the regenerating spinal cord in the tail.

The descending or ascending axons are believed to form up to 2,000 axonal cross-areas, but this high number probably represents not individual axons but sprouting collaterals from descending axons coming from neurons of the stump (Duffy et al. 1990, 1992). Reactive motoneurons undergo a process of swelling during the first few weeks after amputation, with nuclear eccentricity and chromatolysis, all processes derived from the interruption of the axons from their target cells (Giuliani 1878; Marotta 1946; Baffoni 1950; Zannone 1953; Cristino et al. 2000a, b). These neurons later become hypertrophic and their nucleoli also increase in size. The hypertrophic motoneurons of the stump in particular increase their axosomatic synapse coverage since these cells receive more numerous terminals from descending axons of rostral sections of the spinal cord and even from the rhomboencephalon (Duffy et al. 1990).

The direct innervations of the regenerating tail, especially of the new muscles from the motoneurons within the last three segments of the spinal cord (roughly corresponding to the last three ganglia), have been shown using tract-tracing methods (Cristino et al. 2000a, b). No hypertrophic and labeled neurons were found in more rostral areas of the spinal cord (sacral, thoracic, and cervical).

Fig. 2.9 (continued) *L. delicata*. *Bar* 1 μm. **d** Lightly thymidine labeled nucleus (*arrows*) of a CSFCN (the *arrowhead* shows the contact with the central canal) 22 days after injection of the DNA precursor in *L. delicata*. A few silver grains (*double arrowhead*) are present over the chromatin of ependymal cells. *Bar* 1 μm. **e** Silver grains (*arrow*) from injected, tritiated GABA within CSFCNs. *Bar* 0.5 μm. **f** Detail of a synaptic bouton contacting a regenerated neuron. *Arrows* indicate the synaptic thickenings; The *double arrowhead* points to dense core vesicles. *Bar* 250 nm. *ax* axons, *cc* central canal of the ependymal tube, *cy* cytoplasm of postsynaptic neuron, *ep* ependymal cell, *nu* nucleus of CSFCN, *mv* microvilli, *st* stereocilia, *sy* synaptic bouton

Recent molecular analysis in geckos with a regenerating tail has shown that a potent inhibitor of axonal regeneration, identified as a myelin-associated glycoprotein precursor, is downregulated during the first 2 weeks of spinal cord regeneration (Liu et al. 2006). Therefore, a favorable environment is present in the lumbar and caudal spinal cord after transection. Another gene product, brain protein 44-like, is instead upregulated in the transected caudal spinal cord (Jiang et al. 2007). The activity of the latter gene seems to be linked to the stimulation of apoptosis, a process that is probably present during the first 2–3 weeks of spinal cord regeneration in lizards (Alibardi 1986; Alibardi and Sala 1986).

The connection between regenerated and normal spinal cord is quite limited, and even less with the brainstem. The presence of some neurons in rhomboencephalic nuclei, projecting to the regenerating spinal cord or to neurons in the proximal stump spinal cord of the tail, suggests that some mechanoreceptorial stimuli collected in the tail are transmitted to higher centers of the spinal cord and possibly to the brainstem. The resemblance of CSFCNs with inner hair receptors of the utriculus or sacculus has suggested that these neurons may be involved in monitoring the movement of the cerebrospinal fluid or of the Reissner fiber inside the ependymal canal (Alibardi and Meyer-Rochow 1988; Alibardi et al. 1993a). The latter role is not only supported by the cytological characteristics of these cells, but also by some experimental data (Alibardi et al. 1993a). Because these neurons are isolated within the cartilaginous canal, their survival chances decrease after 2 months of regeneration unless they are stimulated. This hypothesis has been tested by increasing the mechanosensory input to lizards during tail regeneration, leaving the animals in cages with 8–10 h/day of gentle but continuous rolling movement alternated with a circling movement for a period of 23 days after the formation of the regenerative blastema. These experimental conditions kept the lizards in continuous movement during the stimulatory period; in particular, the tail of these lizards tended to counterbalance the oscillatory and rotating movements of the body. This condition possibly increased the movement of the cerebrospinal fluid inside the ependymal canal. After 23 days in which lizards were regenerating their tail (6–10 mm long), the tail was analyzed histologically, counting the percentage of CSFCNs present in "stimulated" compared with normal lizards (Fig. 2.10b, c). These initial data indicated a small but significant increase of the percentage of CSFCNs in the experimental group in comparison with the normal group. The experiment suggests that a stimulating environment where more mechanical performances are required may enhance the survival of these cells, further pointing out that they may be receptors of fluid movement.

Other possible roles of CSFCNs within regenerated tails remain speculative, especially as possible trophic source of neurotrophic factors affecting tail regeneration. In fact, the dependence of tail regeneration on the regeneration of the spinal cord has suggested that some neurotrophic molecules released into the spinal fluid in the ependymal ampulla or into the surrounding cells of the blastema may have a possible role in stimulating tail regeneration and

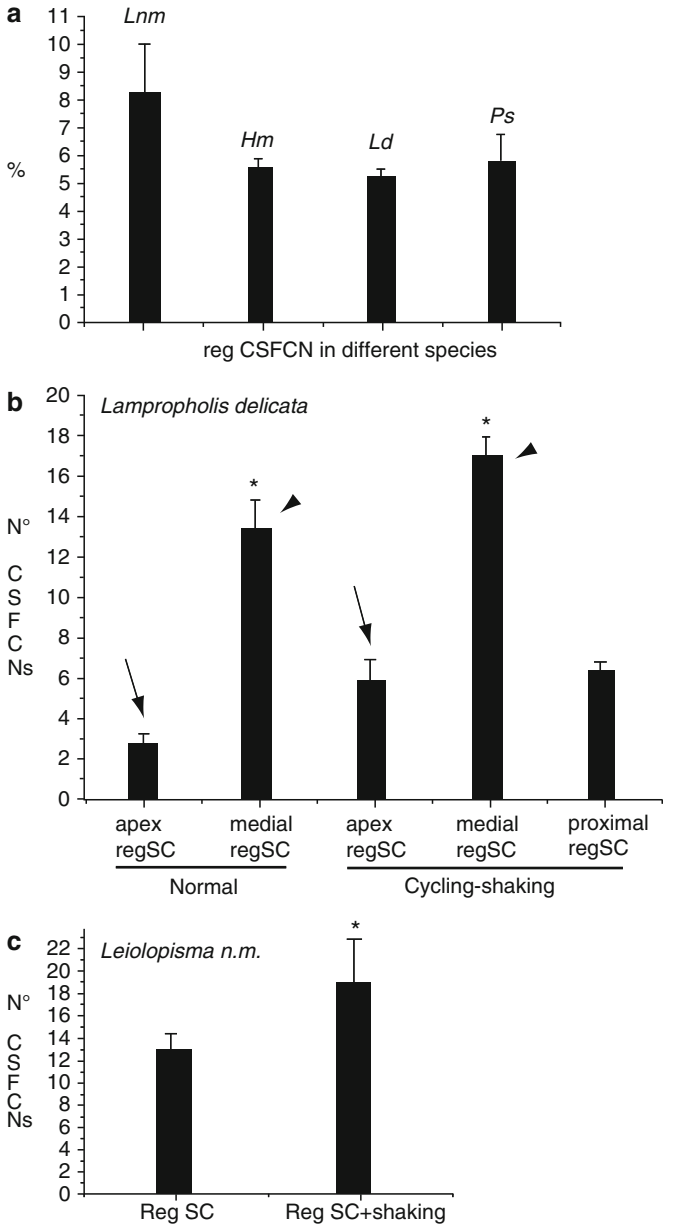

Fig. 2.10 The number of CSFCNs (percentage among ependymal cells, mean, and standard deviation) in different regions of the regenerating tail in normal conditions (**a**) along the entire regenerated spinal cord) and in experimental conditions (**b**, **c**). In **b** *arrows* and *arrowheads* indicate the comparison of the same region of the regenerated spinal cord for normal and experimental conditions. *Asterisks* indicate significant differences. In **c** the medial region of the regenerated spinal cord was counted for cells. *Lmn*, *L. nigriplantare maccanni*, *Ld*, *L. delicata*, *Ps*, *P. sicula*, *Hm*, *H. maculatus*

chondrogenesis (Simpson 1964; Alibardi et al 1988). Further work is, however, required on the latter problem.

2.2.6 Spinal Ganglia and Peripheral Nerves

The innervation of mesenchymal cells and myoblasts by nerves derived from spinal ganglia has been repeatedly observed (Hughes and New 1959; Filogamo and Marchisio 1961; Alibardi and Miolo 1990; Alibardi 1996b). The ultrastructural analysis has shown that many growing axons in the blastema store dense core vesicles of likely peptidergic content. These nerve terminals do not form synaptic specializations with blastema cells but release the content of these vesicles on the surface of blastema cells. Some blastema cells ensheating these terminals appear as Schwann cells mixed with other mesenchymal cells, and they give rise to nonmyelinated axons. Schwann cells actively take up tritiated thymidine and multiply around the growing nerves derived from the last three spinal ganglia in the stump.

In the normal tail, spinal ganglia produce two dorsal and two ventral branches that innervate the muscles and the skin belonging to three caudal segments of the tail, each corresponding to three scale verticals (Terni 1920; Fig. 1.1q). In the regenerating tail, the regenerated, segmental muscles are capable of contraction and are essentially innervated by motor and sensory nerves from the three closest ganglia of the stump, which extend their normal competence to many more targets.

The regeneration of some neurons in the two most proximal ganglia innervating the regenerating tail has been reported (Zannone 1953; Charvat and Kral 1969). However other studies performed using tritiated thymidine have shown that whereas satellite (glial) cells proliferate and increase in number, no new neurons are formed in the proximal ventral horns of the spinal cord or in the spinal ganglia during tail regeneration (Alibardi and Miolo 1990; Duffy et al. 1990, 1992; Alibardi 1995b). Also the tritiated thymidine labeled differentiated neurons observed in a few cases in both spinal cord and ganglia can, however, not indicate that these cells are actually proliferating. The significance of the labeling is related to the amplification of selected DNA fragments (genes) involved in axonal regeneration, and therefore a phenomenon of neuronal plasticity that allows hypertrophy and axonal sprouting (Borrione et al. 1991). In fact, ganglion neurons and those of the spinal cord stump only increase in dimension and cytoplasmic volume, and number of neurofilaments and other organelles including the synaptic input (Pannese 1963; Duffy et al. 1990, 1992; Geuna et al. 1992). Although hypertrophy affects most ganglion neurons, a subtype of ganglion neurons very rich in neurofilaments increased over other types in ganglia of regenerated tails (Geuna et al. 1992). The specific role of these neurons is, however, not known.

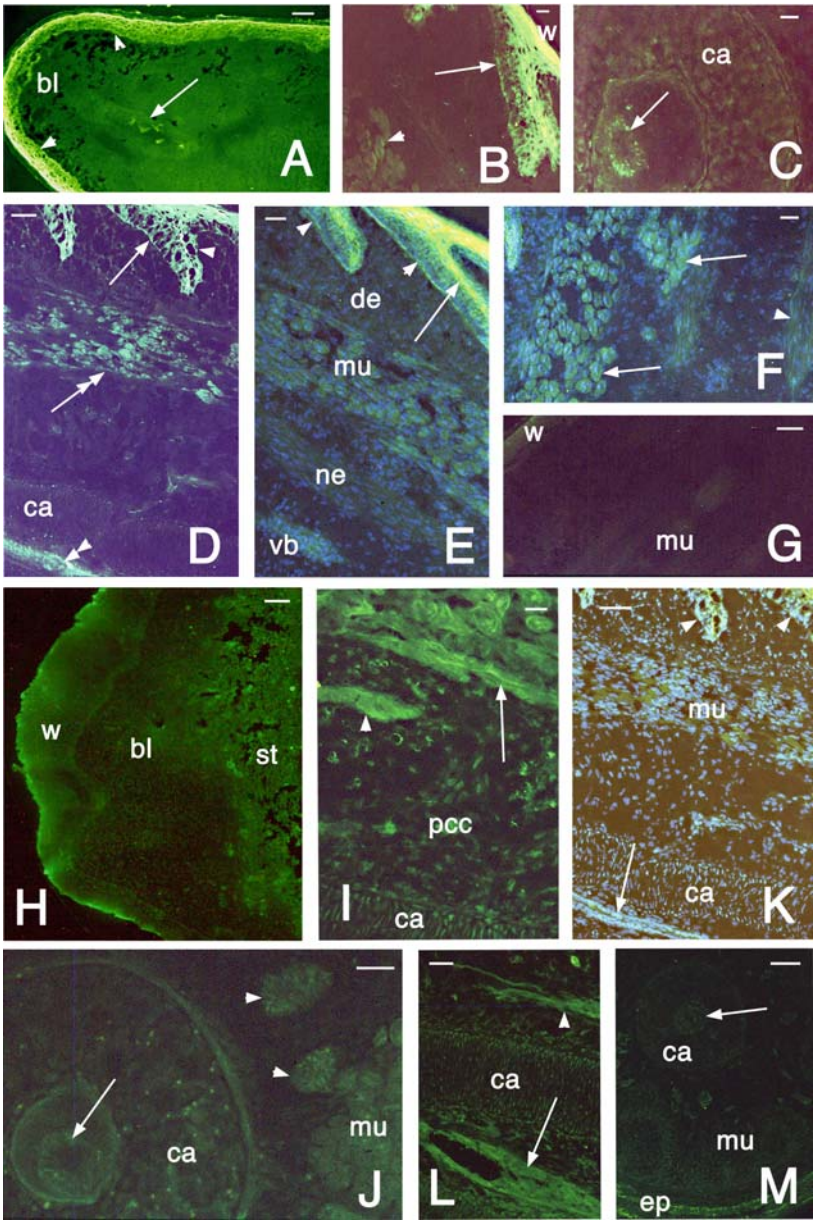

Fig. 2.11 Immunofluorescence localization of fibroblast growth factor 2 (FGF2) (basic, **a**–**g**) and fibroblast growth factor 1 (FGF1) (acidic, **h**–**m**) in the elongating tail of the lizard *L. delicata*. **a** Most immunofluorescence is seen in the wound epidermis (*arrowheads*) and ependymal tube. *Bar* 40 μm. **b** Detail of fluorescence-positive forming scale (*arrow*) and regenerating muscles (*arrowhead*). *Bar* 15 μm. **c** Cross sections showing a detail of

2.3 Growth Factors, Extracellular Matrix Proteins, and Keratins

2.3.1 Growth Factors

The localization, expression, activation, and general effects of growth factors on tissue regeneration in amphibians are known (Mesher 1996; Geraudie and Ferretti 1998; Gianpaoli et al. 2003). Recent studies have also extended this analysis to regenerating tissues in lizards (Alibardi and Loviku 2009). Few growth factors have been studied in the regenerating lizard tail and wounded limb.

Among other growth factors, fibroblast growth factor 1 (FGF1, acidic) and fibroblast growth factor 2 (FGF2, basic) are considered major stimulating molecules capable of replacing most of the activity of the neurotrophic factor as an inducer of organ regeneration in amphibians. The presence of FGF1 and FGF2 in the regenerating tail tissue of lizards has been shown by light and ultrastructural immunocytochemistry and immunoblotting (Alibardi and Loviku 2009, Alibardi, unpublished observations). Specific fibroblast growth factor reactive bands at 16–18 kDa have been identified only in the regenerating blastema and are not present or detectable in the normal tissues of both limb and tail.

The wound epidermis in the apical tail regions is immunofluorescent, whereas the blastema is poorly reactive for FGF2 (Fig. 2.11a). The apical ependymal ampulla and the more proximal regenerating ependymal tube are also immunolabeled (Fig. 2.11b, c). Also, the epidermal pegs of the forming scales, myoblasts aggregating to form segmental muscles, large regenerating nerves and their

Fig. 2.11 (Continued) an immunopositive ependymal tube (*arrow*). *Bar* 15 μm. **d** Longitudinal section of growing tail showing immunolabeled epidermal pegs (*arrow* on the proximal side, *arrowhead* on the distal side), muscles (*double arrow*), and ependyma (*double arrowhead*). *Bar* 16 μm. **e** Double-labeled fluorescence (nuclear labeling with 4′,6-diamidino-2-phenylindole (DAPI) and orange-yellow with fluorescein for FGF2). The *arrow* indicates the distal side and the *arrowheads* indicate the proximal side of epidermal pegs. *Bar* 15 μm. **f** Double labeling for FGF2 (*orange*) and nuclei (*blue*) for regenerating muscles in cross section (*arrows*). *Bar* 15 μm. **g** Nonreactive serum control. *Bar* 20 μm. **h** Blastema showing the higher labeling in the wound epidermis than in the blastema. *Bar* 15 μm. **i** Detail of immunofluorescent myotubes (*arrow*) and a blood vessel (*arrowhead*) within a regenerating tail. *Bar* 10 μm. **j** Cross section showing some labeling in the ependyma (*arrow*), and pericartilaginous nerves (*arrowheads*) and muscles. *Bar* 25 μm. **k** Double labeling for FGF1 (*orange*) and nuclei (*blue*). *Bar* 30 μm. **l** Detail showing the reactive ependyma (*arrow*) and peripheral nerve (*arrowhead*). *Bar* 15 μm. **m** Serum control (the *arrow* indicates the position of the immunonegative ependyma). *Bar* 25 μm. *bl* blastema, *ca* cartilaginous tube, *de* dermis, mu, muscles, *ne* nerve, *pcc* pericartilaginous connective tissue, *st* stump tissues, *vb* blood vessel, *w* wound epidermis

ganglia, and large blood vessels are immunolabeled (Fig. 2.11d, e). The immunofluorescence remains in the external sarcoplasm of growing muscle fibers and in the living epidermis of scales (the fluorescence of the corneous layers is nonspecific). The remaining tissues, such as cartilage, fat, and connective cells, do not show immunolabeling or are weakly labeled.

Within the medioproximal regions of the regenerating spinal cord, numerous immunolabeled nerves are seen, whereas ependymal cells are poorly or patchily labeled. Meninges surrounding the spinal cord appear weakly labeled or not labeled for FGF2. Neurons of the more proximal spinal cord in the stump, closer to the regenerating cord, show higher immunolabeling in comparison with neurons localized in the more distal spinal cord, far from the regenerating tissues (Alibardi and Loviku 2009). It is uncertain whether the few cell bodies showing immunoreactivity for FGF2 represent CSFCNs or macrophages within the ependyma. Control sections (preimmune rabbit serum or antigen-preabsorbed antibodies) confirm that the immunofluorescence is largely specific (Fig. 2.11g).

The antibody against FGF1 shows some reactivity to blastema cells and keratinocytes of the wound epidermis that are medium to strongly reactive (Fig. 2.11h). The apical ependymal ampulla and the more proximal ependymal tube inside the cartilaginous canal also show some immunofluorescence, whereas weak immunofluorescence is present in chondrocytes (Fig. 2.11i–l). FGF1 immunolabeling is also present in the nuclei of mesenchyme, of forming scales, muscles, and in the ependymal cells of the regenerating spinal cord, a different pattern from the immunolabeling for FGF2, where the nuclear labeling is much less evident. The FGF1 antibody also reacts with cells of the dermis beneath the forming scales, but poorly with the cartilaginous tube (except the perichondrium) and the surrounding connective-lipid tissue.

The large regenerating nerves derived from the proximal spinal ganglia are also immunoreactive for FGF1 (Fig. 2.11i, j). A more intense nuclear labeling is present in satellite and Schwann cells, but the labeling is less marked in ganglion neurons. In proximal regions of the regenerating tail at 4–5 weeks after amputation, immunoreactivity remains in the differentiating scales, muscles, and nerves, is scarce in the regenerating cartilage, and is absent in the dermis and pericartilaginous connective tissue. The immunofluorescence of cells in the proximal stump spinal cord is higher than in normal spinal cord. Some immunofluorescent axons in the regenerating spinal cord reach the apical ependymal ampulla (Fig. 2.11l). Control sections confirm that the labeling is largely specific (Fig. 2.11m).

Overall, the pattern of distribution of fibroblast growth factors in regenerating tissues of the lizard tail is similar to that of the regenerating limb and tail of the newt (Geraudie and Ferretti 1998; Gianpaoli et al. 2003). In the newt, FGF1 has been detected in both the wound epidermis, especially in the apical cup, as well as in blastema cells. It is believed that the apical cup produces FGF1, which stimulates the underlying cells of the blastema, or that blastema cells have an autocrine production of FGF1 that stimulates their own proliferation. Also, FGF2 is present

in the apical cup, especially its basal layer, and may stimulate blastema cell multiplication. Preliminary studies have indicated that whereas the wound epithelium of the tail and limb contains FGF2 at 2 weeks after amputation, the epithelium of the limb becomes immunonegative in later stages, in relation to the formation of scar connective tissue (Alibardi, unpublished observations).

TEM analysis (immunogold localization) has shown that FGF2 immunoreactivity is present in the extracellular matrix, especially near the apical wound epithelium contacting mesenchymal cells of the lizard blastema (Fig. 2.12a–c). It remains, however, unclear whether FGF2 moves from the epithelial cells to the mesenchyme or vice versa, and more dynamic studies are required to solve this question.

Fibroblast growth factor immunolocalization in the regenerating and differentiating muscle bundles suggests that such growth factors have autocrine stimulation for their own differentiation and growth. The presence of fibroblast growth factors in numerous blood vessels of the regenerating tail indicates the stimulation of angiogenesis by fibroblast growth factors in forming new blood vessels. The high expression of fibroblast growth factors in the spinal cord, ganglia, and nerves, aside from the stimulation of their own growth, may also be related to the possibility to release these growth factors in the growing blastema, where the factors may be acting as a neurotrophic agent. FGF1 is present in nuclei of reactive satellite cells within spinal ganglia innervating the new tail and this growth factor may stimulate their proliferation. In the regenerating spinal cord of the newt, FGF2 seems to stimulate the proliferation of neural stem cells in the regenerating ependyma (Zhang et al. 2000), and may also induce the proliferation and differentiation of ependymal cells into neurons. The latter effect has to be demonstrated for the lizard spinal cord. Therefore, these initial studies have also indicated that fibroblast growth factors may also be among the main candidates for a neurotrophic factor for tail regeneration in lizards, like in amphibians.

Also transforming growth factor beta-1 (TGF-β_1) and transforming growth factor beta-3 (TGF-β_3) in regenerating tail and limb have been immunolocalized in normal and regenerating limb and tail tissues (Alibardi, In press). TGF-β_1 appears localized in the connective tissue of the stump, but is appears diffusely present in mesenchymal cells of the blastema. A higher level of immunoreactivity is observed in the forming scar tissue of both tail and limb scars (Alibardi, unpublished observations). In this respect, it appears from the initial observations that also in lizards TGF-β_1 presents an overexpression pattern typical of scar tissues in mammals (Ferguson and O'Kane 2004). Preliminary data on TGF-β_3 of 20–22 kDa indicate it is upregulated in the regenerating blastema and in the dermis of the elongating tail, whereas this form is absent or is not detectable in normal tissues. Immunocytochemistry shows that among lesioned stump tissues, some connective cells are particularly rich in TGF-β_3 and they accumulate beneath the wound epidermis, but further analysis is currently in progress.

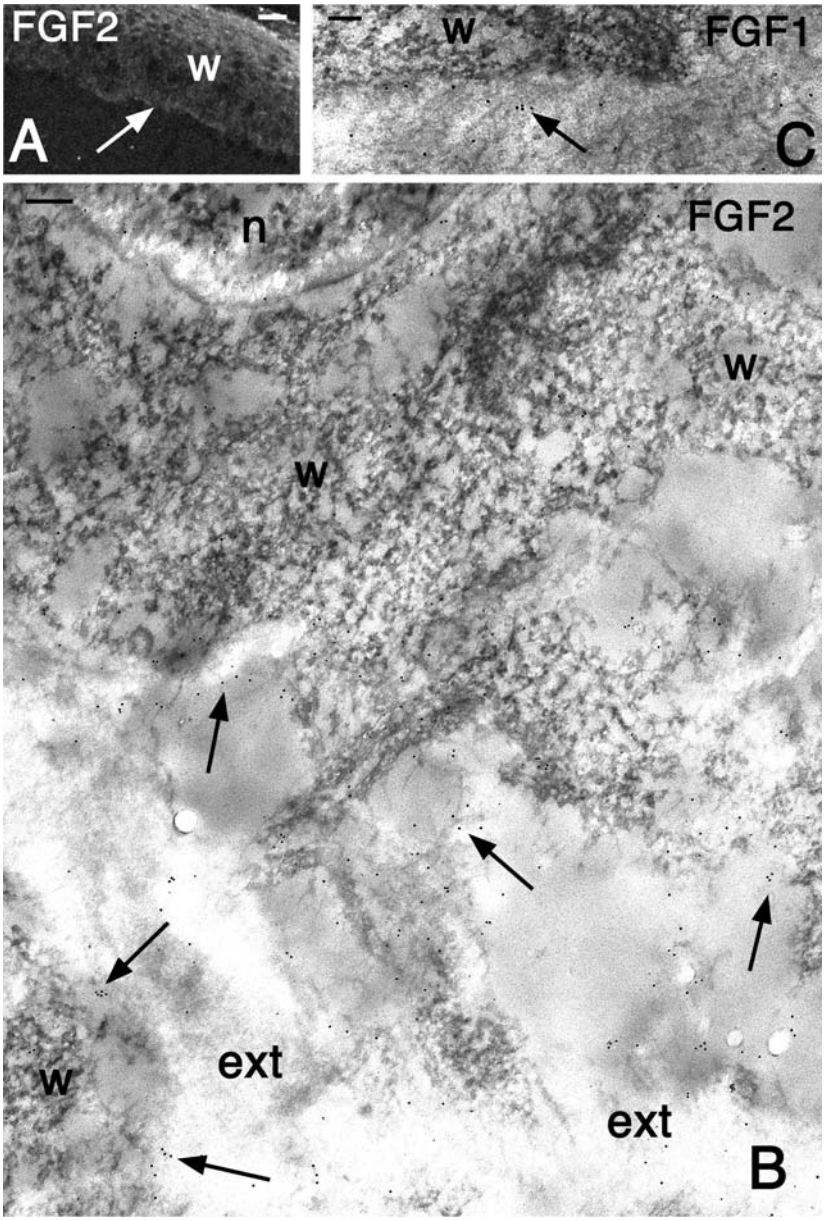

Fig. 2.12 Immunofluorescence (**a**) and immunogold localization (**b**, **c**) of FGF2 in the regenerating wound epithelium of the tail. **a** Immunolabeling along the (incomplete) basement membrane (*arrow*). *Bar* 10 μm. **b** Detail of immunogold labeling (*arrows*) along the basement membrane of wound epidermal cells. *Bar* 200 nm. **c** Detail of the labeling (*arrow*) along the basement membrane. *Bar* 100 nm. *ext* extracellular matrix, *FGF2/1* immunolabeling using FGF2/FGF1 antibody, *n* nucleus, *w* wound epithelium

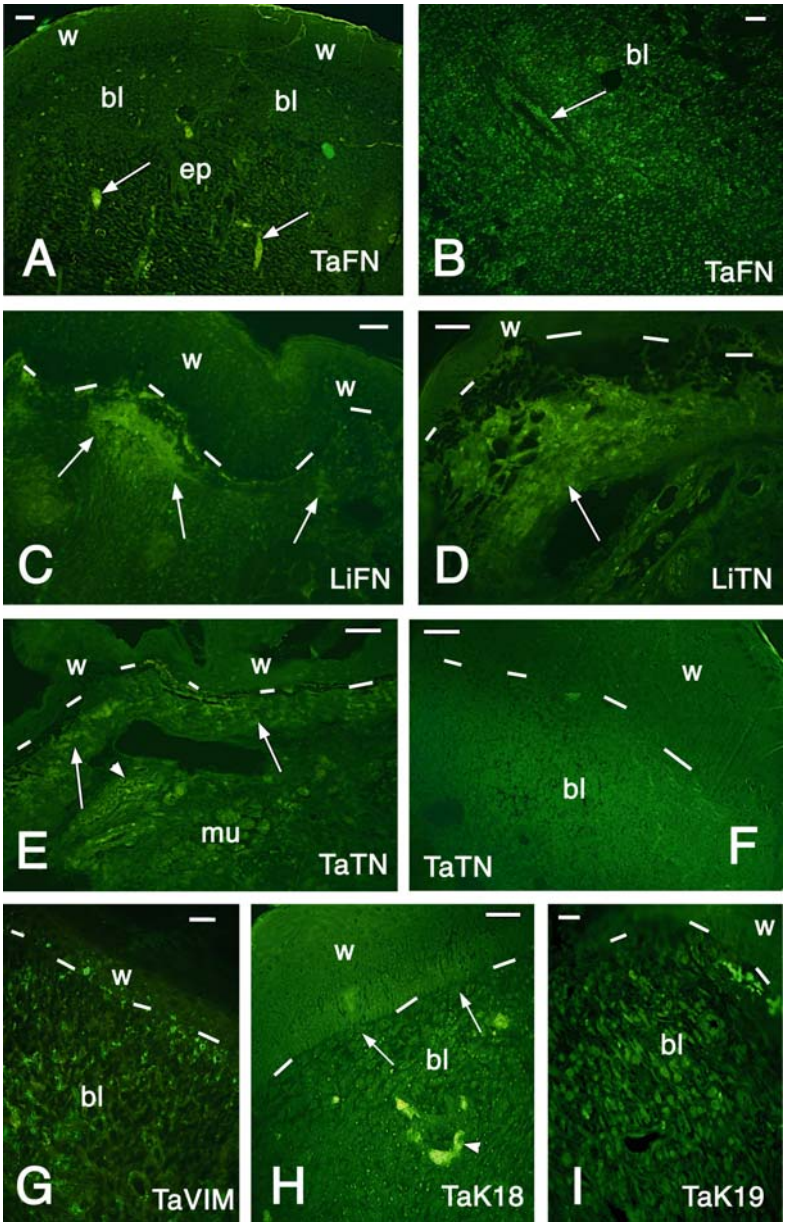

Fig. 2.13 Immunofluorescence images of regenerating tail (**a**, **b**, **e**–**i**) and limb (**c**, **d**) of *P. sicula*. **a** Tail at the cone stage showing a diffuse staining for fibronectin in the blastema but not in the wound epithelium. *Arrows* indicate nonspecific staining of blood vessels. *Bar* 10 μm. **b** Central region of the regenerating cone with fibronectin-immunostained mesenchymal cells and ependyma (*arrow*). *Bar* 15 μm. **c** Limb stump at 16 days after injury.

2.3.2 Extracellular Matrix Proteins

Fibronectin and ternascin are two of the main proteins of the extracellular matrix that have been implicated in the regeneration of amphibian limb and tail, and in the migration of the wound epithelium to cover the stump (see the summary in Geraudie and Ferretti 1998; Harty et al. 2003). Preliminary analysis has also been done in tissues of the lizard *P. sicula* (Alibardi, unpublished observations). Fibronectins of 220–240 kDa, and of lower molecular masses (perhaps degradative products), are present in the dermis of the wounded and regenerating tail and limbs, but not in the epidermis (Fig. 2.13a, b). Together, hyaluronate and fibronectin can stimulate the migration of mesenchymal cells toward the stump of the tail or limb. Also, ependymal cells of the apical ampulla appear to contain some fibronectin. This protein appears to be mainly localized in the connective tissue present beneath the wound epithelium that covers the limb stump at 12–20 days after amputation. The protein is not detectable in normal tissues or is only weakly detectable in the basement membrane of the epidermis. Like in the developing and regenerating limb of amphibians, fibronectin is largely expressed in the mesenchyme and later disappears where differentiating tissues, such as regenerating muscles and cartilage, are formed.

Lizard tenascin has a molecular mass of 220 kDa, although other immunoreactive bands at lower molecular masses are often present, but it is not known whether they represent degradation products. This protein is present in a low amount or is absent in the normal tail and limb connective tissues but becomes immunolocalized underneath the wounded dermis of both limb and tail stumps (Fig. 2.13c–e). The amount of this protein appears to increase in the limb stump beneath the migrating wound epithelium and in the forming basement membrane

Fig. 2.13 (continued) Fibronectin-immunopositive regions of the connective (*arrows*) are observed beneath the wound epithelium. *Bar* 15 μm. **d** Tenascin immunoreactivity in the connective tissue (*arrow*) located beneath the wound epithelium of a limb 13 days after amputation. *Bar* 20 μm. **e** Tenascin-immunoreactive forming blastema cells (*arrows*) 12 days after amputation. Immunofluorescence is also present in the dermis (*arrowhead*) located underneath the wound epithelium covering the tail stump. Also stump muscles appear immunostained. *Bar* 15 μm. **f** Tenascin-positive blastema cells in the tail and unlabeled thick wound epithelium. *Bar* 20 μm. **g** Vimentin-immunolabeled cells of the regenerating tail blastema. The wound epithelium is not labeled. *Bar* 15 μm. **h** Keratin 18 labeled blastema cells and in the wound epithelium (*arrows* on basal cells). *Bar* 20 μm. **i** Keratin 19 immunolabeled cells of the regenerative tail blastema and weakly in the wound epithelium. *Bar* 15 μm. *bl* blastema, *ep* ependymal tube, *LiFN* fibronectin labeling in the limb, *mu* muscles, *LiTN* tenascin labeling in the limb, *TaFN* fibronectin labeling in the tail, *TaK18/19* cytokeratin 18/cytokeratin 19 labeling in the tail, *TaTN* tenascin labeling in the tail, *TaVIM* vimentin labeling of the tail, *w* wound epithelium. *Dashes* underline the epidermis

underlying the nonapical regenerating epidermis. Tenascin immunoreactivity increases in the mesenchyme of the regenerating blastema but is absent in the wound epithelium (Fig. 2.13d). Tenascin has been implicated in the modulation of adhesion of fibroblasts to the epidermis, especially in the basement membrane underlying the wound epidermis.

Laminin of 210–220 kDa, well represented in the basement membrane of normal epidermis, disappears in the regenerative blastema, and is well detectable along the basement membrane of the elongating tail and in the dermis (probably linked to the blood vessel and muscle basement membrane). These preliminary data indicate that the increase of the amount of fibronectin and tenascin is a process that is needed for the migration of wound keratinocytes and the formation of a soft mesenchyme over the tail and limb stump.

2.3.3 Intermediate Filament Proteins

Vimentin and keratins are the main cytoskeletal intermediate filament proteins of the connective cells and epithelial cells, respectively. The presence of vimentin and keratins in the regenerative blastema of the tail has also been analyzed (Alibardi, unpublished data). Vimentin of 42 and 50 kDa is present in mesenchymal cells of the regenerating blastema, but the protein is absent in the wound epithelium (Fig. 2.13g). Vimentin is weakly detected or not visible in connective tissues of the normal tail.

The high expression of a 40–42-kDa keratin in the regenerating blastema or in the apical regions of the elongating tail (Alibardi et al 2000) and of wound keratins of 42–55 kDa (Alibardi and Toni 2005, 2006) has suggested that the mesenchyme of the blastema may contain keratins. This phenomenon was previously shown for the newt blastema (Corcoran and Ferretti 1997; Geraudie and Ferretti 1998). The presence of keratins 6, 16, and 17 in the regenerating tail has been associated with the contraction of migrating keratinocytes over the stump (Fig. 2.14).

Other keratins, however, are expressed more in the blastema than in the wound epithelium. In fact, both keratins 18 and 19 of 42 kDa are present in mesenchymal cells of the lizard blastema (Fig. 2.15h, i), a peculiar phenomenon previously reported for the regenerating blastema of the newt (Corcoran and Ferretti 1997). Keratin 19 is also a marker for stem cells, and the diffuse immunolabeling of blastema cells for this keratin suggests the presence of stem cells among those of the regenerative blastema. This preliminary observation is, however, being analyzed further. Therefore, it seems that also in the tail blastema of lizards, like in that of the newt, mesenchymal cells express typical simple keratins of epithelial tissues, indicating a reversion or dedifferentiation of the connective cells of the stump to embryonic cells (Corcoran and Ferretti 1997). This process in amphibians has been associated with the requirement of dedifferentiating cells to

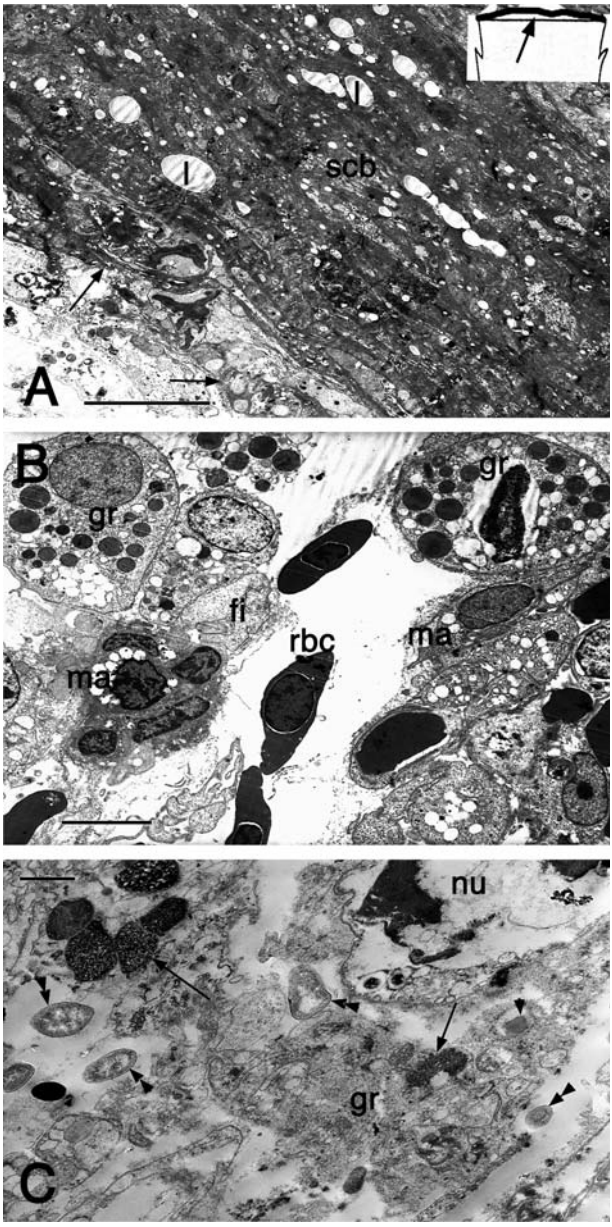

Fig. 2.14 Ultrastructural features of hindlimb stump at 4 days (**a**) and 7 days (**b**, **c**) after amputation in *P. sicula*. **a** Detail of the electron-dense and compact scab with degenerating leukocytes (*arrows*) localized underneath (position indicated by the *arrow* in the *inset*). *Bar* 1 μm. **b** Detail of granulation tissue rich in granulocytes and macrophages among few fibroblasts. *Bar* 3 μm. **c** Detail of spongy-like azurophil granules of granulocytes (*arrows*) that have engulfed some bacteria (*double arrowheads*). *Bar* 250 nm. *l* lipid vesicle, *fi* fibrocyte, *gr* granulocyte, *ma* macrophage, *nu* degenerating nucleus, *rbc* red blood cell, *scb* scab

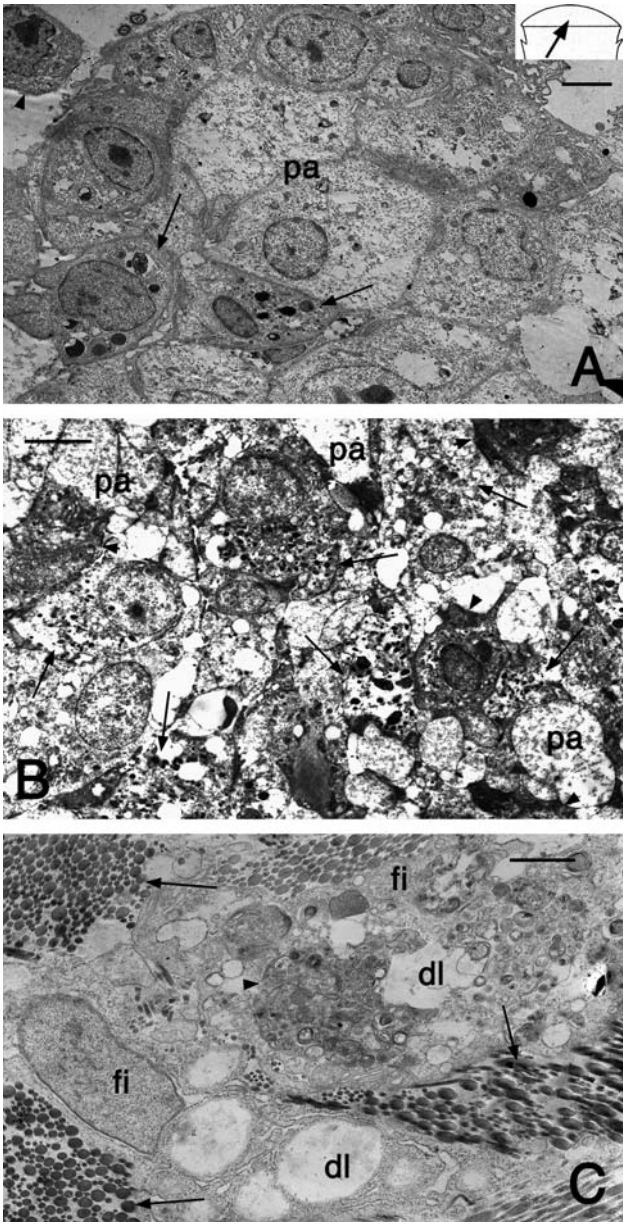

Fig. 2.15 Ultrastructural features of hindlimb stump at 13 days (**a**), 16 days (**b**), and 20 days (**d**) after amputation in *P. sicula*. **a** Epithelioid group of cells located in stump connective tissue, as indicated by the *arrow* in the *inset*. Among pale cells three phagocytes (*arrows*) are seen. A macrophage (*arrowhead*) is contacting this group of cells. *Bar* 1 μm. **b** Area of degenerating cells (*arrowheads* on dark cells) localized beneath the wound epidermis. *Arrows* indicate pale phagocytes rich in granular lysosomes. *Bar* 2.5 μm. **c** Detail of fibrocytes and a macrophage (*arrowhead*) surrounded by large collagen bundles (*arrows*). *Bar* 2 μm. *dl* degenerating lipid vesicles, *fi* fibrocyte, *pa* pale cell

produce a blastematic mass that recapitulates the stages of normal development of the limb (Geraudie and Ferretti 1998). However, this preliminary observation in lizards may also indicate that some blastema cells are derived from an epithelial–dermal transformation, since these epithelial keratins are conserved in mesenchymal-shaped cells. The latter, preliminary observations are presently being analyzed further.

Chapter 3
Limb Regeneration: Ultrastructural and Cytological Aspects

As previously indicated (Sect. 1.8), the injury of a limb in lizards induces large tissue damage that elicits a strong inflammatory reaction. Within 2–3 days after amputation, the reactive process is similar in the stump of the tail and the limb, and numerous granulocytes are present as the main phagocytes and persist in the following week (Alibardi 2009a), when also macrophages of blood origin become numerous. The latter phagocytes complete the tissue debridement but can cause scarring when they are hyperstimulated, for instance, by cauterization or repetitive cutting of the blastema (Alibardi 2009b). Macrophages are more commonly seen than granulocytes after 3 weeks after amputation.

The persistence of leukocytes in the injured limb together with the extensive exudation of fibrin that traps the microorganisms is a potent primitive innate immune defense of reptilian wounds (Huchezermayer and Cooper 2000). The permanence of active granulocytes for 1 week in the wounded tail and for over 3 weeks in wounded limbs indicates that these cells continue to be stimulated probably by a persistence of microbes and unknown chemical factors derived from tissue destruction (especially in the limb stump). In the injured tissues of the limb at 30–40 days after amputation, granulocytes within wounded tissues show an increased irregular surface and blebbing and contain activated (spongy-like) azurophil granules. These granules may store potent antimicrobial molecules that block the spreading of infection of injured lizard tissues of the stump.

3.1
Wound Healing and Blastema Formation

During the first 2–7 days after amputation of the limb, there is a strong infiltration of leukocytes among damaged tissues (muscles, connective tissue, nerves, and bone) within 0.3–0.5 mm in the stump (Alibardi 2009a; Fig. 1.8a, b).

Two to 3 days after amputation, on the surface of the limb stump a scab made of electron-dense cell remnants from blood cells and platelets, like in the tail stump, is formed (Fig. 2.14a). Beneath the scab, a region of injured or necrotic epithelial and connective cells is present in which numerous phagocytes are localized (Fig. 2.14b, c). Some of the phagocytes are poorly differentiated

epidermal cells, as indicated by the few bundles of keratin and desmosomal remnants that they contain. Other degenerating cells are granulocytes and most of their ribosomes and other organelles are lost; in addition, an intense vacuolation is present. The nuclear membrane of these degenerating granulocytes is broken and is often associated with prominent heterochromatin clumps. Other phagocytes beneath the scab, which are also localized among wound keratinocytes, are recognizable as heterophil granulocytes (the reptilian counterpart of neutrophil granulocytes in mammals). These cells contain small granules (specific, 0.1–0.2 μm) or larger granules (nonspecific or azurophilic; Fig. 2.14b, c). Another type of phagocyte is rich in small granules and is recognized as a monocyte. These cells possess a pale cytoplasm, an electron-dense nucleus with heterochromatin clumps, and cytoplasmic stout blebs. The latter feature indicates amoeboid movement and phagocytosis.

At 6–7 days after trauma, migrating epithelial cells cover a large part of the stump surface underneath the scab. Flat and elongated keratinocytes are still mixed with phagocytes, mainly heterophil granulocytes with large, azurophilic granules of 0.4–1.5 μm or, less commonly, with granulocytes containing small granules (0.05–0.2 μm). Migrating keratinocytes contain small keratin bundles and numerous, irregular pale vesicles of the endoplasmic reticulum, and secondary lysosomes. No cell junctions between keratinocytes and granulocytes are seen, and the latter cells possess cytoplasmic stout blebs infiltrated among keratinocytes. Some bacteria are seen within granulocytes, and most of their azurophilic granules at 6–18 days after amputation show a spongy texture or even broad pale areas among the dense material.

At 12–16 days after amputation, granulocytes are still numerous among the granulation tissues where numerous cells are still degenerating as in a condition of chronic inflammation. Aside from free granulocytes, clusters of phagocytes with degenerating cells are also present (Fig. 2.15a, b). This mass of cells resembles the granulomas described in mammalian tissues under chronic inflammation, and similar cell aggregates are also present at 18–22 days after amputation. The presence of granules and lobed or multiple nuclei in the degenerating cells indicates that they are granulocytes. Degenerating granulocytes contain dense and heterochromatic nuclei, and granules of different size and heterogeneous aspect or containing dense or spongy material. Pale lipid material is present in some vesicles within granulocytes, whereas most organelles are degenerated and swollen. The plasma membrane in some areas is discontinuous and the cell content is apparently released from the degenerating cells.

In these cell clumps, most pale and few darker cells are present, both representing degenerating cells (Fig. 2.15b). Sparse junctional remnants join these cells together, forming an epithelioid structure. Sparse lymphocytes are also seen among damaged tissues or within blood vessels at 6–16 days after amputation. Sparse among these granuloma-like tissues, empty spaces, derived from tissue degeneration, are present in the limb stump, another sign of the intense inflammatory reaction produced in this organ after amputation.

At 18–22 days after amputation, the cell composition of the granulation tissues of the limb stump changes and numerous fibroblasts and collagen fibrils become prevalent, as well as numerous macrophages (Fig. 2.15c). The differentiated fibroblasts are surrounded by irregular bundles of parallel collagen fibrils, which form large collagenous fibers. The latter give rise to the dense, irregular fibrotic dermis of the scarred limb. Fibrobasts contain numerous ribosomes and sparse parallel cisternae of rough endoplasmic reticulum. Basophil granulocytes are also seen among the irregular dense connective tissue at 18–22 days. A complete and continuous basement membrane separates the differentiated epidermis from the underlying, fibrous connective tissue.

In conclusion, the limb stump initially contains interstitial tissue made of prevalent hematogenous elements involved in microbe phagocytosis and cell debridement. The limb granulation tissue is replaced in 6–10 days by mesenchymal cells in the tail stump, but remains prevalently hematogenous in the limb, up to 14–18 days after amputation, when fibrocytic fibroblasts cause the rapid evolution of the granulation tissue into scar connective tissue. In comparison with the tail stump, the reepithelialization, healing, and inflammatory period in the limb are extended for 10–20 days longer with respect to that in the tail. The intense inflammation can lasts over 30 days when the bone remains protruding from the stump (Barber 1944; Kudokotsev 1960). The presence of areas containing pus in limbs at 12–22 days after amputation indicates a chronic inflammatory status in the limb stump and may also stimulate some immune reaction. Neither granulomas nor cyst or pus is formed in the tail stump. Granulocytes and macrophages remain in the stump for over 20 days after amputation, and later numerous macrophages remain among the tissue of the limb, whereas these phagocytes are less frequently seen and appear to be not activated in the regenerating tail (Alibardi and Sala 1988a, b). The tail appears to regenerate from mesenchymal cells largely derived from autotomy planes of the connective septa and intervertebral fracture planes (Quattrini 1954; Bellairs and Bryant 1985), perhaps containing stem cells. Although autotomy planes are absent in the limb, the presence of stem cells is not known. Another phenomenon that can increase the number of blastema cells in both the tail and the limb stump is the epidermal–mesenchymal transformation (Hay 1996). It is unknown whether an epidermal–dermal transformation may occur during lizard tail and limb regeneration.

3.2 Scar Formation in the Limb as Compared with the Inducement of Tail Scarring

In mammals, granulocytes do not produce chemokines for fibroblast recruitment and proliferation like macrophages, but are mainly involved in microbe destruction. The extensive damage of tissues in the limb stimulates a persistent secretion of fibroblast growth factor, platelet-derived growth factor (PDGF), and transforming

growth factor beta-1 (TGF-β_1) from macrophages which results in the recruitment and proliferation of fibroblasts capable of synthesizing a high amount of collagen and therefore inducing scarring (Kovacs and DiPietro 1994; Ferguson and O'Kane 2004). During chronic inflammation in mammals, lymphocytes and wound keratinocytes produce interleukin-1 and interferon gamma, two molecules that stimulate macrophage proliferation and indirectly scarring. In the case of lizards, no biochemical information is available on similar molecules.

The intense inflammatory reaction and the presence of a granulomatous reaction within the limb stump do not allow the establishment of a mesenchymal population, and the rapid formation of a continuous dense lamella in the basement membrane blocks any dermal–epidermal interaction to sustain the elongation of the initial limb outgrowth. These combined effects determine the origin of a variably short scar. Even in the few cases of initial blastema formation, the permanence of leukocytes and of macrophages among injured tissue causes the initial mesenchymal cell population to rapidly differentiate into fibrocytes, whereas the wound epithelium forms a basement membrane.

The confirmation that a strong inflammatory reaction, aside from the sparse recruitment of stem or undifferentiated cells, is the main cause for the unsuccessful limb regeneration derives from the study of the process of scarring in the tail after cauterization, or from other experimental manipulations (Marcucci 1914–1915; Bellairs and Bryant 1985). After cauterization of the tail stump (Fig. 1.9g), the damaged surface forms a dark necrotic tissue that produces a thick scab at 14–16 days after cauterization (Alibardi 2009b. Beneath the scab a soft dark mound of less than 1 mm in length is formed, which initially resembles a blastema. In the following week, the soft mound can grow to 1–3 mm, but it rapidly turns into a pale and scaled scar by about 1 month after cauterization (similar to those shown in Fig. 1.11g, h). The scaling pattern and the pigmentation of the outgrowths are irregular as pigment cells are distributed at random in the epidermis and also in the dermis.

Aside from tissue necrosis, cauterization also produces damage affecting the permeability of blood vessels with the consequent loss of a large amount of fibrin. The latter is still present among tissues at 14–20 days after cauterization. The ultrastructural analysis of the soft outgrowths at 14 days after cauterization shows numerous fibroblasts with well-developed ergastoplasm, surrounded by a fibrinous exudate containing collagen fibrils. The latter form a characteristic "alveolate intercellular matrix" among densely packed fibroblasts (Fig. 1.13e). The cytoplasm of these fibroblasts contains sparse bundles of microfilaments, an indication that these cells may represent myofibroblasts, the key cell leading to scarring in mammalian tissues (Wynn 2008). Numerous macrophages are present among fibroblasts and both cell types appear trapped within a dense collagenous network of bundles. Another common cell type encountered among fibroblasts is the electron-dense granulocyte with large, 0.2–0.5-μm granules with a characteristic spongy texture and an irregular cell surface with frequents blebs. Also, the numerous melanophores present in the outgrowth appear trapped within the fibrin–collagenous extracellular

matrix. The regenerated epidermis contains a continuous dense lamella that is contacted by anchoring fibrils from fibroblasts. Hemidesmosomes are commonly present, like in the normal epidermis. The rapid formation of a differentiated basal lamina with a continuous dense lamella in the cauterized tail stump as well as in the amputated limb contrasts with the presence of a discontinuous lamella dense in the blastema of the regenerating tail (Alibardi 1994a, b; 1995; Alibardi and Toni 2005).

From 16 to 20 days after cauterization, the connective tissue of the outgrowth forms scar tissue, made of elongated fibrocytes within a dense matrix, like in the stump of the limb. At 20–30 days after cauterization, fibrocytes adopt a perpendicular orientation with respect to the basement membrane of the epidermis, like in the limb. The presence of numerous macrophages, heterophils, or other types of granulocytes for over 20 days after injury in both cauterized tissues of the tail and the stump of the limb probably stimulates the recruitment of scarring fibroblasts, a phenomenon well known in mammalian chronic inflammation. Cauterization stimulates the excessive migration of macrophages that, through the liberation of fibrogenic cytokines (TGF-β_1, PDGF, etc.), attract the numerous fibrocytes responsible for the production of scar connective tissue. It is likely that cauterization in lizards gives rise to a population of myofibroblasts, like in mammalian fibrosis (Wynn 2008; Alibardi 2009b). The latter cells determine the rapid contraction of the wound and also the deposition of a large amount of collagen. In the tail scars, not only the cell composition is changed in comparison with normal blastema, but also the degradation of the collagen may take place at a lower rate than its production, with the consequent net increase of collagen fibrils.

The above observations indicate that the lizard model of regeneration can be utilized to study scarring mechanisms in amniotes in general as it resembles the process present in mammals. The condition of the mesenchyme and that of the extracellular matrix in the normal regenerative tail blastema are comparable to those present in mammalian embryonic tissues or in tissues of fetuses (Adzick and Longaker 1992; Martin 1997). It is known that mammalian fetal wounds produce little or no inflammation and that they repair well without scarring (Ferguson and O'Kane 2004). Among other growth factors, also the TGF-β_1, produced by macrophages, stimulates fibrocyte recruitment. In contrast, in embryonic/fetal wounds the amount of an isoform of transforming growth factor, transforming growth factor beta-3, is increased and this isoform favors regeneration without scarring. This factor is also present in lizard tissues after wounding and regeneration (Alibardi, unpublished observations).

Chapter 4
Conclusion and Perspectives: Implications for Human Regeneration

The introductory discussion on the biological conditions that might have allowed the evolution of tail regeneration in lizards (Sect. 1.2) indicated that the mechanisms for organ regeneration may be induced by medical treatments that utilize knowledge of the biological process responsible for organ regeneration in amniotes. These medical interventions should aim to limit inflammation, to increase the number of stem cells, and to stimulate dermal–epidermal interactions by removing the early formation of the barrier represented by a stable basement membrane between epidermis and dermis. Lizards represent a good model to study all these conditions, especially when comparing inflammation and scarring in the limb (or in the cauterized tail) with healing in the normal tail. Therefore, the lizard model is useful for studies that aim to detect the factors involved in the delicate equilibrium between regeneration (the environment present in the normal tail stump) and scarring (the environment present in the limb stump or in the manipulated tail stump).

Although detailed cytological information on the process of tail and limb regeneration in lizards is now available, there is little molecular information on specific genes and proteins activated during regeneration. Furthermore, the role of these genes in the process of regeneration in lizards remains completely unknown (Liu et al. 2006; Jiang et al. 2007).

In conclusion, the use of the lizard model in research on the mechanisms of tissue and organ regeneration is particularly interesting. Among others, three main topics are presently under analysis: (1) the presence of potent antimicrobial molecules produced after wounding; (2) the mechanisms limiting limb and digit regeneration; (3) the mechanisms implicated in the limited regeneration of the lumbar and thoracic spinal cord.

1. The innate immunity of wounded tissues of lizards to avoid infection and then septicemia may lead to the discovery of potent antimicrobial molecules like the defensins or cathelicidins, effective antimicrobial peptides present in most vertebrates (Zasloff 2002). Studies in this direction are presently under way to characterize possible antimicrobial molecules present in azurophil granules of granulocytes and dense granules or the cytoplasm of wound keratinocytes (Fig. 2.1b, 2.14b, c).

2. Future studies on lizard tissue regeneration should focus on the molecules exchanged between the apical cup or the wound epidermis and the underlying mesenchyme, an interaction that maintains the apical center for the growth of the tail. One of these molecules is fibroblast growth factor, but other growth factors (transforming growth factor, epidermal growth factor, etc.) may also be involved. The localization and expression of growth factors and of other signaling molecules (Sonic hedgehog, Gremlin, bone morphogenetic protein, MSx, etc.; see Sanz-Ezquerro and Tockle 2003) in the regenerating blastema of the tail compared with that of the limb should be determined. These growth factors can be administered or placed in specific areas of the amputated limbs to see whether they can stimulate regeneration, in particular whether they can induce the formation of the autopodium and digits. This can be done by the application of microbeads releasing the molecule being tested in the limited cases of limb outgrowths (Fig. 1.2).
3. The recovery from paraplegia observed in numerous cases of spinal cord injury in lizards (Raffaelli and Palladini 1969; Alibardi, unpublished observations) should also be analyzed for a possible medical follow-up. It is known that the lumbar or thoracic spinal cord allows the regeneration of axons when it is autotransplanted into the tail, in relation to the presence of a regenerative tail blastema (Simpson and Pollack 1985). The complete resection of the spinal cord at lumbar and thoracic levels in the lizard *Anolis carolinensis* produces a permanent paralysis (Simpson 1961, 1970, 1983; Simpson and Duffy 1994). However, other studies on the wall lizards *Podarcis muralis* and *Podarcis sicula*, species that regenerate a larger tail than *A. carolinensis*, have indicated that after the resection of the lumbar spinal cord, the initial paraplegia can recover in 25–45 days after the operation (Raffaelli and Palladini 1969; Alibardi, unpublished observations). In these cases, the microscopic analysis of the lesioned spinal cord has shown that some regenerating nerves can bypass the gap of the sectioned spinal cord. However, the careful histological control of the lizards operated on has also shown that in animals that recovered limb motility the spinal cord was not completely transected (Furieri 1957). Therefore, in these cases, it is likely that some of the bridge nerves have rebuilt the intrinsic local spinal locomotor circuits present in the spinal cord (Bernstein 1983; Schwab and Bartholdi 1996; Sharma and Peng 2001; Borgens 2003). The latter possibility, however, does not diminish the value of the lizard model, since most spinal cord injuries in humans do not completely transect the spinal cord, and therefore the lizard model can be of interest in the study of the reestablishment of local spinal locomotor circuits. This is interesting considering that after lumbar lesion of the spinal cord the tail was also amputated and it regenerates normally (Alibardi, unpublished observations). Present analysis is trying to evaluate whether the presence of regenerating tissues at 1–2 cm from the lumbar injury stimulates the regeneration of long spinal cord nerves to cross the gap and progress into the regenerating tail.

The ultrastructural analysis of the complete or largely transected spinal cord of the lumbar spinal cord has indicated that some axons cross the scarring gap in the presence of a nearby regenerating tail. The reactive proximal spinal cord (upstream of the lesion) remains viable, whereas the distal spinal cord (downstream of the lesion) is more affected and most neurons disappear and axons degenerate. However, after 20–30 days from the lesion, numerous, small glial cells of undetermined nature, and sparse neurons are still viable in the proximal and even in the distal spinal cord. The lizard model therefore represents a unique experimental case in which the influence of a target tissue (the regenerating blastema) may stimulate the regrowth of axons within some 1–2-cm distance from the lesioned lumbar spinal cord. The clarification of this issue using the lizard model may allow the discovery of trophic factors involved in the guidance of transected axons over a long distance within the spinal cord.

In conclusion, if the last issues presented in this review stimulate some researchers to adopt and exploit the lizard model of amniote regeneration, my effort in summarizing the topic will have largely achieved one of its main goals.

References

Adzick NS, Longaker MT (1992) Fetal wound healing. Elsevier, New York

Agaiby AD, Dyson M (1999) Immuno-inflammatory cell dynamics during cutaneous wound healing. J Anat 195:531–542

Alberio SO, Diniz JA, Silva EO, deSouza W, DaMatta RA (2005) Cytochemical and functional characterization of blood and inflammatory cells from the lizard *Ameiva ameiva*. Tiss Cell 37:193–202

Alibardi L (1986) Fenomeni degenerativi nell' ependima durante la rigenerazione codale di alcuni sauri. Atti Mem Acc Patav Sci Lett e Arti 98:55–64

Alibardi L (1990–1991) Electron microscopic observations on the myelination of the long-term regenerated caudal spinal cord in lizards and *Sphenodon*. Biol Struct Morphog 3:147–158

Alibardi L (1992) Ultrastructural observations on blood vessels surrounding normal and regenerating spinal cord in newt. Arch Ital Anat Embriol 97:257–272

Alibardi L (1993a) H3-labeled cerebrospinal fluid contacting cells in the regenerating caudal spinal cord of the lizard *Lampropholis*. Annals Anat 176:347–356

Alibardi L (1993b) Observations on the ultrastructure of blood capillaries in the regenerating blastema of lizard in relation to the blood-brain barrier. Eur Arch Biol 104:21–27

Alibardi L (1994a) Fine autoradiographical study on scale morphogenesis in the regenerating tail of lizards. Histol Histopath 9:119–134

Alibardi L (1994b) Modifications of the dermis during scale regeneration in the lizard tail. Histol Histopath 9:733–745

Alibardi L (1994c) Production of immature erythrocytes in lizard during tail regeneration. Anim Biol 3:139–147

Alibardi L (1995a) Cytological localization of 3H-Proline in the regenerating spinal cord of the lizard *Lampropholis*. Ann Sci Natur (Paris) 16:137–143

Alibardi L (1995b) Development of the axial cartilaginous skeleton in the regenerating tail of lizards. Bull Associat Anatomist 79:3–9

Alibardi L (1995c) Electron microscopic analysis of the regenerating scales in lizard. Boll Zool 62:109–120

Alibardi L (1995d) Histogenesis of fat tissue in the regenerating tail of the lizard (*Lampropholis* spp). Canad J Zool 73:1077–1084

Alibardi L (1995e) Muscle differentiation and morphogenesis in the regenerating tail of lizards. J Anat 186:143–151

Alibardi L (1996a) Autoradiographic ultrastructural observation on the meninges of the regenerating tail of lizards. Bull Soc Anatom 80:5–9

Alibardi L (1996b) Observations on proliferating sheath cells in the regenerating nerves of lizard. Histol Histopath 11:937–942
Alibardi L (1996c) Differentiation of the epidermis during scale formation in embryos of lizard. J Anat 192:173–186
Alibardi L (1998) Presence of acid phosphatase in the epidermis of the regenerating tail of the lizard (*Podarcis muralis*) and its possible role in the process of shedding and keratinization. J Zool 246:379–390
Alibardi L (1999) Keratohyalin-like granules in embryonic and regenerating epidermis of lizards and *Sphenodon punctatus* (Reptilia, Lepidosauria). Amphibia-Reptilia 20:11–23
Alibardi L (2000) Ultrastructural localization of alpha-keratins in the regenerating epidermis of the lizard *Podarcis muralis* during formation of the shedding layer. Tiss Cell 32:153–162
Alibardi L (2001) Keratohyalin-like granules in lizard epidermis: evidence from cytochemical, autoradiographic and microanalytic studies. J Morphol 248:64–79
Alibardi L (2009a) Ultrastructural features of the process of wound healing after tail and limb amputation in lizard. Acta Zool (In press)
Alibardi L (2009b) Ultrastructural observations on the process of cicatrization in the cauterized tail and the amputated limb of lizard as compared to the normal regenerative blastema of the tail. NW J Zool (In press)
Alibardi L, Loviku JF (2009) Immunolocalization of FGF1 and FGF2 in the regenerating tail of the lizard *Lampropholis guichenoti*: implications for FGFs as trophic factors in tail regeneration. Acta Histoch (In press)
Alibardi L, Maderson PFA (2003) Observations on the histochemistry and ultrastructure of regenerating caudal epidermis of the tuatara *Sphenodon punctatus* (Sphenodontida, Lepidosauria, Reptilia). J Morphol 256:134–145
Alibardi L, Meyer-Rochow VB (1988) Ultrastructure of the neural component of the regenerating spinal cord of three species of New Zealand lizards (*Leiolopisma nigriplantare maccanni*, *Lampropholis delicata*, and *Hoplodactylus maculatum*). New Zeal J Zool 15:535–550
Alibardi L, Meyer-Rochow VB (1989) Comparative fine structure of the axial skeleton inside the regenerated tail of lizards and the tuatara (*Sphenodon punctatus*). Gegenb Morphol Jahrb (Leipzig) 135:705–716
Alibardi L, Meyer-Rochow VB (1990) Fine structure of regenerating caudal spinal cord in the Tuatara (*Sphenodon punctatus*). J Hirnf 31:613–621
Alibardi L, Miolo V (1990) Fine observations on nerves colonizing the regenerating tail of the lizard *Podarcis sicula*. Histol Histophat 5:387–396
Alibardi L, Sala M (1981) Indagini istochimiche sulla struttura della cartilagine rigenerata nella coda di *Lacerta sicula*. Arch Ital Anat Embr 88:163–182
Alibardi L, Sala M (1983) Distribuzione di sostanze d' importanza morfogenetica in tessuti rigeneranti di *Lacerta sicula*, *Triturus alpestris* e *Rana dalmatina*. Atti Mem Acc Patav Sci Lett e Arti 95:100–151
Alibardi L, Sala M (1986) Eterogeneita' e neurogenesi nell' ependima rigenerante di alcuni sauri (Reptilia). Arch Ital Anat Embriol 91:29–41
Alibardi L, Sala M (1988a) Fine structure of the blastema in the regenerating tail of the lizard *Podarcis sicula*. Boll Zool 55:307–313
Alibardi L, Sala M (1988b) Presence of liquor contacting neurons in the regenerating spinal cord of lizard. Monit Zool Ital NS 22:263–269
Alibardi L, Sala M (1989) Ependymal fine structure and secretory activity during early phases of tail regeneration in lizard. Arch Ital Anat Embriol 94:55–69
Alibardi L, Toni M (2005) Wound keratins in the regenerating epidermis of lizard suggest that the wound reaction is similar in the tail and limb. J Exp Zool 303A:845–860
Alibardi L, Toni M (2006) Cytochemical, biochemical and molecular aspects of the process of keratinization in the epidermis of reptilian scales. Prog Histoch Cytoch 40:73–134

Alibardi L, Sala M, Meneghini C (1987) Effect of treatment with GABA on regenerating ependyma in lizards. Acta Embr Morphol Exper NS 8:181–185
Alibardi L, Sala M, Miolo V (1988) Morphology of experimentally produced tails in lizards. Acta Embr Morph Exper NS 9:181–194
Alibardi L, Gibbons J, Simpson SB Jr (1992) Fine structure of cells in the young regenerating spinal cord of the lizard *Anolis carolinensis* after H3-Thymidine administration. Biol Struct Morphog 4:45–52
Alibardi L, Wibel R, Simpson SB Jr (1993a) Scanning electron microscopic observations on the central canal of the regenerating tail spinal cord in lizard. Boll Zool 60:245–252
Alibardi L, Gibbons J, Simpson SB Jr (1993b) 3H-GABA administration during tail regeneration of lizards and autoradiographical localization. J Hirnfor 34:67–77
Alibardi L, Maurizii MG, Taddei C (2000) Immunocytochemical and electrophoretic distribution of cytokeratins in the regenerating epidermis of the lizard *Podarcis muralis*. J Morphol 246:179–181
Alvarado SA (2000) Regeneration in metazoans: why does it happen? BioEssay 22:548–590
Arnold EN (1984) Evolutionary aspects of tail shedding in lizards and their relatives. J Nat Hist 18:127–169
Arnold N (1990) The throwaway tail. New Scientist 3 February 22–25, Magazine issue 1702
Arsanto JP, Diano M, Thouveny Y, Thiery JP, Levi G (1990) Patterns of tenascin expression during tail regeneration of the amphibian urodele *Pleurodeles waltl*. Development 109:177–188
Avel M, Verrier ML (1930) Un cas de regeneration hypotypique de la patte chez *Lacerta vivipara*. Bull Biol France-Belg 64:198–204
Baffoni GM (1950) Fenomeni reattivi e degenerativi delle cellule nervose nei processi di cicatrizzazione del moncone caudale dei sauri. Rend Acc Naz Lincei 8:389–393
Ballinger RE (1973) Experimental evidence of the tail as a balancing organ in lizard, *Anolis carolinensis*. Herpetologica 29:65–66
Ballinger RE, Tinkle DW (1979) On the cost of tail regeneration to body growth in lizards. J Herpetol 13:374–375
Baranowitz SA, Maderson PF, Connelly TG (1979) Lizard and newt tail regeneration: a quantitative study. J Exp Zool 210:17–37
Barber LW (1944) Correlations between wound healing and regeneration in fore-limbs and tails of lizards. Anat Rec 89:441–453
Bauer AM (1998) Morphology of the adhesive tail tips of carphodactyline geckos (Reptilia: Diplodactylidae). J Morphol 235:41–58
Bayne EK, Simpson SB Jr (1977) Detection of myosin in prefusion G0 lizard myoblasts in vitro. Dev Biol 55:306–319
Beazley LD, Sheard PW, Tennant M, Starac D, Dunlop SA (1997) Optic nerve regenerates but does not restore topographic projections in the lizard *Ctenophorous ornatus*. J Comp Neurol 377:105–120
Bellairs A d'A, Bryant SV (1985) Autotomy and regeneration in reptiles. In: Gans C, Billet F, Maderson PFA (eds) "Biology of the Reptilia" vol 15B. Wiley, New York, pp 302–410
Bernstein JJ (1983) Successful spinal cord regeneration: known biological strategies. In: Reier PJ, Bunge RP, Seil FJ (eds) Current Issues in neural regeneration. Alan Liss Inc, New York, pp 331–341
Boilly B, Cavanaugh KP, Thomas D, Hondermarck H, Bryant SV, Bradshaw RA (1991) Acidic fibroblast growth factor is present in regenerating limb blastemas of axolots and binds specifically to blastema tissue. Dev Biol 145:302–310
Borgens RB (2003) Restoring function to the injuered human spinal cord. Adv Anat Embryol Cell Biol 171:1–161
Boring AM, Chang LF, Chang WH (1948) Autotomy and regeneration in the tails of lizards. Peking Nat Hist Bull 17:85–108

Borrione P, Cervella P, Geuna S, Giacobini-Robecchi MG, Poncino A, Silengo L (1991) Electrophoretic analysis of neuronal genomic DNA from hypertophic spinal ganglia during lizard tail regeneration. Neurosci Lett 113:245–248

Bottazzi-Bacchi A, Sassu G (1973) On the fine structure of the motor plates during muscular regeneration in *Gongylus ocellatus*. Acta Anat 85:580–592

Brawick RE (1959) The life history of the common New Zealand skink *Leiolepisma zelandia* (Gray, 1943). Trans Roy Soc NZ 86:331–380

Brazaitis P (1981) Maxillary regeneration in a marsh crocodile, *Crocodylus palustris*. J Herpeth 15:360–362

Brookes JP, Kumar A, Velloso CP (2001) Regeneration as an evolutionary variable. J Anat 199:3–11

Brunetti PM (1948) Istogenesi e morfogenesi dei muscoli nella rigenerazione della coda di lucertola in seguito a mutilazione spontanea. Monit Zool Ital 57:244–248

Bryant SV (1970) Regeneration in amphibians and reptiles. Endeavour 29:12–17

Bryant SV, Bellairs AA (1967a) Tail regeneration in the lizards *Anguis fragilis* and *Lacerta dugesii*. J Linn Soc Zool 46:297–305

Bryant SV, Bellairs AA (1967b) Amnio-allantoic constriction bands in lizard embryos and their effects on tail regeneration. J Zool Lond 152:155–161

Bryant SV, Bellairs AA (1970) Development of regenerative ability in the lizard, *Lacerta vivipara*. Am Zool 10:167–173

Bryant SV, Wozny KJ (1974) Stimulation of limb regeneration in the lizard *Xantusia vigilis* by means of ependymal implants. J Exp Zool 189:339–52

Byerly TC (1925) Note on the partial regeneration of the caudal region of *Sphenodon punctatus*. Anat Rec 30:61–66

Calori L (1858) Sullo scheletro della *Lacerta viridis* Linn., sulla riproduzione della coda nelle lucertole, e sulle ossa cutanee del teschio dei sauri. Mem Att Acc Sci Bologna 9:46–50

Carlson BM (1970) Relationship between thze tissue and epimorphic regeneration of muscle. Amer Zool 10:175–185

Carlson BM (2007) Principles of regenerative biology. Academic Press-Elsevier, USA

Chakko TV, Mariamma PJ (1981) Changes in lipid composition of regenerating tail of the lizard *Hemidactylus flaviviridis*. Ind J exp Biol 19:979–981

Charvat Z, Kral B (1969) Development of new spinal ganglia during regeneration of spinal cord after autotomy of tail in *Lacerta vivipara*. West Afr Med J Niger Pract 18:3–6

Chernoff EAG (1996) Spinal cord: a phenomen unique to urodeles? Int J Dev Biol 40:823–831

Chlebowsky JS, Przybylski RJ, Cox PG (1973) Ultrastructural studies of lizard (*Anolis carolinensis*) myogenesis in vitro. Dev Biol 33:80–99

Clause AR, Capaldi EA (2006) Caudal autotomy and regeneration in lizards. J Exp Zool 305B:965–973

Colbert EH, Morales M, Minkoff EC (2001) Colbert's evolution of the vertebrates, 5th edn. Wiley-Liss, New York

Congdon JD, Vitt LJ, King WW (1974) Geckos: adaptive significance and energetics of tail autotomy. Science 184:1379–80

Cooper EL, Klempau AE, Zapata AG (1985) Reptilian immunity. In: Gans C, Billett F, Maderson PFA (eds) Biology of the Reptilia 14A. Wiley, New York, pp 799–878

Corcoran JP, Ferretti P (1997) Keratin 8 and 18 expression in mesenchymal progenitor cells of regenerating limbs is associated with cell proliferation and differentiation. Dev Dyn 210:355–370

Cox PG (1969a) Some aspects of tail regeneration in the lizard *Anolis carolinensis* I. A description based on histology and autoradiography. J Exp Zool 171:127–150

Cox PG (1969b) Some aspects of tail regeneration in the lizard, *Anolis carolinensis* II. The role of the peripheral nerves. J Exp Zool 171:151–160

Cristino L, Pica A, Della Corte F, Bentivoglio M (2000a) Plastic chages and nitric oxide synthase induction in neurons that innervate the regenerated tail of the lizard *Gekko gecko* I. Response of spinal motoneurons to tail amputation and regeneration. J Comp Neurol 417:60–72

Cristino L, Pica A, Della Corte F, Bentivoglio M (2000b) Plastic chages and nitric oxide synthase induction in neurons that innervate the regenerated tail of the lizard *Gekko gecko* II. The resposnse of dorsal root ganglion cells to tail amputation and regeneration. Brain Res 871:83–93

d'A BA, Bryant SV (1968) Effects of amputation of limbs and digits of lacertid lizards. Anat Rec 161:489–95

Dalla Valle L, Toffolo V, Belvedere P, Alibardi L (2005) Isolation of a mRNA encoding a glycine-proline-rich beta-keratin expressed in the regenerating epidermis of lizard. Dev Dyn 234:934–947

Daniels CB (1984) The importance of caudal lipid in the gecko *Phyllodactylus marmoratus*. Herpetologica 40:337–344

Daniels CB, Lewis BC, Tsopelas C, Munns SL, Orgeig S, Baldwin ME, Stacker SA, Achen MG, Chatterton BE, Cooter RD (2003) Regenerating lizard tail: a new model for investigating lymphangiogenesis. FASEB 17:479–481

Del Grande P, Minelli G, Franceschini V, Vughi F (1981) Regenerative capacity of the optic tectum in *Lacerta viridis*. Boll Zool 48:113–119

Desai K, Thomas E, Akhuji UU (1977) Neurosecretion and tail regeneration in the indian gecko Hemidactilys flavivirisis. Ruppel Ann Zool (India) 13:93–107

Dufaure JP, Hubert J (1961) Table de developpement du lezard vivipare: *Lacerta (Zootoca) vivipara* Jacquin. Arch Anat Micr Morph Exp 50:309–327

Duffy MT, Simpson SB, Liebich DR, Davis BM (1990) Origin of spinal cord axons in the lizard regenerating tail: supernormal projections from local spinal neurons. J Comp Neurol 293:208–222

Duffy MT, Liebich DR, Garner LK, Hawrych A, Simpson SB, Daviv BM (1992) Axonal sprouting and frank regeneration in the lizard tail spinal cord: correlation between chages in synaptic circuitry and axonal growth. J Comp Neurol 316:363–374

Duffy MT, Hawrych A, Liebich DR, Simpson SB (1993) Regeneration of cerebro-spinal fluid contacting neurons (CSFCN) in regenerated tail spinal cord of the lizard *Anolis carolinesis*. Soc Neurosci 19:707 Abstract

Dungan KM, Wel TY, Nace JD, Polun ML, Chiu IM, Lang JC, Tassava RA (2002) Expression and biological effect of urodele fibroblast growth factor 1: relationship to limb regeneration. J exp Zool 292:540–554

Dunlop SA, Tee LBG, Stirling RV, Taylor AL, Runham PB, Barber AB, Kutchling G, Rodger J, Roberts JD, Harvey AR, Beazley LD (2004) Failure to restore vision after optic nerve regeneration in reptiles: interspecies variation in response to axotomy. J Comp Naurol 478:292–305

Egar M, Simpson SB, Singer M (1970) The growth and differentiation of the regenerating spinal cord of the lizard, *Anolis carolinensis*. J Morphol 131:131–51

Estrada CM, Park CD, Castilla M, Tassava RA (1993) Monoclonal antibody WE6 identifies an antigen that is u-regulated in the wound epthelium of newts and frogs. In: Fallon JF, Goetinck PF, Kelley RO, Stocum DL (eds) Limb development and regeneration. Wyley-Liss, New York, pp 271–282

Evans SE (2003) At the feet of the dinosaurs: the early history and radiation of lizards. Biol Rev 78:513–551

Evans SE, Bellairs AA (1983) Histology of a triple tail regenerate in a gecko, *Hemidactylus persicus*. Br J Herpetol 6:319–322

Ferguson MWJ, O'Kane S (2004) Scar-free healing: from embryonic mechanisms to adult therapeutic intervention. Phil Trans R Sco London B 359:839–850

Filogamo G, Marchisio PC (1961) Sulla sede delle placche motrici della musculatura della coda rigenerata dei sauri. Rendic Acc Naz Lincei (Sci Mat Fis Nat) 30:933–938

Fitch HS (2003) A comparative study of loss and regeneration of lizard tails. J Herpethol 37:395–399

Font E, Garcia-Verdugo JM, Alcantara S, Lopez-Garcia C (1991) Neuron regeneration reverses 3-acetylpyridine-induced cell loss in the cerebral cortex of adult lizards. Brain Res 551:230–235

Fox SF, Rostker MA (1982) Social cost of tail loss in *Uta stansburiana*. Science 218:692–693

Fraisse P (1885) Die Regeneration von Geweben und Organen bei den Wirbeltieren besonders bei Amphibien und Reptilien. Fischer, Berlin

Furieri P (1956) Struttura anatomica e rigenerazione della coda della *Tarentula mauritanica* L. Monit Zool Ital 64:30–4

Furieri P (1957) Lesione delle vertebre e del midollo spinale nella regione presacrale di *Lacerta* e *Tarentola*. Monit Zool Ital 65:7–18

Gabella G (1961) Sulla sede delle placche motrici nei sauri (*Lacerta muralis*, Laur. *E Lacerta viridis*, Laur.). Boll Soc Ital Biol Sperim 42:405–408

Galis F, Wagner GP, Jockusch EL (2003) Why is limb regeneration possibile in amphibians but not in reptiles, birds, and mammals? Evol Dev 5:208–220

Geraudie J, Ferretti P (1998) Gene expression during amphibian limb regeneration. Int Rev Cytol 180:1–50

Geuna S, Giacobini-Robechhi MG, Poncino A, Filogamo G (1992) Nuclear hypertrophy and hyperdiploidy in lizard root ganglion neurons during innervation of the regenerating tail. Eur Arch Biol 103:63–70

Gianpaoli S, Bucci S, Ragghianti M, Mancino G, Zhang F, Ferretti P (2003) Expression of FGF2 in the limb blastema of two salamandridae correlates with their regenerative capability. Proc Royal Soc London 270B:2197–2205

Giuliani M (1878) Sulla struttura del midollo spinale. Sulla riproduzione della coda della *Lacerta viridis*. Ric Lab Anat Norm (Ed G Todaro) Vol. I–II, 137–150

Goss RJ (1969) Principles of regeneration. Academic Press, New York and London

Goss RJ (1987) Why mammals don't regenerate- or do they? NIPS 2:112–115

Guyenot E (1928) Territoire de régénération chez le lézard (*Lacerta muralis*). CR Soc Biol (Paris) 99:27–28

Guyenot E, Matthey R (1928) Les processus regeneratifs dans la patte posterieure du lezard. W. Roux Arch Entwick Organ 113:520–529

Han M, Yang X, Taylor G, Bursdal CA, Anderson RA, Muneoka K (2005) Limb regeneration in higher vertebrates: developing a roadmap. Anat Rec 287B:14–24

Hardy CJ, Hardy CM (1977) Tail regeneration and other observations in a species of agamid lizard. Aust Zool 19:141–148

Harty M, Neff AW, King MW, Mesher AL (2003) Regeneration and scarring: an immunologic perspective. Dev Dyn 226:268–279

Hay ED (1996) An overview of epithelio-mesenchymal transformation. Acta Anat 154:8–20

Hellmich WG (1951) A case of limb regeneration in the Chilean iguanid *Liolaemus*. Copeia 1951:241–242

Hiradar PK, Kotari JS, Shah RV (1979) Studies on changes in blood-cell populations during tail regeneration in the gekkonid lizard, *Hamidactylus flaviviridis*. Neth J Zool 29:129–136

Huchezermayer FW, Cooper JE (2000) Fibrishess, not abscess, resulting from a localized inflammatory response to infection in reptiles and birds. Veter Rec 147:515–517

Hughes A, New D (1959) Tail regeneration in the geckonid lizard, *Sphaerodactylus*. J Embryol Exp Morphol 7:281–302

Irwin CR, Ferguson MWJ (1986) Fracture repair of reptilian dermal bones: can reptiles form secondary cartilage? J Anat 146:53–64

Jamison JJ (1964) Regeneration subsequent to intervertebral amputation in lizards. Herpetologica 20:145–149

Jiang M, Gu X, Feng X, Fan Z, Ding F, Liu Y (2007) The molecular characterisation of the brain protein 44-like (Brp44l) gene of *Gekko japonicum* and its expression changes in spinal cord after tail amputation. Mol Biol Reports 36:215–220

Kamrin RP, Singer M (1955) The influence of the spinal cord in regeneration of the tail of the lizard, *Anolis carolinensis*. J Exp Zool 128:611–627
Kinariwala RV, Shah RV, Ramachandran AV (1978) Tail regeneration and lipid metabolism: changes in the content of total hepatic lipids, glycerides and total blood lipids in the scincid lizard, *Mabuya carinata*. J Anim Morph Physiol 25:153–160
Kovacs EJ, DiPietro LA (1994) Fibrogenic cytokines and connective tissue production. FASEB J 8:854–861
Kuchling G (2005) Bifid tail regeneration in a turtle, *Emydura* sp. (testudines: Chelidae). Chelon Cons Biol 4:935–937
Kudokotsev VP (1960) Regeneration of the limb in the desert snake-eyed skink (*Ablepharus deserti* Strauch). Dokl Ak Sci SSSR 126:464–467
Leblond CP (1991) Time dimension in biology. A radioautographic survey of the dynamic features of cells, cell components, and extracellular matrix. Protoplasma 160:5–38
Licht P, Howe NR (1969) Hormonal dependence of tail regeneration in the lizard *Anolis carolinensis*. J Exp Zool 171:75–84
Liu HC, Maneely RB (1969a) Observations on the development and regeneration of tail epidermis in *Hemidactylus bowringi* (Gray). Acta Anat (Basel) 72:549–83
Liu HC, Maneely RB (1969b) The development of muscle spindles in the embryonic and regenerative tail of *Hemidactylus bowringi* (Gray). Acta Anat (Basel) 72:63–74
Liu Y, Ding F, Jiang M, Yang H, Feng X, Gu X (2006) EST-based identification of genes expressed in brain and spinal cord of *Gekko japonicus*, a species demonstrating intrinsic capacity of spinal cord regeneration. J Molec Neurosci 29:21–27
Lopez-Garcia C, Molowny A, Martinez-Guijarro FJ, Blasco-Ibanez JM, Luis de la Iglesias JA, Barnabeu A, Garcia-Verdugo JM (1992) Lesion and regeneration in the medial cerebral cortex of lizards. Histol Histopath 7:725–746
Maderson PFA (1971) The regeneration of caudal epidermal specialisations in *Lygodactylus picturatus keniensis* (Gekkonidae, Lacertilia). J Morphol 134:467–478
Maderson PFA (1985) Some developmental problems of the reptilian integument. In: Gans C, Billett F, Maderson PFA (eds) Biology of Reptilia, vol 14B. Wiley, New York, pp 525–598
Maderson PF, Licht P (1968) Factors influencing rates of tail regeneration in the lizard *Anolis carolinensis*. Experientia 24:1083–6
Maderson PFA, Roth SI (1972) A histological study of early stages of cutaneous wound healing in lizards in vivo and in vitro. J Exp Zool 180:175–186
Maderson PFA, Baranowitz S, Roth SI (1978) A histological study of the long term response to trauma of squamate integument. J Morphol 157:121–136
Maginnis TL (2006) The cost of autotomy and regeneration in animals: a review and framework for future research. Behav Ecol 17:857–872
Magon DK (1975) Changes in the thyroid activity in the house lizard, *Hemidactylus flaviviridis*, during different phases of regeneration in the different seasons of the year. Broteria 44:113–120
Magon DK (1977) Glucose metabolism in the regenerating tail of the scincid lizard, *Mabuya striata*: glycogen, phosphorylase and aldolase activity. J Nat Hist 11:121–126
Magon DK (1978) Hexose monophosphate oxydative cycle in the regenerating tail of scincid lizard Mabuya striata. Indian J Expl Biol 16:1–2
Marcucci E (1915a) Anche nella *Lacerta muralis* si può inibire la rigenerazione della coda. Boll Soc Nat Napoli 27:249–255
Marcucci E (1915b) Gli arti e la coda della *Lacerta muralis* rigenerano nello stadio embrionale? Boll Soc Nat Napoli 27:98–101
Marcucci E (1925) La rigenerazione degli arti nei rettili. Boll Soc Natur (Napoli) 38:8–17
Marcucci E (1930a) Il potere rigenerativo degli arti nei Rettili Ricerche sperimentali sopra alcune specie di Sauri. Archo Zool Ital 14:27–252
Marcucci E (1930b) La rigenerazione nei rettili. Arch Zool Ital 16:455–458

Marcucci E (1932) Trapianti di pelle e rigenerazione in *Lacerta muralis*. Archo Zool Ital 17:435–446
Marotta M (1946) Sulla rigenerazione del midollo spinale dei rettili. Atti Acc Naz Lincei 1:1367–1371
Martin P (1997) Wound healing. Aiming for perfect skin regeneration. Science 276:75–81
Mather CM (1978) A case of limb regeneration in *Sceloporus variabilis* (Reptilia, Lacertilia, Iguanidae). J Herpethol 12:263
Marusich MF, Simpson SB (1983) Changes in cell surface antigens during in vitro lizard myogenesis. Dev Biol 97:313–328
McGowan K, Coulombe PA (1998) The wound repar-asociated keratins 6, 16, and 17. In: Herman H, Harris JR (eds) Subcellular biochemistry: intermediate filaments, vol 31. Plenum Press, New York, pp 173–202
Mesher AL (1996) The cellular basis of limb regeneration in urodeles. Int J Dev Biol 40:785–795
Minelli G, Del Grande P, Manbelli MC (1978) Preliminary study of the regenerative process of the dorsal cortex of the telencephalon of *Lacerta viridis*. Z Mikrosk Anat Forsch 91:241–246
Minelli G, Del Grande P, Vighi F, Franceschini V (1980) Alcuni aspetti sperimentali sulla rigenerazione del sistema nervoso centrale in anfibi, rettili e mammiferi. Rendic Atti Acc Sci Bologna 13:161–175
Misuri A (1910) Ricerche sulla struttura della coda normale e rigenerata nella *Lacerta muralis* Merr. Boll Soc Zool Ital 11:103–135
Moffat LA, Bellairs AD (1964) The regenerative capacity of the tail in embryonic and post-natal lizards (*Lacerta vivipara* Jacquin). J Embryol Exp Morphol 12:769–86
Montali RJ (1988) Comparative pathology of inflammation in the higher vertebrates (reptiles, birds and mammals). J Comp Path 99:1–26
Mufti SA, Iqbal J (1975) Tail regeneration after amputation in *Hemidactylus flaviviridis*. Pakistan J Zool 7:15–28
Mufty SA, Mahmood S (1970) Muscle regeneration in a reptile, Uromastix Hardwicki. Pakist J Zool 8:85–92
Mufti SA, Munir M (1973) Analysis of tail regeneration in *Hemidactylus flaviviridis*. Biologia, Lahore 19:183–193
Mufti SA, Simpson SB (1972) Tail regeneration following autotomy in the adult salamander *Desmognatus fuscus*. J Morphol 136:297–312
Muthukkaruppan VR, Borysenko M, El Ridi R (1982) RES structure and function of the reptilia. In: Cohen N, Sigel MM (eds) The reticuloendothelial system, phylogeny and ontogeny, vol 3. Plenum Press, New York and London, pp 461–508
Neufeld DA, Day FA (1996) Perspective: a suggested role for basement membrane structures during newt limb regeneration. Anat Rec 246:155–161
Noble GK, Bradley HT (1933) The effect of temperature on the scale form of regenerated lizard skin. J Exp Zool 65:1–16
Noble GK, Clausen HJ (1936) Factors controlling the form and colour of scales on the regenerated tail of lizards. J Exp Zool 73:209–229
Nodler S, Martin P (1997) Wound healing in embryos: a review. Anat Embryol 195:215–228
Odelberg SJ (2005) Cellular plasticity in vertebrate regeneration. Anat Rec 287B:25–35
Pannese E (1963) Investigations on the ultrastructural changes of the spinal ganglion neurons in the course of axon regeneration and cell hypertophy. Zeitschr Zellf 60:711–740
Peadon AM, Singer M (1966) The blood vessels of the regenerating limb of the adult newt, *Triturus*. J Morphol 118:79–86
Pouling ML, Patrie KM, Botelho MJ, Tassava RA, Chiu IM (1993) Heterogeneity in the expression of fibroblast growth factor receptors during limb regeneration in newts (*Notophtalmus viridescens*). Development 119:353–361
Poyntz SV, Bellairs AA (1965) Natural limb regeneration in *Lacerta vivipara*. Br J Herpetol 3:204–205

Pritchard JJ, Ruzicka AJ (1950) Comparison of fracture repair in the frog, lizard and rat. J Anat 84:236–262
Purvis MD (1979) Early stages of tail regeneration in *Lampropholis guichenoti*. Aust Zool 20:289–296
Quattrini D (1952a) Ricerche anatomiche e sperimentali sulla autotomia della coda delle lucertole. I. Dinamica dell'autotomia e conseguenza nel tegumento (Osservazioni nella *Lacerta sicula sicula* Raf.). Arch Zool Ital 37:131–170
Quattrini D (1952b) Ricerche anatomiche e sperimentali sull'autotomia della coda delle lucertole. II. Muscolatura, adipe sottomuscolare e scheletro. (Osservazioni nella *Lacerta sicula sicula* Raf. e nella *L. sicula campestris* De Betta). Arch Zool Ital 37:465–515
Quattrini D (1953a) Autotomia e struttura anatomica della coda dei Rettili. (Altre osservazioni in *Lacerta vivipara* Jacq. e *L. viridis* Laur.). Monit Zool Ital 61:36–48
Quattrini D (1953–1954) Superrigenerazione della coda nei rettili. Monit Zool Ital 62(suppl): 466–470
Quattrini D (1954) Piano di autotomia e rigenerazione della coda nei Sauri. Archo ital Anat Embriol 59:225–282
Quattrini D (1955) Richerche sperimentali sulla rigenerazine della coda dei Sauri (Osservazioni in *Lacerta sicula campestris* de Betta e *L. muralis* Brueggemanni Bedr.). Monit Zool Ital 62:210–222
Radhakrishnan N, Shah RV (1973) Studies on the levels of glycogen and phosphorylase in the normal and regenerating tail of the scincid lizard, *Mabuya carinata*: a quantitative and histochemical analysis. J Anim Morph 20:150–159
Raffaelli E, Palladini G (1969) Rigenerazione delle cellule nervose delle cellule e degli assoni del midollo spinale dorsal di *Lacerta sicula*. Boll Zool 36:105–110
Ramachandran AV, Kinariwala RV, Shah RV (1983) Haemopoiesis and regeneration: changes in the liver, spleen, bone marrow and hepatic ion content during tail regeneration in the scincid lizard, *Mabuya carinata* (Boulenger). Amph Rept 6:377–386
Reichman OJ (1984) Evolution of regeneration capabilities. Amer Natur 123:752–763
Repesh LA, Fitzgerald TJ, Furcht LT (1982) Changes in the distribution of fibronectin during limb regeneration in newts using immunocytochemistry. Differentiation 22:125–131
Sabrazes J, Muratet L (1924) Les globules blancs du sangg de *Lacerta muralis* a l'état normal et pathologique. CR Soc Biol (Paris) 91:44–46
Sanz-Ezquerro JJ, Tockle C (2003) Digital development and morphogenesis. J Anat 202:51–58
Sassu G, Marchisio PC (1963) La giunzione neuromuscolare nella coda rigenerata di *Gongylus ocellatus*. Studi Sassaresi 41:32–38
Scadding SR (1977) Phylogenetic distribution of limb regeneration capacity in adult Amphibia. J exp Zool 202:57–68
Schall JJ, Bromwich CR, Werner YL, Midlege J (1989) Clubbed regenerated tails in *Agama agama* and their possible use in social interactions. J Herpetol 23:303–305
Schmidt AJ (1967) Cellular biology of vertebrate regeneration and repair. The University of Chicago Press, Chicago
Schwab ME, Bartholdi D (1996) Degeneration and regeneration of axons in the lesioned spinal cord. Physiol Rev 76:319–370
Shah RV, Chakko TV (1966) Histochemical localisation of acid phophatase in the adult normal and regenerating tail of *Hemidactylus flaviviridis*. J Anim Morph Physiol 13:169–188
Shah RV, Chakko TV (1971) Histochemical localization of cholinesterase in the normal and regenerating tail of the house lizard, *Hemidactylus flaviviridis*. J Anim Morphol Physiol 18:158–163
Shah RV, Chakko TV (1972) Histochemical localisation of nucleic acids in the normal and regenerating tail of the house lizard, *Hemidactylus flaviviridis*. J Anim Morph Physiol 19:28–33

Shah RV, Hiradhar PK (1974) Studies on glycogen, glycogen synthetase and respiratory quotient in the normal and regenerating tail of the house lizard, *Hemidactylus flaviviridis*. Netherlands J Zool 24:1–9

Shah RV, Hiradhar PK (1975) Glycosaminoglycans during tail regeneration in the house lizard, *Hemidactylus flaviviridis* (Lacertilia: Gekkonidae). J Anim Morph Physiol 22:43–50

Shah RV, Kinariwala RV, Ramachandran AV (1980) Haematopoiesis and regeneration: changes in the cellular elements of blood and haemoglobin during tail regeneration in the adult scincid lizard *Mabuya carinata* (Boulenger). Monit Zool Ital NS 14:137–150

Sharma K, Peng CY (2001) Spinal motor circuits: merging development and function. Neuron 29:321–324

Simpson SB (1961) Induction of limb regeneration in the lizard Lygosoma laterale, by augmentation of the nerve supply. Proc Soc exp Biol Med 107:108–111

Simpson SB Jr (1964) Analysis of tail regeneration in the Lizard *Lygosoma Laterale* I. Initiation of regeneration and cartilage differentiation: the role of ependyma. J Morphol 114:425–35

Simpson SB (1965) Regeneration of the lizard tail. In: Kiortsis V, Trampusch HAL (eds) Regeneration in animals and related problems. North-Holland, Amsterdam, pp 431–443

Simpson SB Jr (1968) Morphology of the regenerated spinal cord in the lizard, *Anolis carolinensis*. J Comp Neurol 134:193–210

Simpson SB Jr (1970) Studies on regeneration of the lizard's tail. Am Zool 10:157–65

Simpson SB (1983) Fasiculation and guidance of regenerating central axons by the ependyma. In: Kao CC, Bunge RP, Reier PJ (eds) Spinal cord reconstruction. Raven Press, New York, pp 151–162

Simpson SB Jr, Cox PG (1967) Vertebrate regeneration system: culture in vitro. Science 157:1330–1332

Simpson SB, Bayne EK (1979) In vivo and in vitro studies of regenerating muscle in the lizard Anolis. In: Mauro A (ed) Muscle regeneration. Raven Press, New York, pp. 189–200.

Simpson SB, Duffy MT (1994) The lizard spinal cord: a model system for the study of spinal cord injury and repair. Prog Brain Res 103:229–241

Simpson SB, Pollack K (1985) Ependyma-mesenchyme interactions during spinal cord regeneration. Soc Neurosci Abstr 10:1027

Singer M (1961) Induction of regeneration of body parts in the lizard, *Anolis*. Proc Soc exp Biol Med 107:106–108

Singer M (1978) On the nature of the neurotrophic phenomenon in urodele limb regeneration. Amer Zool 18:829–841

Smith DA, Barker IK (1988) Healing of cutaneous wounds in the common garter snake (*Thamnopis sirtalis*). Can J Vet res 52:111–119

Tassava RA, Goss RJ (1966) Regeneration rate and amputation level in fish fins and lizard tails. Growth 30:9–21

Tassava RA, Mesher AL (1975) The role of injury, nerves and wound epidermis during the initiation of amphibian limb regeneration. Differentiation 4:23–24

Tassava RA, Olsen CL (1982) Higher vertebrates do not regenerate digits and legs because the wound epidermis is not functional. A hypothesis. Differntiation 22:151–155

Terni T (1915) Studio anatomico di una coda doppia. Arch Ital Anat Embryol 14:290–314

Terni T (1920) Sulla correlazione fra amplezza del territorio di innervazioni e grandezza della cellule gangliare. 2. Richerche sui gangli spinali che innervano la coda rigenerata, dei Sauri (*Gongylus ocellatus*). Arch Ital Anat Embriol 17:507–543

Terni T (1922) La rigenerazione del simpatico nella coda rigenerata dei Sauri. Monit Zool Ital 33:58–62

Thermes G (1951) Autonomia rigenerativa e rigenerazione inversa nel segmento codale di *Lacerta muralis* interrotto dal restante neurasse. Rend Fac Sci Univ Cagliari 20:1–12

Thomas BP, Varia MR, Ansari MM, Menon GN (1972) Lack of talidomide induced aplasia in regenerating tail of lizard, *Hemidactylus flaviviridis*. Indian J exp Zool 10:316–318

Toole BP, Gross J (1971) The extracellular matrix of regenerating newt limbs: synthesis and removal of hyaluronate prior to differentiation. Dev Biol 25:57–77
Tsonis PA (2002) Regenerative biology: the emerging field of tissue repair and restoration. Differentiation 70:397–409
Tuchunduva M, Borelli P, Silva JRM (2001) Experimental study of induced inflammation in the Brazilian boa (*Boa constrictor constrictor*). J comp Pathol 125:174–181
Turner JE (1972) Effects of hypophysectomies and thyroxine replacement upon the initiation of tail regeneration in the lizard, *Anolis carolinensis*. J Morphol 137:449–462
Turner JE, Singer M (1973) Some morphological and ultrastructural changes in the ependyma during early regeneration of the tail in the lizard, *Anolis carolinensis*. J Morphol 140:257–270
Turner JE, Tipton SR (1971) The role of the lizard thyroid gland in tail regeneration. J Exp Zool 178:63–84
VanBekkum DW (2004) Phylogenetic aspects of tissue regeneration: role of stem cells. A concise overview. Blood Cells Mol Dis 32:11–16
VanDen Boom R, Wilmink JM, O'Kane S, Wood J, Ferguson MWJ (2002) Transforming growth factor- levels during second-intention healing are related to the different course of wound contraction in horses and ponies. Wound Heal Reg 10:188–194
Vitt LJ (1983) Tail loss in lizards: the significance of foraging and predator escape modes. Herpetologica 39:151–165
Volante F (1923) Contributo alla conoscenza della superrigenerazione nei rettili. Monit Zool Ital 34:185–201
Wake DB, Dresner JG (1967) Functional morphology and evolution of tail autotomy in salamanders. J Morphol 122:265–306
Webb G, Manoli C (1989) Crocodiles of Australia. Reed, Chatswood, Australia
Werber I (1905) Regeneration der Kiefer bei der Eidechse Lagerta agilis. Wilhelm Roux Arch Entw Mech Org 19:248–258
Werner YL (1967a) Regeneration of specialised scales in tails of *Teratoscincus* (Reptilia: Gekkonidae). Senck Biol 48:117–124
Werner YL (1967b) Regeneration of the caudal axial skeleton in a gekkonid lizard (*Hemidactylus*) with particular reference to the "latent" period. Acta Zool Stockn 48:103–125
Werner YL (1968) Regeneration frequencies in geckos of two ecological types (Reptilia: Gekkonidae). Vie et Milieu 19:199–222
Werner YL (1971) The ontogenic development of the vertebrae in some gekkonid lizards. J Morphol 133:41–92
Whimster IW (1978) Nerve supply as a stimulator of the growth of tissues including skin II. Animal evidence. Clin exp Dermatol 3:389–410
White CP (1925) Regeneration of the lizard's tail. J Path Bact 28:63–68
Woodland WNF (1920) Some observations on caudal autotomy and regeneration in the gecko (*Hemidactylus flaviviridis*, Ruppel), with notes on the tails of *Sphenodon* and *Pygopus*. QJ Microsc Sci 65:63–100
Wynn TA (2008) Cellular and molecular mechanism of fibrosis. J Pathol 214:199–210
Zannone L (1953) Fenomeni rigenerativi nervosi in rapporto con la rigenerazione della coda di Geko (*Tarentola mauritanica*). Ric Morfologia 22:183–2000
Zasloff M (2002) Antimicrobial peptides of multicellular organisms. Nature 415:389–395
Zhang F, Clarke JDW, Ferretti P (2000) FGF-2 up-regulation and proliferation of neural progenitors in the regenerating amphibian spinal cord in vivo. Dev Biol 225:381–391
Zika JM (1969) A histological study of the regenerative response in a lizard, *Anolis carolinensis*. J Exp Zool 172:1–8
Zika J, Singer M (1965) The relation between nerve fiber number and limb regenerative capacity in the lizard, Anolis. Anat Rec 152:137–40